algorithms

MDPI

Article

Hybrid Four Vector Intelligent Metaheuristic with Differential Evolution for Structural Single-Objective Engineering Optimization

Hussam N. Fakhouri [1], Ahmad Sami Al-Shamayleh [2,*], Abdelraouf Ishtaiwi [1], Sharif Naser Makhadmeh [3,4], Sandi N. Fakhouri [3] and Faten Hamad [3,5]

[1] Data Science and Artificial Intelligence, Faculty of Information Technology, University of Petra, Amman 11196, Jordan; hussam.fakhouri@uop.edu.jo (H.N.F.); aishtaiwi@uop.edu.jo (A.I.)
[2] Department of Data Science and Artificial Intelligence, Faculty of Information Technology, Al-Ahliyya Amman University, Amman 19328, Jordan
[3] The University of Jordan, Amman 11942, Jordan; sharif.makhadmeh@uop.edu.jo (S.M.); san9220489@ju.edu.jo (S.N.F.); f.hamad@ju.edu.jo (F.H.)
[4] Artificial Intelligence Research Center (AIRC), College of Engineering and Information Technology, Ajman University, Ajman P.O. Box 346, United Arab Emirates
[5] Information Studies, Sultan Qaboos University, Muscat 123, Oman
* Correspondence: a.alshamayleh@ammanu.edu.jo

Abstract: Complex and nonlinear optimization challenges pose significant difficulties for traditional optimizers, which often struggle to consistently locate the global optimum within intricate problem spaces. To address these challenges, the development of hybrid methodologies is essential for solving complex, real-world, and engineering design problems. This paper introduces FVIMDE, a novel hybrid optimization algorithm that synergizes the Four Vector Intelligent Metaheuristic (FVIM) with Differential Evolution (DE). The FVIMDE algorithm is rigorously tested and evaluated across two well-known benchmark suites (i.e., CEC2017, CEC2022) and an additional set of 50 challenging benchmark functions. Comprehensive statistical analyses, including mean, standard deviation, and the Wilcoxon rank-sum test, are conducted to assess its performance. Moreover, FVIMDE is benchmarked against state-of-the-art optimizers, revealing its superior adaptability and robustness. The algorithm is also applied to solve five structural engineering challenges. The results highlight FVIMDE's ability to outperform existing techniques across a diverse range of optimization problems, confirming its potential as a powerful tool for complex optimization tasks.

Keywords: metaheuristic; intelligent; optimization; engineering design

Citation: Fakhouri, H.N.; Al-Shamayleh, A.S.; Ishtaiwi, A.; Makhadmeh, S.N.; Fakhouri, S.N.; Hamad, F. Hybrid Four Vector Intelligent Metaheuristic with Differential Evolution for Structural Single-Objective Engineering Optimization. *Algorithms* **2024**, *17*, 417. https://doi.org/10.3390/a17090417

Academic Editor: Frank Werner

Received: 17 July 2024
Revised: 10 September 2024
Accepted: 11 September 2024
Published: 20 September 2024

1. Introduction

Metaheuristic techniques represent a prominent area of study in the field of computational optimization, offering a variety of methods for solving complex and often intractable problems across various domains [1]. These techniques, characterized by their ability to escape local optima and explore the global search space, have gained substantial traction due to their versatility and efficacy in tackling a wide array of optimization challenges [2].

The genesis of metaheuristic algorithms can be traced back to the 1960s and 1970s, with the advent of strategies like Genetic Algorithms (GAs) [3] and Simulated Annealing (SA) [4], which drew inspiration from biological evolution and thermodynamics, respectively. However, the term "metaheuristic" was formally coined in the late 1980s and early 1990s and began to see widespread adoption in academic and research circles. This period marked a paradigm shift in optimization techniques, moving from traditional, deterministic methods to more stochastic and heuristic-based approaches [5].

At its core, a metaheuristic is a high-level problem-independent algorithmic framework that provides a set of guidelines or strategies to develop heuristic optimization algorithms.

Metaheuristics do not guarantee an optimal solution [6]; instead, they seek to find a sufficiently good solution within a reasonable time frame, making them particularly useful for practical applications where time and resources are limited [7].

The landscape of metaheuristic techniques is diverse, encompassing a broad spectrum of algorithms inspired by natural phenomena, psychological processes, and even human-made systems, including Evolutionary Algorithms (EAs) [8], Swarm Intelligence (SI)-based [9] algorithms like Particle Swarm Optimization (PSO) [10] and Ant Colony Optimization (ACO) [11], and physics-based methods like the Gravitational Search Algorithm (GSA) [12]. Each of these algorithms operates on the principle of iterative improvement, where a set of candidate solutions undergoes various processes such as selection, crossover, mutation (in the case of EAs), or movement and updating of positions (in swarm intelligence algorithms) to converge towards an optimal or near-optimal solution [13].

The application of metaheuristic techniques spans numerous domains, ranging from engineering design optimization to financial modeling [14], from logistics and supply chain management to bioinformatics, and from machine learning to network design. Their adaptability and robustness in handling multi-modal, non-linear, and high-dimensional problems make them an indispensable tool in the arsenal of modern-day researchers and practitioners [15,16]. However, there are several limitations and challenges associated with metaheuristics, including the risk of premature convergence, the balance between exploration and exploitation, and the need for parameter tuning [17]. Thus, the choice of a suitable metaheuristic algorithm is decided based on the specific nature and requirements of the problem at hand.

In the evolving landscape of metaheuristic algorithms, a notable gap exists in their ability to fully meet the intricate requirements of complex engineering optimization problems. This gap analysis identifies these shortcomings and explores how the Hybrid FVIMDE Algorithm aims to address them, enhancing the overall efficacy of optimization processes.

Further, the No-Free-Lunch (NFL) Theorem asserts that no single optimization algorithm is universally superior across all problem types. Established by Wolpert and Macready, it emphasizes that an algorithm's effectiveness is highly problem-specific, challenging the notion of a one-size-fits-all solution in algorithm design. This theorem asserts the importance of selecting the right algorithm based on the specific characteristics of the problem at hand and has encouraged the development of more adaptive, hybrid algorithms that combine the strengths of various approaches to address a broader range of optimization challenges [18].

The proposed FVIMDE method is designed to bridge these gaps by combining the strong exploration capabilities of FVIM with the focused exploitation proficiency of DE. The main contributions of introducing the proposed methods are:

- The HybridFour Vector Intelligent Metaheuristic and Differential Evolution (FVIMDE) algorithm is introduced, merging the advantages of both optimizers to enhance optimization efficiency.
- The FVIMDE algorithm integrates FVIM's four-vector strategy with DE's mutation and crossover strategies, utilizing the average mean of the four best solutions for exploration and DE strategies for exploitation.
- The FVIMDE algorithm is implemented and evaluated using unimodal, multimodal, hybrid, and composition benchmark functions from the 2022 and 2017 IEEE Congress on Evolutionary Computation and challenging benchmark function that consists of complex, hybrid, and composite functions.
- The FVIMDE algorithm is validated on complex real-world engineering design problems such as welded beam design, pressure vessel design, spring design, speed reducer design, cantilever beam design, and three-bar truss design, showing superior performance when compared to 12 well-known and state-of-the-art optimization algorithms, such as GWO, WOA, MFO, and MVO.

The rest of this paper is organized as follows: Section 2 provides a detailed review of the recent related work, and Section 3 focuses on the foundational concepts of the

Four-Vector Intelligent Metaheuristic (FVIM) and Differential Evolution (DE), highlighting their key characteristics and applications. In Section 4, we introduce the proposed Hybrid FVIMDE Algorithm, detailing its conceptual framework and operational mechanics, and discuss how it integrates the strengths of FVIM and DE. It also presents the mathematical model of FVIMDE, including variable definitions, mutation and crossover processes, and the FVIM position-update mechanism. In addition, it explores the strategic components of exploration and exploitation within the hybrid algorithm, describing the balance between these elements to optimize performance. Section 5 delves into the experimental analysis and results, presents evaluations using benchmark functions, and discusses the algorithm performance relative to other optimization algorithms. Section 7 applies the FVIMDE algorithm to real-world engineering design problems, discussing optimization constraints and parameter settings. Finally, Section 9 concludes the paper by summarizing the findings, reiterating the advantages of the hybrid algorithm, and suggesting future research directions.

2. Related Work

Hybrid optimization algorithms have been increasingly adopted to tackle complex engineering and industrial design challenges, leveraging the strengths of multiple metaheuristic approaches. Huang and Hu [19] and Tang et al. [20] developed hybrid algorithms that combine existing techniques to improve performance in structural design and engineering optimization, with each study demonstrating enhanced efficiency and effectiveness over traditional methods.

Several researchers have focused on enhancing exploration and exploitation capabilities within hybrid algorithms. Liu et al. [21] proposed hybrid methods that integrate diverse strategies to prevent local optima entrapment and improve solution diversity. Their algorithms have shown significant improvements in convergence speed and robustness across various benchmark and engineering problems.

In the realm of uncertainty handling and specific applications, Cheng et al. [22] and Dhiman [23] presented hybrid approaches that cater to engineering structures and constrained optimization scenarios, respectively. Their work highlights the need for algorithms capable of addressing complex uncertainties and optimizing highly constrained environments.

Further contributions include Qin and Han's [24] Hybrid Quantum Particle Swarm Optimization and Chu et al.'s [25] Hybrid Parallel Willow Catkin Optimization Algorithm, both of which incorporate unique strategies to improve global search capabilities and convergence rates, particularly in multidimensional and real-world engineering problems.

Finally, addressing the balance between exploration and exploitation, which remains a significant challenge in metaheuristic optimization, has been a central theme across these studies [9]. The development of robust, adaptable algorithms capable of handling the diversity of engineering design problems remains an ongoing pursuit, motivating the proposal of the FVIMDE hybrid optimization algorithm.

A primary challenge in current metaheuristic algorithms is striking the right balance between exploration and exploitation. Exploration involves diversifying the search across the solution space, while exploitation focuses on intensifying the search in promising regions. Many algorithms excel in exploration, but fall short in exploitation, or vice versa, leading to either suboptimal solutions or inflated computation times. This imbalance is a critical issue that needs to be addressed [26].

Another gap is in handling multimodal landscapes—common in engineering design problems—which are characterized by numerous local optima. Existing algorithms often struggle to distinguish between local and global optima, leading to premature convergence on suboptimal solutions. This limitation can severely impede the effectiveness of the optimization process [9].

In addition, the diversity of engineering design problems calls for algorithms that are robust and adaptable to various problem structures without the need for extensive modifications. This flexibility is often lacking in existing algorithms, limiting their applicability

across different types of engineering challenges [27], and this motivates us to develop the hybrid FVIMDE optimization algorithm.

3. Technical Background

3.1. Overview of the Four Vector Intelligent Metaheuristic (FVIM)

The Four Vector Intelligent Metaheuristic (FVIM) [28] is an innovative optimization algorithm designed to overcome the challenges associated with traditional swarm-based algorithms, such as Particle Swarm Optimization (PSO). At its core, FVIM is structured to strike a balance between exploration and exploitation within the search space, thereby enhancing the probability of converging to a global optimum solution. This algorithm builds upon a mathematical framework that integrates multiple agent behaviors and dynamically adjusts their movements to avoid premature convergence, which is considered a common issue in many optimization algorithms.

3.2. Algorithmic Overview

FVIM operates through a sequence of well-defined stages, beginning with an initialization phase where key parameters are set, and agents are randomly positioned within the solution space. This is followed by an iterative process where agents update their positions based on a set of four mathematical models, each contributing to the overall search strategy. The final stage of the algorithm focuses on identifying the optimal solution by comparing the outcomes of these iterations against the predefined objective function.

3.3. Algorithm Flow

The FVIM algorithm can be summarized as follows:

1. Initialization Phase: Define and randomly initialize the key parameters and agent positions. Set the upper and lower boundaries of the search space.
2. Iterations Phase: Update the agents' positions using the four mathematical models, iterating until the stopping conditions are met.
3. Finding Optimal Solution Phase: Identify the best solution by evaluating the fitness of each agent's position and comparing it to the objective function.

FVIM leverages four leading agents Alpha, Beta, Gamma, and Delta to guide the search process. These four vectors are actual candidate solutions within the population, and they are dynamically updated during each iteration of the FVIM phase. The four vectors (Alpha, Beta, Gamma, and Delta) represent the four best candidate solutions within the population at any given iteration. Specifically:

- Alpha: The best solution found so far.
- Beta: The second-best solution.
- Gamma: The third-best solution.
- Delta: The fourth-best solution.

These vectors are actual members of the population and are updated based on their fitness values. Their role is to influence the position updates of all other particles in the population, thereby guiding the search toward promising regions of the solution space.

3.4. Mathematical Foundation

FVIM [28] introduced an innovative exploration strategy into the optimization process by the use of four vectors (Alpha, Beta, Gamma, and Delta), as shown in Equations (1) and (2), with each vector representing a distinct subset of top-performing solutions within the search space. This multi-vector structure allows FVIM to conduct a more effective exploration compared to traditional single-point search methods [28].

$$\mathbf{X}_{n,i} = \mathbf{P}_{n,i} + (\alpha \times 2 \times \xi_1 - \alpha) \times \left|\xi_2 \times \mathbf{P}_{n,i} - \overline{\mathbf{P}}_i\right| \times \begin{cases} 1, & \text{if } \xi_3 < 0.5, \\ -1, & \text{otherwise} \end{cases}, \quad \text{for } n \in \{1,2,3,4\}. \tag{1}$$

$$\overline{\mathbf{P}}_i = \frac{\mathbf{X}_{1,i} + \mathbf{X}_{2,i} + \mathbf{X}_{3,i} + \mathbf{X}_{4,i}}{4} \tag{2}$$

where, $\mathbf{X}_{n,i}$ represents the updated position for the n^{th} best agent in the i^{th} dimension. $\mathbf{P}_{n,i}$ is the current position of the n^{th} best agent in the i^{th} dimension. $\overline{\mathbf{P}}_i$ represents the current average position of all agents in the i^{th} dimension. α is a coefficient. ξ_1, ξ_2, and ξ_3 represent random numbers uniformly distributed in **[0, 1]**.

The mechanism of these vectors is central to FVIM's functionality. The search space is navigated using the Alpha, Beta, Gamma, and Delta vectors, which are dynamically updated according to their fitness values. Each vector is responsible for guiding a segment of the population, promoting a diversified exploration approach. The Alpha vector takes the lead in the search, followed in the hierarchy of Beta, Delta, and Gamma, with each focusing on exploring different regions of the solution space. This hierarchical model is instrumental in maintaining a strategic balance between discovering new areas and capitalizing on known promising regions [28]. A key attribute of FVIM is its search strategy. FVIM incorporates dynamic parameters that adjust the influence of each vector on the search agents. This adaptability allows FVIM to navigate various regions of the solution space effectively, be they sparsely or densely populated with potential solutions [28].

The balance between exploration and exploitation is another critical aspect of FVIM. Exploration is facilitated through the stochastic nature of the vector updates, ensuring FVIM avoids premature convergence to local optima. In contrast, exploitation is managed by concentrating the search around the best solutions identified by the vectors. This equilibrium between exploration and exploitation is essential in FVIM's capability to uncover high-quality solutions, enhancing the overall efficacy of the optimization process [28].

3.5. Overview of Differential Evolution (DE)

Differential Evolution (DE) [29] is known for its efficiency and effectiveness in the exploitation phase of optimization tasks. Grounded in evolutionary principles, the typical workflow of DE encompasses initializing a population of candidate solutions, performing mutation and crossover on each individual to create a trial vector, evaluating the fitness of these trial vectors, and applying a selection to establish the population for the next generation. This process is repeated until a predefined stopping criterion is met [30]. In addition, DE employs a straightforward yet potent set of operators (mutation, crossover, and selection) to maneuver through the solution space and refine solutions toward the global optimum. DE's approach is centered on a population-based methodology. It operates on a pool of candidate solutions, iteratively working through them to explore and exploit the solution space. Each candidate, also referred to as an individual or a vector, represents a possible solution to the optimization problem at hand. A critical aspect of DE is its mutation strategy, which plays a pivotal role in introducing variability and novel traits into the population [30].

The mutation strategy in differential evolution (DE) is encapsulated by an equation that outlines the process of mutated vector generation for each population member. This generation is accomplished by adding the weighted difference between two distinct, randomly chosen population members, X_{r2} and X_{r3}, to a third member, X_{r1} [30]. The formula illustrating this mutation strategy is presented in Equation (3):

$$V_i = X_{r1} + F \cdot (X_{r2} - X_{r3}) \tag{3}$$

where V_i represents the mutated vector, X_{r1}, X_{r2}, and X_{r3} are the three distinct, randomly selected vectors from the population, and F is a scaling factor that controls the mutation extent.

Following mutation, DE employs a crossover operation to further diversify the population. This operation integrates the mutated vector with an existing population member, creating a trial vector. It operates by interchanging components between both vectors, influenced by a crossover probability CR, to enhance the search of the solution space [30].

The selection mechanism in DE hinges on the comparative fitness of the trial vector and the original individual. The one exhibiting superior fitness is retained for the next generation, fostering gradual enhancement in the overall quality of the population.

The Role of Crossover in the DE Phase

While the traditional role of the crossover operator in Differential Evolution (DE) is to introduce diversity by mixing components from the mutant and target vectors, it is important to address a subtle aspect of its function in our implementation. Specifically, the crossover operator can sometimes reverse parts of the mutation operation, which may give the impression that it is primarily a corrective mechanism rather than one that enhances diversity.

Reversing Mutation:

In our approach, the crossover operation decides whether to retain components from the target vector $\mathbf{P}_i(j)$ or incorporate components from the mutant vector $\mathbf{V}_i(j)$. Due to this decision-making process, particularly when the crossover rate C_r is low, the crossover may indeed undo some of the changes introduced by mutation. This occurs when more components from $\mathbf{P}_i(j)$ are retained, effectively reversing parts of the mutation's effects on those components.

Introducing Diversity:

However, the crossover operation still plays a crucial role in maintaining diversity within the population. By selectively incorporating components from the mutant vector $\mathbf{V}_i(j)$, especially when C_r is high, the crossover ensures that new information is introduced into the trial vector $\mathbf{U}_i$. This mixing of components from both the mutant vector and the target vector allows the trial vector to benefit from the exploratory nature of the mutation while preserving some of the original solution's structure. Therefore, even though crossover may reverse some aspects of the mutation, it does not completely negate the contribution of mutation, and diversity is maintained.

The balance between reversing mutation and introducing new diversity is controlled by the crossover rate C_r. By adjusting this parameter, we can fine-tune the algorithm's exploration and exploitation capabilities, allowing the algorithm to effectively search the solution space while avoiding premature convergence to suboptimal solutions.

While the crossover operator may occasionally reverse the effects of mutation, its primary role remains the introduction of diversity into the population. The crossover rate C_r serves as a key parameter to balance these effects, ensuring that the DE algorithm maintains its effectiveness in exploring and exploiting the search space.

4. Proposed Hybrid FVIMDE Algorithm

In this section, we present the Hybrid Four Vector Intelligent Mechanism with Differential Evolution (FVIMDE) algorithm, a novel optimization technique designed to effectively balance exploration and exploitation within the search space. The proposed algorithm integrates the strengths of Differential Evolution (DE), known for its robust exploration capabilities, with the Four Vector Intelligent Mechanism (FVIM), which excels at fine-tuning solutions in promising regions of the search space.

The FVIMDE algorithm operates in two distinct phases. The first phase involves the application of Differential Evolution to explore the global search space, identifying potential areas where optimal or near-optimal solutions may reside. During this phase, the population undergoes initialization, mutation, crossover, and selection processes to iteratively improve the quality of solutions. The second phase transitions into the FVIM, where the best solution obtained from the DE phase is refined through a strategic position update mechanism involving the Alpha, Beta, Gamma, and Delta particles.

By combining these two powerful optimization techniques, the FVIMDE algorithm leverages the global search capability of DE and the local search efficiency of FVIM, en-

suring a comprehensive search process that effectively avoids premature convergence and improves the likelihood of finding the global optimum. The following subsections provide a detailed explanation of the steps involved in each phase of the proposed algorithm.

4.1. Mathematical Model of the Hybrid DE-FVIM Optimizer

The Hybrid DE-FVIM optimizer is a two-phase optimization algorithm that combines Differential Evolution (DE) with the Four Vector Intelligent Mechanism (FVIM). The optimizer iterates over a predefined number of iterations, Max_iter, which is divided into two phases: the DE phase and the FVIM phase.

4.1.1. DE Phase

The DE phase is executed during the first half of the total iterations, i.e., $\frac{\text{Max\_iter}}{2}$.

4.1.2. Initialization

Initially, a population $\mathbf{P}$ of size $N \times D$ is generated randomly within the search space bounds. The position of each individual i in the population is initialized, as shown in Equation (4):

$$\mathbf{P}(i,j) = \text{lb}(j) + \text{rand}(0,1) \times (\text{ub}(j) - \text{lb}(j)), \quad i = 1,\ldots,N,\ j = 1,\ldots,D \tag{4}$$

where N is the population size, D is the dimensionality of the problem, $\text{lb}(j)$ and $\text{ub}(j)$ are the lower and upper bounds for dimension j, respectively.

4.1.3. Mutation and Crossover

For each individual i, a mutant vector $\mathbf{V}_i$ is generated using the DE/rand/1 strategy, as shown in Equation (5):

$$\mathbf{V}_i = \mathbf{P}_{r_1} + F \times (\mathbf{P}_{r_2} - \mathbf{P}_{r_3}) \tag{5}$$

where r_1, r_2, r_3 are distinct indices randomly selected from the population, and F is the scaling factor.

Following mutation, a trial vector $\mathbf{U}_i$ is generated through binomial crossover, as defined in Equation (6). The crossover generates a trial vector by combining elements from the mutant vector and the target vector. The goal of this operation is to introduce variability in the population while preserving some of the characteristics of the current solution.

The crossover operator used is a binomial crossover, where each element of the trial vector $\mathbf{U}_i$ is taken from either the mutant vector $\mathbf{V}_i$ or the target vector $\mathbf{P}_i$, based on a crossover probability C_r. The equation used to generate the trial vector is as follows:

$$\mathbf{U}_i(j) = \begin{cases} \mathbf{V}_i(j) & \text{if rand}(0,1) \leq C_r \text{ or } j = j_{\text{rand}} \\ \mathbf{P}_i(j) & \text{otherwise} \end{cases} \tag{6}$$

where C_r is the crossover rate and j_{rand} is a randomly chosen index to ensure that at least one element is inherited from $\mathbf{V}_i$.

In this equation, $\mathbf{U}_i(j)$ is the j-th component of the trial vector for individual i, $\mathbf{V}_i(j)$ is the j-th component of the mutant vector for individual i, and $\mathbf{P}_i(j)$ is the j-th component of the target vector for individual i. The crossover rate C_r determines the probability of taking a component from the mutant vector, and j_{rand} is a randomly chosen index that ensures at least one element is inherited from the mutant vector. This prevents the trial vector from being identical to the target vector.

The crossover process operates as follows.

For each dimension j of the solution vector, a random number is generated. If this random number is less than or equal to the crossover rate C_r, or if the index j equals j_{rand}, the corresponding component from the mutant vector $\mathbf{V}_i(j)$ is copied into the trial vector $\mathbf{U}_i(j)$. If neither condition is met, the component from the target vector $\mathbf{P}_i(j)$ is retained in the trial vector.

To ensure diversity in the population, the inclusion of j_{rand} guarantees that at least one component from the mutant vector is always included in the trial vector. This prevents the trial vector from being a direct copy of the target vector, maintaining variability in the population.

The crossover operation iterates over each individual in the population (using the loop 'for i = 1:pop') and each dimension of the solution vector (using the loop 'for j = 1:dim'). Inside the nested loop, a random index 'jrand' is selected once for each individual, ensuring that at least one component from the mutant vector $\mathbf{V}_i$ is copied into the trial vector $\mathbf{U}_i$. For each dimension, a random number is generated. If this random number is less than or equal to the crossover rate (set to 0.9 in the code), or if the current index j equals j_{rand}, the corresponding component from the mutant vector is copied into the trial vector. Otherwise, the component from the target vector is retained.

4.1.4. Selection

The selection process decides whether the trial vector $\mathbf{U}_i$ replaces the target vector $\mathbf{P}_i$. This decision is made based on their fitness values, as described in Equation (7):

$$\mathbf{P}_i = \begin{cases} \mathbf{U}_i & \text{if } f(\mathbf{U}_i) < f(\mathbf{P}_i) \\ \mathbf{P}_i & \text{otherwise} \end{cases} \tag{7}$$

where $f(\cdot)$ denotes the fitness function. The best individual in the population after the DE phase is identified as $\mathbf{P}_{\text{best}}$.

4.2. FVIM Phase

The FVIM phase begins after the DE phase and utilizes the best solution from DE as the initial position for the alpha particle. The FVIM phase continues for the remaining half of the total iterations.

4.3. Population Size and Role of the Four Vectors

In the FVIM phase, the population size remains the same as in the DE phase and is denoted as N.

Position Update

During the FVIM phase, the position of each particle is updated based on the positions of the Alpha, Beta, Gamma, and Delta particles. The new position for each particle is computed as the average of four intermediate positions, as given in Equation (8):

$$\mathbf{X}_{i,j} = \frac{\mathbf{X}^1_{i,j} + \mathbf{X}^2_{i,j} + \mathbf{X}^3_{i,j} + \mathbf{X}^4_{i,j}}{4} \tag{8}$$

where $\mathbf{X}^1, \mathbf{X}^2, \mathbf{X}^3, \mathbf{X}^4$ are position updates influenced by the Alpha, Beta, Gamma, and Delta particles, respectively, as shown in Equation (9).

Each intermediate position $\mathbf{X}^k_{i,j}$ is calculated as follows:

$$\mathbf{X}^k_{i,j} = \begin{cases} \mathbf{P}_{k,j} + a \times (2 \times \text{rand}(0,1) - 1) \times |\text{rand}(0,1) \times \mathbf{P}_{k,j} - \mathbf{X}_{i,j}| & \text{if rand}(0,1) < 0.5 \\ \mathbf{P}_{k,j} - a \times (2 \times \text{rand}(0,1) - 1) \times |\text{rand}(0,1) \times \mathbf{P}_{k,j} - \mathbf{X}_{i,j}| & \text{otherwise} \end{cases} \tag{9}$$

where $k \in \{\text{Alpha}, \text{Beta}, \text{Gamma}, \text{Delta}\}$, and a is a linearly decreasing coefficient calculated as shown in Equation (10):

$$a = 2 - \text{iteration} \times \frac{2}{\text{Max\_iter} - \text{DE\_iter}} \tag{10}$$

where iteration is the current iteration number, and $\text{DE\_iter} = \frac{\text{Max\_iter}}{2}$.

4.4. Combined Optimization Process

The overall optimization process combines the DE phase and FVIM phase. The DE phase aims to explore the search space and identify promising regions, while the FVIM phase exploits these regions to refine the solution. The combination of these two phases enhances the optimizer's performance in terms of exploration and exploitation balance.

4.5. Hybrid FVIMDE Algorithm Stages

The Hybrid FVIMDE Algorithm as shown in Algorithm 1, consists of two main stages, each designed to complement the other in optimizing complex functions by effectively balancing exploration and exploitation. The source code is available at https://www.mathworks.com/matlabcentral/fileexchange/171204-hybrid-four-vector-intelligent-metaheuristic-with-de (accessed on 17 July 2024).

Algorithm 1 Hybrid FVIMDE Algorithm Pseudocode

Initialize population $\mathbf{P}$ of size $N \times D$ within the bounds $[\text{lb}, \text{ub}]$ using Equation (4).
Evaluate the fitness of each individual in $\mathbf{P}$.
Set DE_iter = $\frac{\text{Max\_iter}}{2}$ (number of iterations for DE phase).
for each iteration $l = 1$ to DE_iter **do**
    for each individual $i = 1$ to N **do**
        Generate mutant vector $\mathbf{V}_i$ using Equation (5).
        Generate trial vector $\mathbf{U}_i$ using crossover as shown in Equation (6).
        Apply boundary handling to $\mathbf{U}_i$.
        Evaluate the fitness of $\mathbf{U}_i$.
        Perform selection between $\mathbf{P}_i$ and $\mathbf{U}_i$ using Equation (7).
    end for
    Update the best solution $\mathbf{P}_{\text{best}}$ if a better solution is found.
end for
Initialize positions for FVIM with $\mathbf{P}_{\text{best}}$ as the alpha particle's position.
Set FVIM_iter = Max_iter − DE_iter (number of iterations for FVIM phase).
for each iteration $itr = 1$ to FVIM_iter **do**
    Update the coefficient a using Equation (10).
    for each individual $i = 1$ to N **do**
        for each dimension $j = 1$ to D **do**
            Calculate the position updates $\mathbf{X}^1_{i,j}, \mathbf{X}^2_{i,j}, \mathbf{X}^3_{i,j}, \mathbf{X}^4_{i,j}$ using Equation (9).
            Update the position $\mathbf{X}_{i,j}$ using Equation (8).
        end for
        Evaluate the fitness of $\mathbf{X}_i$.
        Update Alpha, Beta, Gamma, and Delta positions if necessary.
    end for
    Record the best solution $\mathbf{P}_{\text{best}}$.
end for
Return the best solution $\mathbf{P}_{\text{best}}$ and its fitness value.

4.5.1. Stage 1: Differential Evolution (DE) Phase

The first stage of the algorithm is the Differential Evolution (DE) phase, which focuses on exploring the global search space. This phase is executed over the first half of the total iterations. The process begins with the initialization of a population of candidate solutions within the defined search space bounds. Each individual in the population is then evaluated based on the objective function. During each iteration of the DE phase, new candidate solutions are generated using mutation and crossover operators. Mutation involves creating a mutant vector by perturbing existing solutions, as described by the DE/rand/1 strategy. The crossover operator then combines elements from the mutant vector and the current solution to create a trial vector. This trial vector undergoes boundary handling to ensure it remains within the permissible search space. The selection process follows, where the trial vector replaces the current solution if it offers a better fitness

value. Throughout the DE phase, the algorithm continuously tracks the best solution found, setting it up as the foundation for the next stage.

4.5.2. Stage 2: Four Vector Intelligent Mechanism (FVIM) Phase

The second stage is the Four Vector Intelligent Mechanism (FVIM) phase, which is designed to exploit the most promising regions identified during the DE phase. The best solution obtained from the DE phase is used as the initial position for the alpha particle, a key element in the FVIM. The FVIM phase begins by reinitializing the population with the alpha particle as a reference. Each iteration involves updating the positions of the population based on the influence of four key particles: Alpha, Beta, Gamma, and Delta. These particles represent different levels of solution quality, with alpha being the best. The position updates are governed by a coefficient that decreases linearly over time, encouraging convergence as the algorithm progresses. The updated positions are evaluated, and the best positions are continuously refined. This phase focuses on intensively searching around the best-known solutions, aiming to improve them further. The process concludes when the maximum number of iterations is reached, and the algorithm returns the best solution found during both stages.

4.6. Exploration and Exploitation Behavior

The effectiveness of the Hybrid FVIMDE Algorithm is largely attributed to its ability to balance exploration and exploitation throughout the optimization process. These two behaviors are critical for ensuring that the algorithm can thoroughly search the solution space and converge to the global optimum.

4.6.1. Exploration Behavior

Exploration refers to the algorithm's ability to investigate diverse regions of the search space. This behavior is crucial for avoiding local optima and ensuring that the algorithm can discover the most promising areas where the global optimum may reside. In the Hybrid FVIMDE Algorithm, the exploration is predominantly handled during the Differential Evolution (DE) phase.

During the DE phase, the population is subjected to operations such as mutation and crossover, which introduce variability among candidate solutions. The mutation operation, defined by Equation (5), generates mutant vectors by combining different individuals from the population. This process creates new potential solutions that may lie far from the current population's centroid, effectively enabling the algorithm to explore distant and unexplored regions of the search space. The crossover operation further contributes to exploration by mixing components of the mutant vector and the target vector, thus maintaining diversity within the population. As the DE phase progresses, the algorithm explores various areas of the search space, laying the groundwork for subsequent exploitation.

4.6.2. Exploitation Behavior

Exploitation, on the other hand, refers to the algorithm's ability to intensively search within promising regions of the search space that have already been identified as potentially containing optimal solutions. This behavior is essential for refining solutions and converging toward the global optimum with high precision. In the Hybrid FVIMDE Algorithm, exploitation is primarily managed during the Four Vector Intelligent Mechanism (FVIM) phase.

The FVIM phase leverages the best solution found during the DE phase as a starting point for further refinement. The position updates in this phase are guided by the influence of the Alpha, Beta, Gamma, and Delta particles, with a particular emphasis on the alpha particle, which represents the best solution. The balance between exploration and exploitation is controlled by the alpha particle's dominant role, ensuring that the search remains focused on the most promising regions. Additionally, the process involves a controlled reduction in the exploration range, governed by a linearly decreasing coefficient

a, as described in Equation (10). As iterations progress, the influence of the alpha particle becomes increasingly dominant, while the random perturbations decrease. This narrows the search to a smaller region of the search space, focusing on refining the best solutions identified so far.

4.6.3. Balancing Exploration and Exploitation

The Hybrid FVIMDE Algorithm is designed to strike an optimal balance between exploration and exploitation. The DE phase illustrates that the algorithm does not get trapped in local optima by maintaining population diversity and searching broadly across the search space. In contrast, the FVIM phase capitalizes on the information gathered during the DE phase to focus on refining the best solutions. By transitioning from global exploration to local exploitation, the algorithm effectively navigates the trade-off between exploring new areas and exploiting known good solutions, thereby enhancing its ability to find the global optimum in complex optimization problems.

4.7. Computational Complexity

The computational complexity of the Hybrid FVIMDE Algorithm can be determined by analyzing the operations performed in each phase of the algorithm. Let us break it down step by step.

First, consider the initialization phase. The population **P** is initialized by generating $N \times D$ random values. This step has a time complexity of $O(N \times D)$, as shown in Equation (11). Additionally, evaluating the fitness of each individual in the population requires $O(N)$ operations, as indicated in Equation (12).

$$O(N \times D) \tag{11}$$

$$O(N) \tag{12}$$

Next, in the Differential Evolution (DE) phase, the algorithm runs for $\text{DE\_iter} = \frac{\text{Max\_iter}}{2}$ iterations. During each iteration, mutation, crossover, and selection are performed for each individual. Each of these operations is linear with respect to the dimensionality D. Consequently, the complexity of these steps is $O(N \times D \times \text{DE\_iter})$, as shown in Equation (13). After generating the trial vector, the fitness of the new vector is evaluated, leading to a complexity of $O(N \times \text{DE\_iter})$, as indicated in Equation (14).

$$O(N \times D \times \text{DE\_iter}) \tag{13}$$

$$O(N \times \text{DE\_iter}) \tag{14}$$

In the FVIM phase, which runs for $\text{FVIM\_iter} = \text{Max\_iter} - \text{DE\_iter}$ iterations, the position of each individual in every dimension is updated. This involves calculating intermediate positions and updating the current position, requiring $4 \times D$ operations per individual. Thus, the complexity of position updates is $O(N \times D \times \text{FVIM\_iter})$, as shown in Equation (15). Additionally, after updating positions, the fitness of each individual is evaluated, with a complexity of $O(N \times \text{FVIM\_iter})$, as indicated in Equation (16).

$$O(N \times D \times \text{FVIM\_iter}) \tag{15}$$

$$O(N \times \text{FVIM\_iter}) \tag{16}$$

The computational complexity of FVIMDE Algorithm is the sum of the complexities of the initialization, DE phase, and FVIM phase. This can be expressed as shown in Equation (17).

$$
\begin{aligned}
&O(N \times D) + O(N) + O(N \times D \times \frac{\text{Max\_iter}}{2}) \\
&+ O(N \times \frac{\text{Max\_iter}}{2}) + O(N \times D \times (\text{Max\_iter} - \frac{\text{Max\_iter}}{2})) \\
&+ O(N \times (\text{Max\_iter} - \frac{\text{Max\_iter}}{2}))
\end{aligned} \tag{17}
$$

Simplifying this expression, we obtain the overall computational complexity of the algorithm, as shown in Equation (18):

$$O(N \times D \times \text{Max\_iter}) \tag{18}$$

This complexity reflects the FVIMDE's dependence on the population size N, the dimensionality of the problem D, and the total number of iterations Max_iter.

5. Implementation and Comparison

5.1. IEEE CEC-2022 Benchmark Test Functions Description

The CEC2022 benchmark suite, as detailed in Table A1 [31], was used to evaluate our evolutionary computation algorithms. The benchmarks include unimodal, multimodal, hybrid, and composition functions, each selected to challenge different aspects of algorithm performance. Unimodal functions test straightforward convergence, while multimodal functions assess FVIMDE's ability to navigate complex landscapes with multiple optima. Hybrid and composition functions combine these challenges, simulating complex real-world problems. All functions were tested within a uniform domain of $[-100, 100]$ across 30 dimensions, ensuring consistency and comparability in our evaluations. An illustration of sample objective space from CEC2022 benchmark functions (F1–F4) is shown in Figure 1.

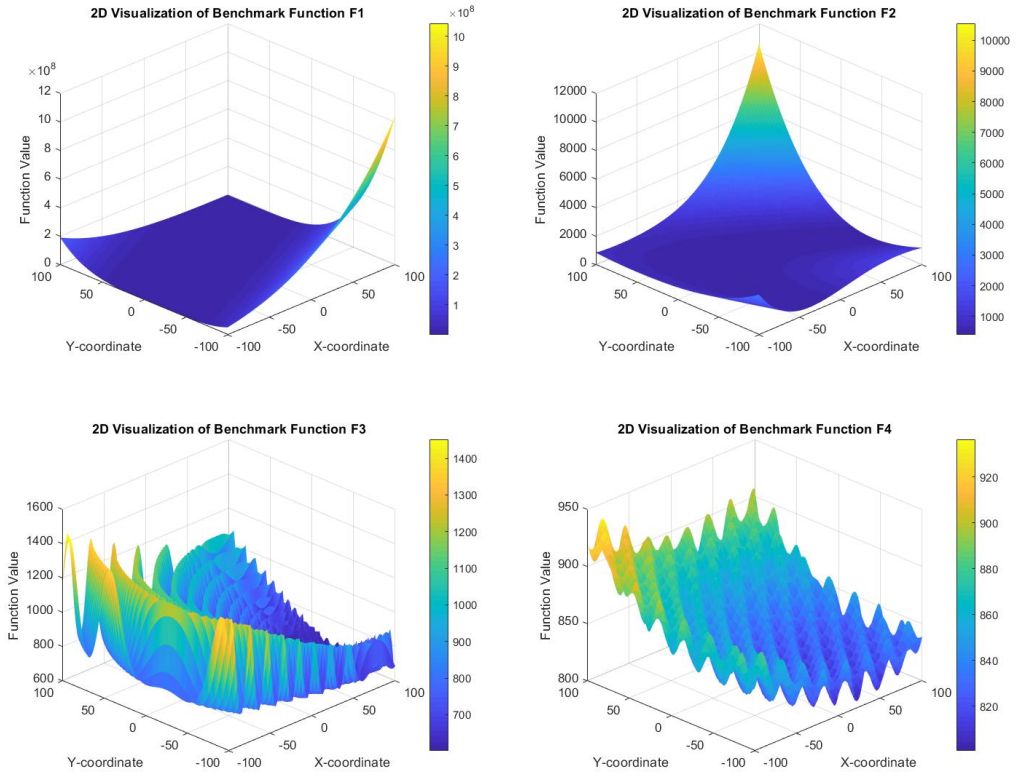

Figure 1. Illustration of sample objective space from CEC2022 Benchmark Functions (F1–F4).

5.2. IEEE CEC-2017 Benchmark Test Functions Description

The first benchmark function used is the CEC2017 competition benchmark function [32], which is a comprehensive suite of benchmark functions that serve to rigorously evaluate the performance of evolutionary computation algorithms, as seen in Table A2 [32]. This suite is meticulously curated to present a variety of optimization landscapes, each designed to assess different aspects of algorithmic behavior in seeking optimal solutions. The suite begins with a series of unimodal benchmark functions. These functions are crucial for testing the exploitation abilities of an algorithm due to their singular global optima. Examples include the shifted and rotated Bent Cigar and Zakharov functions, which challenge FVIMDE with narrow ridge solutions and a combination of quadratic and quartic components, respectively. The shifted and rotated Rosenbrock's function, with its notorious narrow, parabolic-shaped valley, and the shifted and rotated Rastrigin's function, a unimodal adaptation of a typically multimodal function, are designed to test precision in locating the global optimum. The suite also includes the shifted and rotated expanded Scaffer's F6 function, which presents a landscape characterized by sharp valleys and ridges [33].

Following the unimodal functions are the simple multimodal functions. These functions are embedded with numerous local optima, thus evaluating the exploration capabilities of an algorithm and its effectiveness in distinguishing global optima from local ones. The suite features the shifted and rotated Lunacek Bi_Rastrigin function, which combines the Rastrigin function's properties with a dual sphere structure, and the shifted and rotated non-continuous Rastrigin's function, which introduces complexity with its discontinuities. Additionally, the shifted and rotated Levy function and the deceptive shifted and rotated Schwefel function require robust strategies to navigate their complex landscapes [34].

The hybrid functions in the suite, such as the various iterations of Hybrid function 6, represent a synthesis of unimodal and multimodal characteristics, creating a diverse and dynamic optimization environment. These functions test FVIMDE's adaptability and capacity to manage transitions between different function characteristics effectively. The composition functions are the most intricate, constructed by integrating multiple basic functions with varied weights and biases. These functions, ranging from Composition function 1 to 10, replicate the complex, multimodal landscapes akin to real-world optimization scenarios. They require sophisticated exploration and exploitation strategies to navigate the intricately woven global and local optima.

5.3. Description of the 50 Benchmarks

The first set (F1–F25) of 50 benchmark functions, as shown in Table A3, include various functions, such as "Steptint", "Step", "Sphere", "SumSquares", "Quartic", and "Beale", and primarily feature unimodal and separable characteristics. These functions typically involve simple algebraic formulas, which make them useful for evaluating basic aspects of optimization algorithms, such as convergence rate and precision. For example, the "Steptint" and "Step" functions, with their use of the floor operation, challenge an algorithm's ability to handle discontinuities within a defined range. The "Sphere" and "SumSquares" functions are quintessential for testing an algorithm's performance in handling different scales of variables due to their simple, sum-of-squares form. The inclusion of a random component in the "Quartic" function adds a stochastic element to the evaluation, providing insights into how algorithms cope with noise [35].

Furthermore, the second set (F26–F50) also includes benchmarks in Tables A4 and A5 and has complexity with functions like "Booth", "Rastrigin", "Schwefel", and "Michalewicz" models, which introduce multimodal characteristics and often non-separable dimensions. These functions are designed to test more advanced capabilities of optimization algorithms, such as escaping local minima and exploring multiple basins of attraction effectively. The "Rastrigin" function, for instance, is notorious for its large number of local minima, making it an excellent testbed for an algorithm's global search capabilities. The "Michalewicz" function, varying with dimensions, specifically challenges an algorithm's ability to solve prob-

lems that become progressively difficult as dimensions increase. Functions like "Schwefel" and "Six Hump Camel Back" further emphasize handling irregularities and asymmetries in the search space [36].

5.4. Configuration of Experiment Parameters

The computational device used for the optimization evaluation in this study consists of a high-performance server running Windows Server 2016 Standard. The server is equipped with an Intel(R) Xeon(R) Silver 4314 CPU operating at 2.40 GHz, featuring 32 processing cores, and 128 GB of installed RAM.

However, all compared algorithms have been implemented and run in the same environment to provide a fair comparison (run = 30, FES = 1000, agents No. = 30).

The parameter configuration is critical for the consistent evaluation of optimization algorithms using the benchmark functions. However, the CEC 2022 and CEC 2017 parameters utilized in these benchmarks provide a controlled environment to compare the performance of various evolutionary algorithms. These parameters are summarized in Tables 1 and 2.

Table 1. Instance parameter Settings.

Parameter	Value
Dimensionality (D)	10
Search Range	$[-100, 100]^D$
Rotation	Applied to all rotated functions
Shift	Applied to all shifted functions

Table 2. Algorithm parameter.

Parameter	Value
Population Size	30
Maximum Function Evaluations	1000

A population size of 30 and a dimensionality of 10 provide a balance between computational feasibility and complexity. The maximum number of function evaluations is defined as 1000, offering sufficient iterations for algorithms to demonstrate convergence without excessive computational overhead. The search range of $[-100, 100]^D$ illustrates a broad and consistent search space across all dimensions.

The functions often include both rotation and shifting to increase complexity, simulating more realistic optimization challenges. Noise is intentionally omitted to ensure that results focus on algorithm robustness in navigating challenging landscapes, rather than random perturbations. This uniform framework allows a fair comparison of different algorithms, highlighting their strengths and weaknesses across the wide range of benchmark functions.

6. Evaluated Algorithms

A diverse array of optimization algorithms have been chosen (See Table 3) to provide a comprehensive comparison across various metaheuristic approaches. This selection is motivated by the need to evaluate the effectiveness, versatility, and robustness of different optimization techniques across a range of problem domains. The algorithms selected span several decades of development, beginning with foundational methods like the Genetic Algorithm (GA) introduced in the 1960s and the Simulated Annealing (SA) algorithm from the early 1980s, both of which have become standard benchmarks in the field of optimization. These classical algorithms have been widely studied and provide a solid reference point for evaluating newer methods.

Our selection also includes some of the most influential and widely used swarm intelligence algorithms such as Particle Swarm Optimization (PSO), Grey Wolf Optimizer

(GWO), and Whale Optimization Algorithm (WOA), which have demonstrated remarkable performance in solving complex optimization problems. These algorithms have been chosen not only for their proven efficacy but also for their varying strategies in exploring and exploiting the search space, thereby providing insights into how different mechanisms influence the optimization process.

In addition to these, we have included several recent and innovative algorithms such as the Synergistic Swarm Optimization Algorithm (SSOA), Frilled Lizard Optimization (FLO), Four Vector Optimizer (FVIM), and Chinese Pangolin Optimizer (CPO). These algorithms represent the latest advancements in metaheuristic optimization, incorporating novel mechanisms and hybrid strategies that potentially offer improved performance and faster convergence rates. By including these cutting-edge techniques, we aim to assess whether they can outperform or complement the established methods in terms of solution quality, computational efficiency, and adaptability to different problem landscapes.

Furthermore, we have integrated a variety of nature-inspired algorithms like the Success History Intelligent Optimizer (SHIO), Remora Optimization Algorithm (ROA), and Sooty Tern Optimization Algorithm (STOA), each inspired by different biological and ecological phenomena. These algorithms introduce unique heuristics and search patterns that contribute to the diversity of approaches in our comparison. The Zebra Optimization Algorithm (ZOA), Dingo Optimization Algorithm (DOA), and Aquila Optimizer (AO) add further variety by bringing in concepts from animal behavior and ecological systems, which are particularly interesting for their balance between exploration and exploitation.

By covering a wide range of algorithmic strategies, from evolutionary algorithms, swarm intelligence, and hybrid methods to algorithms based on ecological and animal behavior, we ensure that our comparative analysis is not only thorough but also reflective of the current state-of-the-art in optimization research. This diverse selection allows us to examine the performance of each algorithm under various scenarios, thereby identifying the most suitable techniques for different types of optimization problems. Additionally, by comparing these algorithms against both classical and contemporary benchmarks, we aim to provide valuable insights into their relative strengths and weaknesses, contributing to the ongoing development and refinement of optimization algorithms.

Table 3. Optimization Algorithms.

Acronym	Algorithm Name	Year
SSOA	Synergistic Swarm Optimization Algorithm [37]	2024
FLO	Frilled Lizard Optimization [38]	2024
CPO	Chinese Pangolin Optimizer [39]	2024
FVIM	Four Vector Optimizer [40]	2024
SHIO	Success History Intelligent Optimizer [41]	2022
ZOA	Zebra Optimization Algorithm [42]	2022
DOA	Dingo Optimization Algorithm [43]	2021
ROA	Remora Optimization Algorithm [44]	2021
AO	Aquila Optimizer [45]	2021
CHIMP	Chimp Optimization Algorithm [46]	2020
STOA	Sooty Tern Optimization Algorithm [47]	2019
SOA	Seagull Optimization Algorithm [48]	2019
SCSO	Sand Cat Optimization Algorithm [49]	2023
MVO	Multi-Verse Optimizer [50]	2016
WOA	Whale Optimization Algorithm [51]	2016
SCA	Sine Cosine Algorithm [52]	2016
MFO	Moth-Flame Optimization Algorithm [53]	2015
GWO	Grey Wolf Optimizer [54]	2014
PSO	Particle Swarm Optimization [55]	1995
SA	Simulated Annealing Algorithm [56]	1983
GA	Genetic Algorithm [57]	1960

6.1. Quantitative Evaluation

To robustly assess the performance of various optimization algorithms, we utilized several statistical measures: mean, standard deviation, standard error of the mean (SEM), and the Wilcoxon sum-rank test. The mean indicates the average performance over multiple trials, while the standard deviation measures variability, reflecting the algorithm's reliability. The rank is used to compare the relative performance of algorithms, with lower-ranked algorithms showing superior performance. Specifically, the rank for an algorithm is calculated based on the ordering of mean values across all compared algorithms, as described by the following equation:

$$\text{Rank}(x_i) = \text{RANK}(x_i, \{x_1, x_2, \ldots, x_n\}, order)$$

where x_i is the value to be ranked, $\{x_1, x_2, \ldots, x_n\}$ is the set of values to rank against, and 1 indicates ascending order.

Additionally, the Wilcoxon sum-rank test was used to evaluate the statistical significance of performance differences between two independent samples.

6.2. Results on Benchmark of IEEE Congress on Evolutionary Computation 2022 (CEC2022)

The FVIMDE algorithm showcases exceptional performance across the CEC2022 benchmark functions, as shown in Tables 4 and 5, significantly outperforming the compared optimizers. For instance, in functions such as F1 and F2, FVIMDE achieves the lowest mean values, highlighting its superior optimization ability. In F1, FVIMDE records a mean value of 3.01E+02, which is notably lower than that of FVIM (4.64E+03), STOA (1.88E+03), and other competitive algorithms like Chimp (2.42E+03) and CPO (1.58E+03). Similarly, in F2, FVIMDE leads with a mean value of 4.06E+02, surpassing other algorithms such as FLO (1.27E+03) and SOA(9.44E+02).

When compared to other optimizers, FVIMDE consistently outperforms both classical algorithms like GA and SA, as well as modern metaheuristic optimizers like WOA and PSO. For example, in F7, FVIMDE achieves a mean value of 2.02E+03, outperforming SA (2.03E+03) and WOA (2.06E+03), which are commonly employed for solving complex optimization problems. Additionally, in F6, FVIMDE delivers a mean value of 1.80E+03, significantly lower than that of GA (1.53E+07) and SA (4.49E+03), further demonstrating its capacity to provide more accurate and consistent results.

The robustness of FVIMDE is also evident in its lower standard deviations and standard errors across these functions, indicating not only its ability to find optimal solutions but also to do so reliably and consistently. This is a critical advantage in practical applications where stability and predictability are as crucial as achieving the best solution.

As can be seen in Figures A1 and A2, the boxplot results of the FVIMDE algorithm compared to other optimizers across various functions in the CEC2022 benchmarks demonstrate that FVIMDE consistently exhibits lower error measures and less variability. In most F1–F12 functions, FVIMDE consistently ranks among the algorithms with the smallest error measures, indicating high accuracy and precision. In contrast, other optimizers, such as FLO and SSOA, show significantly higher error measures and greater variability, as evidenced by larger interquartile ranges and more frequent outliers. This suggests that FVIMDE offers robust performance across different test functions, maintaining stability where other algorithms struggle with either high error rates or inconsistency in their results.

As seen in Tables A6 and A7, the Wilcoxon rank-sum test results provide a comprehensive analysis of how FVIMDE compares with various other optimizers across the CEC2022 benchmark functions (F1–F12). The test results are categorized as significant (S), non-significant (N), or equal (E), indicating whether FVIMDE's performance is significantly different, not significantly different, or statistically equal to that of the other algorithms.

For most functions, FVIMDE demonstrates statistically significant superiority over other algorithms, with the majority of the results marked as S (significant). For instance, in functions like F1–F9, FVIMDE consistently achieves significant results against

all competitors. This is evidenced by extremely low p-values, such as 3.02E-11, indicating that the observed differences in performance are highly unlikely to be due to chance. These consistent S results across multiple functions underscore FVIMDE's strong optimization capabilities.

However, there are a few instances where FVIMDE's performance is either equal or not significantly different from that of other algorithms. For example, in F4, while FVIMDE outperforms most optimizers, its comparison with the AO algorithm results in a non-significant (N) outcome, suggesting that both algorithms perform similarly for this particular function. Similarly, in F10, although FVIMDE shows a strong performance, the comparison with some optimizers results in a mix of S and N outcomes, reflecting closer competition.

The few E (equal) results, such as in F4 and F12, when compared to specific algorithms, indicate scenarios where FVIMDE and the competing algorithms perform almost identically. These E results highlight that while FVIMDE is generally superior, there are certain cases where it matches the performance of other algorithms rather than exceeding it.

Table 4. Comparison results over CEC2022 benchmarks (F1–F12), run = 30, FES = 1000, agents No. = 30.

Function		FVIMDE	FVIM	FLO	STOA	SOA	SPBO	AO	SSOA	Chimp	CPO	ROA
F1	Mean	3.01E+02	4.64E+03	8.72E+03	1.88E+03	2.80E+03	3.23E+04	1.59E+03	1.03E+04	2.42E+03	1.58E+03	8.32E+03
	Std	1.29E+00	3.02E+03	1.32E+03	1.62E+03	2.91E+03	9.71E+03	1.13E+03	5.23E+03	9.72E+02	2.43E+03	1.50E+03
	Rank	1	14	16	11	13	21	8	17	12	7	15
F2	Mean	4.06E+02	4.39E+02	1.27E+03	4.17E+02	4.80E+02	9.44E+02	4.08E+02	1.25E+03	5.22E+02	4.06E+02	5.14E+02
	Std	2.62E+00	3.01E+01	5.53E+02	2.05E+01	1.31E+02	1.52E+02	1.03E+01	3.09E+02	7.96E+01	3.75E+00	2.85E+01
	Rank	1	13	22	6	15	20	3	21	17	2	16
F3	Mean	6.00E+02	6.02E+02	6.49E+02	6.12E+02	6.09E+02	6.74E+02	6.13E+02	6.61E+02	6.23E+02	6.46E+02	6.38E+02
	Std	6.22E-02	2.19E+00	1.43E+01	7.65E+00	5.26E+00	6.33E+00	6.03E+00	4.62E+00	5.26E+00	1.11E+01	1.36E+01
	Rank	1	3	19	8	6	22	9	21	14	18	16
F4	Mean	8.14E+02	8.24E+02	8.43E+02	8.23E+02	8.25E+02	8.98E+02	8.26E+02	8.65E+02	8.29E+02	8.32E+02	8.41E+02
	Std	1.04E+01	7.88E+00	1.84E+01	1.01E+01	2.68E+00	9.08E+00	6.74E+00	9.95E+00	7.99E+00	5.43E-01	1.15E+01
	Rank	1	7	18	5	8	22	9	19	11	14	16
F5	Mean	9.00E+02	9.06E+02	1.33E+03	9.54E+02	9.94E+02	3.75E+03	9.57E+02	1.70E+03	1.20E+03	1.46E+03	1.27E+03
	Std	1.16E-01	1.09E+01	1.77E+02	3.11E+01	9.31E+01	7.05E+02	4.23E+01	1.80E+02	1.37E+02	2.47E+02	1.82E+02
	Rank	1	2	15	5	9	22	6	20	13	17	14
F6	Mean	1.80E+03	5.00E+03	5.44E+07	1.69E+04	2.01E+04	2.41E+08	7.33E+03	1.84E+08	1.21E+06	4.86E+03	5.36E+04
	Std	1.58E+00	1.91E+03	3.34E+07	6.33E+03	9.40E+03	1.03E+08	2.21E+03	1.89E+08	1.48E+06	2.86E+03	6.98E+04
	Rank	1	10	20	13	14	22	12	21	16	9	15
F7	Mean	2.02E+03	2.03E+03	2.09E+03	2.04E+03	2.03E+03	2.17E+03	2.03E+03	2.15E+03	2.06E+03	2.07E+03	2.07E+03
	Std	5.42E+00	1.10E+01	3.07E+01	6.81E+00	8.54E+00	3.46E+01	6.24E+00	1.67E+01	8.08E+00	1.79E+01	1.24E+01
	Rank	1	6	19	7	5	22	4	21	13	16	17
F8	Mean	2.21E+03	2.23E+03	2.26E+03	2.23E+03	2.23E+03	2.66E+03	2.23E+03	2.38E+03	2.28E+03	2.28E+03	2.23E+03
	Std	5.50E+00	1.33E+00	3.81E+01	3.23E+00	2.50E+00	7.91E+02	1.14E+00	1.01E+02	6.54E+01	5.91E+01	2.85E+00
	Rank	1	6	17	10	9	22	5	21	18	19	15
F9	Mean	2.53E+03	2.60E+03	2.76E+03	2.57E+03	2.56E+03	2.73E+03	2.57E+03	2.77E+03	2.58E+03	2.58E+03	2.67E+03
	Std	5.30E-09	3.24E+01	1.20E+02	4.49E+01	4.00E+01	6.54E+01	3.06E+01	2.86E+01	2.16E+01	5.92E+01	3.15E+01
	Rank	1	15	21	11	6	20	8	22	13	12	18
F10	Mean	2.51E+03	2.60E+03	2.81E+03	2.50E+03	2.50E+03	2.59E+03	2.55E+03	2.59E+03	2.70E+03	2.64E+03	2.57E+03
	Std	2.92E+01	5.39E+01	1.44E+02	1.83E-01	6.36E-02	5.49E+01	6.11E+01	5.55E+01	4.38E+02	7.71E+01	8.45E+01
	Rank	6	17	21	1	2	16	9	15	20	19	13
F11	Mean	2.60E+03	2.93E+03	3.69E+03	2.72E+03	2.78E+03	3.60E+03	2.66E+03	3.73E+03	3.29E+03	2.78E+03	2.87E+03
	Std	1.67E-01	2.08E+02	4.85E+02	5.57E+01	1.43E+01	3.03E+02	7.94E+01	4.08E+02	7.33E+01	1.81E+02	8.20E+01
	Rank	1	17	21	6	9	20	4	22	19	10	16
F12	Mean	2.86E+03	2.88E+03	3.05E+03	2.86E+03	2.86E+03	2.89E+03	2.87E+03	3.10E+03	2.87E+03	2.95E+03	2.95E+03
	Std	1.59E+00	1.99E+01	6.06E+01	5.46E-01	3.50E-01	6.08E+00	5.10E+00	1.63E+02	1.36E-01	1.04E+02	3.46E+01
	Rank	1	13	21	3	4	15	8	22	6	19	18

Table 5. Continue comparison results over CEC2022 benchmarks (F1–F12), run = 30, FES = 1000, agents No. = 30.

Function		WOA	PSO	MFO	SHIO	ZOA	MTDE	SCA	DOA	SCSO	GA	SA
F1	Mean	1.39E+04	7.13E+02	1.79E+03	1.20E+03	4.84E+02	1.38E+04	1.72E+03	1.54E+03	5.11E+02	5.16E+04	1.07E+04
	Std	7.02E+03	5.97E+02	2.08E+03	1.07E+03	3.34E+01	3.65E+03	3.92E+02	1.31E+03	1.95E+02	1.37E+04	2.34E+03
	Rank	20	4	10	5	2	19	9	6	3	22	18
F2	Mean	4.20E+02	4.12E+02	4.26E+02	4.10E+02	4.36E+02	5.38E+02	4.62E+02	4.36E+02	4.36E+02	7.77E+02	4.20E+02
	Std	3.00E+01	1.43E+01	3.31E+01	1.12E+01	2.67E+01	2.57E+01	1.44E+01	3.96E+01	3.89E+01	2.98E+02	5.01E+00
	Rank	8	5	9	4	11	18	14	10	12	19	7
F3	Mean	6.39E+02	6.00E+02	6.03E+02	6.07E+02	6.13E+02	6.33E+02	6.16E+02	6.18E+02	6.14E+02	6.59E+02	6.11E+02
	Std	9.65E+00	7.64E-02	5.46E+00	9.03E+00	5.24E+00	4.88E+00	1.69E+00	1.19E+01	9.72E+00	1.25E+01	3.00E+00
	Rank	17	2	4	5	10	15	12	13	11	20	7
F4	Mean	8.29E+02	8.21E+02	8.28E+02	8.22E+02	8.23E+02	8.71E+02	8.36E+02	8.22E+02	8.31E+02	8.67E+02	8.42E+02
	Std	1.61E+01	2.19E+00	4.62E+00	4.06E+00	4.84E+00	7.80E+00	6.10E+00	1.11E+01	8.66E+00	2.02E+01	8.79E+00
	Rank	12	2	10	4	6	21	15	3	13	20	17
F5	Mean	1.79E+03	9.07E+02	9.35E+02	9.76E+02	1.01E+03	1.50E+03	9.69E+02	1.11E+03	1.06E+03	1.36E+03	1.47E+03
	Std	6.44E+02	5.68E+00	4.03E+01	1.44E+02	6.07E+01	1.92E+02	1.65E+01	1.31E+02	2.09E+02	1.02E+02	1.24E+02
	Rank	21	3	4	8	10	19	7	12	11	16	18
F6	Mean	3.19E+03	3.89E+03	5.21E+03	2.81E+03	3.06E+03	9.43E+06	1.58E+06	2.00E+03	4.14E+03	1.53E+07	4.49E+03
	Std	1.43E+03	2.41E+03	2.92E+03	9.00E+02	1.35E+03	8.21E+06	1.87E+06	1.61E+02	1.74E+03	1.88E+07	2.15E+03
	Rank	5	6	11	3	4	18	17	2	7	19	8
F7	Mean	2.06E+03	2.02E+03	2.04E+03	2.06E+03	2.04E+03	2.08E+03	2.05E+03	2.04E+03	2.06E+03	2.12E+03	2.03E+03
	Std	1.63E+01	3.94E-01	3.42E+01	3.75E+01	2.03E+01	6.82E+00	9.86E+00	2.31E+01	1.63E+01	2.19E+01	2.24E+00
	Rank	15	2	8	14	9	18	11	10	12	20	3
F8	Mean	2.23E+03	2.23E+03	2.23E+03	2.23E+03	2.22E+03	2.24E+03	2.23E+03	2.23E+03	2.22E+03	2.32E+03	2.23E+03
	Std	5.45E+00	2.32E+00	4.13E+00	7.04E+00	1.86E+00	1.12E+01	3.54E+00	6.79E+00	3.55E+00	6.58E+01	2.79E+00
	Rank	14	8	7	11	2	16	13	12	3	20	4
F9	Mean	2.54E+03	2.55E+03	2.53E+03	2.58E+03	2.62E+03	2.63E+03	2.56E+03	2.57E+03	2.57E+03	2.73E+03	2.53E+03
	Std	1.86E+01	2.11E+01	1.41E+00	3.07E+01	4.78E+01	4.12E+01	9.42E+00	5.07E+01	5.24E+01	7.33E+01	1.87E+00
	Rank	4	5	2	14	16	17	7	10	9	19	3
F10	Mean	2.53E+03	2.57E+03	2.50E+03	2.61E+03	2.55E+03	2.51E+03	2.50E+03	2.55E+03	2.58E+03	2.86E+03	2.50E+03
	Std	6.65E+01	5.98E+01	1.64E+00	7.69E+01	6.89E+01	1.05E+01	2.88E-01	7.18E+01	6.81E+01	6.49E+02	2.44E-01
	Rank	8	12	4	18	10	7	5	11	14	22	3
F11	Mean	2.87E+03	2.65E+03	2.66E+03	2.81E+03	2.71E+03	2.86E+03	2.78E+03	2.74E+03	2.84E+03	3.26E+03	2.78E+03
	Std	2.08E+02	7.09E+01	8.71E+01	1.62E+02	9.68E+01	7.05E+01	6.92E+00	5.04E+01	2.06E+02	4.94E+02	7.56E+00
	Rank	15	2	3	12	5	14	8	7	13	18	11
F12	Mean	2.88E+03	2.86E+03	2.86E+03	2.88E+03	2.92E+03	2.89E+03	2.87E+03	2.91E+03	2.87E+03	3.04E+03	2.87E+03
	Std	2.66E+01	1.82E+00	1.08E+00	1.87E+01	2.10E+01	2.84E+00	1.68E+00	6.40E+01	5.77E+00	8.20E+01	7.08E-01
	Rank	12	5	2	11	17	14	9	16	10	20	7

6.3. Results over 2017 IEEE Congress on Evolutionary Computation (CEC2017)

The FVIMDE algorithm continues to demonstrate its robustness and efficiency across the CEC2017 benchmark functions, as shown in Tables 6 and 7, outperforming many other algorithms in various instances. For example, in F1, FVIMDE achieves a mean value of 3.21E+03, which is significantly better than those obtained by algorithms like FLO (1.14E+10) and ROA (4.06E+09). This highlights FVIMDE's ability to find more optimal solutions where other optimizers struggle. Similarly, in F2, FVIMDE's mean of 1.51E+03 outperforms FVIM (3.00E+07) and STOA (1.98E+07), showcasing its efficiency in dealing with complex optimization landscapes.

In addition to these successes, FVIMDE outperforms several modern metaheuristic optimizers. For instance, in F3, FVIMDE achieves a mean value of 3.01E+02, outclassing MFO (1.60E+04) and SHIO (7.13E+03). Moreover, in F5, FVIMDE leads with a mean value of 5.17E+02, demonstrating its superiority over FVIM (5.25E+02) and STOA (5.24E+02). This trend of outperformance continues in F6, where FVIMDE ranks first with a mean value of 6.00E+02, outperforming even well-regarded algorithms like PSO (6.15E+02) and SA (6.12E+02).

Table 6. Comparison results over CEC2017 benchmarks (F1–F30), run = 30, FES = 1000, agents No. = 30.

Function		FVIMDE	FVIM	FLO	STOA	SOA	SPBO	AO	SSOA	Chimp	CPO	ROA
F1	Mean	3.21E+03	5.68E+06	1.14E+10	1.99E+08	3.47E+08	8.71E+09	8.43E+05	1.17E+10	1.52E+09	2.21E+03	4.06E+09
	Std	1.66E+03	1.03E+07	3.75E+09	2.05E+08	1.81E+08	3.09E+09	4.58E+05	2.56E+09	1.50E+09	2.21E+03	1.97E+09
	SEM	6.78E+02	4.19E+06	1.53E+09	8.38E+07	7.41E+07	1.26E+09	1.87E+05	1.04E+09	6.14E+08	9.03E+02	8.03E+08
	Rank	3	6	20	11	12	19	4	21	15	1	17
F2	Mean	1.51E+03	3.00E+07	4.12E+11	1.98E+07	2.08E+07	3.76E+10	6.11E+06	6.28E+12	6.65E+08	7.42E+03	9.54E+10
	Std	3.21E+03	7.31E+07	5.31E+11	2.14E+07	2.28E+07	3.94E+10	8.48E+06	1.03E+13	1.03E+09	1.05E+04	1.26E+11
	SEM	1.31E+03	2.98E+07	2.17E+11	8.75E+06	9.30E+06	1.61E+10	3.46E+06	4.22E+12	4.21E+08	4.29E+03	5.15E+10
	Rank	2	11	19	8	10	17	6	20	16	3	18
F3	Mean	3.01E+02	5.93E+03	1.40E+04	2.79E+03	1.72E+03	4.09E+04	9.28E+02	1.49E+04	2.95E+03	3.56E+02	1.13E+04
	Std	1.08E+00	5.23E+03	2.79E+03	1.47E+03	1.66E+03	7.70E+03	4.53E+02	3.14E+03	1.12E+03	6.92E+01	4.29E+03
	SEM	4.40E-01	2.14E+03	1.14E+03	6.00E+02	6.78E+02	3.14E+03	1.85E+02	1.28E+03	4.58E+02	2.83E+01	1.75E+03
	Rank	1	13	17	9	7	20	4	18	10	3	15
F4	Mean	4.01E+02	4.15E+02	1.24E+03	4.50E+02	4.72E+02	1.32E+03	4.19E+02	1.23E+03	5.81E+02	4.06E+02	7.31E+02
	Std	4.07E-01	1.88E+01	2.73E+02	2.94E+01	4.62E+01	3.14E+02	2.20E+01	4.56E+02	1.42E+02	1.14E+00	1.40E+02
	SEM	1.66E-01	7.66E+00	1.11E+02	1.20E+01	1.88E+01	1.28E+02	8.98E+00	1.86E+02	5.81E+01	4.66E-01	5.72E+01
	Rank	1	4	20	11	13	21	6	19	16	3	17
F5	Mean	5.17E+02	5.25E+02	5.92E+02	5.24E+02	5.25E+02	6.09E+02	5.25E+02	6.05E+02	5.59E+02	5.71E+02	5.77E+02
	Std	8.72E+00	5.05E+00	1.86E+01	4.43E+00	9.76E+00	1.04E+01	5.40E+00	1.67E+01	1.32E+01	1.89E+01	1.36E+01
	SEM	3.56E+00	2.06E+00	7.59E+00	1.81E+00	3.98E+00	4.25E+00	2.20E+00	6.80E+00	5.38E+00	7.70E+00	5.57E+00
	Rank	1	4	18	2	5	21	3	20	15	16	17
F6	Mean	6.00E+02	6.02E+02	6.55E+02	6.13E+02	6.14E+02	6.71E+02	6.15E+02	6.60E+02	6.24E+02	6.45E+02	6.44E+02
	Std	2.45E-02	1.33E+00	1.08E+01	4.47E+00	6.79E+00	1.03E+01	5.18E+00	4.61E+00	6.74E+00	1.34E+01	1.30E+01
	SEM	9.99E-03	5.45E-01	4.40E+00	1.82E+00	2.77E+00	4.22E+00	2.11E+00	1.88E+00	2.75E+00	5.47E+00	5.32E+00
	Rank	1	2	18	6	7	20	8	19	13	17	16
F7	Mean	7.23E+02	7.34E+02	8.16E+02	7.60E+02	7.57E+02	1.17E+03	7.49E+02	8.23E+02	8.01E+02	7.89E+02	8.06E+02
	Std	1.21E+01	1.44E+01	1.41E+01	7.93E+00	2.13E+01	4.57E+01	1.66E+01	1.97E+01	2.00E+01	3.72E+01	3.07E+01
	SEM	4.95E+00	5.86E+00	5.75E+00	3.24E+00	8.71E+00	1.86E+01	6.79E+00	8.03E+00	8.17E+00	1.52E+01	1.25E+01
	Rank	1	2	17	10	8	21	6	19	15	13	16
F8	Mean	8.13E+02	8.11E+02	8.66E+02	8.28E+02	8.27E+02	9.27E+02	8.25E+02	8.72E+02	8.39E+02	8.35E+02	8.49E+02
	Std	6.82E+00	3.20E+00	1.31E+01	1.25E+01	1.01E+01	1.19E+01	9.62E-01	7.60E+00	9.41E+00	3.98E-01	9.34E+00
	SEM	2.78E+00	1.31E+00	5.36E+00	5.09E+00	4.11E+00	4.87E+00	3.93E-01	3.10E+00	3.84E+00	1.63E-01	3.81E+00
	Rank	2	1	18	8	6	21	5	19	14	11	17
F9	Mean	9.00E+02	9.64E+02	1.55E+03	9.98E+02	9.96E+02	4.17E+03	1.03E+03	1.87E+03	1.62E+03	1.83E+03	1.71E+03
	Std	7.02E-02	1.01E+02	1.81E+02	8.59E+01	4.52E+01	5.29E+02	1.18E+02	3.84E+02	2.91E+02	2.13E+02	3.35E+02
	SEM	2.87E-02	4.12E+01	7.37E+01	3.51E+01	1.85E+01	2.16E+02	4.82E+01	1.57E+02	1.19E+02	8.69E+01	1.37E+02
	Rank	1	2	14	5	4	21	9	19	15	18	16
F10	Mean	1.45E+03	1.65E+03	2.79E+03	1.88E+03	2.05E+03	2.65E+03	1.97E+03	3.25E+03	2.94E+03	2.73E+03	2.40E+03
	Std	6.81E+01	3.57E+02	1.40E+02	3.27E+02	2.66E+02	8.75E+01	2.48E+02	2.66E+02	9.78E+01	6.54E+02	4.72E+02
	SEM	2.78E+01	1.46E+02	5.72E+01	1.33E+02	1.09E+02	3.57E+01	1.01E+02	1.09E+02	3.99E+01	2.67E+02	1.93E+02
	Rank	1	3	18	6	10	15	8	21	19	17	13
F11	Mean	1.11E+03	1.90E+03	4.42E+03	1.26E+03	1.25E+03	4.21E+03	1.21E+03	6.78E+03	1.29E+03	1.24E+03	4.29E+03
	Std	5.02E+00	1.84E+03	2.70E+03	8.33E+01	9.09E+01	8.75E+02	5.16E+01	3.89E+03	1.15E+02	9.75E+01	4.07E+03
	SEM	2.05E+00	7.49E+02	1.10E+03	3.40E+01	3.71E+01	3.57E+02	2.10E+01	1.59E+03	4.70E+01	3.98E+01	1.66E+03
	Rank	1	16	19	12	11	17	8	21	13	10	18
F12	Mean	1.65E+03	7.80E+05	5.00E+08	8.21E+05	1.99E+06	8.12E+08	3.07E+06	4.92E+08	6.80E+06	4.01E+06	3.72E+07
	Std	1.97E+02	6.24E+05	3.76E+08	6.17E+05	3.24E+06	2.09E+08	2.63E+06	5.76E+08	3.19E+06	5.35E+06	3.35E+07
	SEM	8.04E+01	2.55E+05	1.54E+08	2.52E+05	1.32E+06	8.55E+07	1.08E+06	2.35E+08	1.30E+06	2.18E+06	1.37E+07
	Rank	1	6	20	7	9	21	10	19	13	11	17
F13	Mean	1.32E+03	1.32E+04	1.22E+07	1.78E+04	2.14E+04	2.39E+08	8.04E+03	1.40E+07	2.90E+04	1.37E+04	7.98E+04
	Std	3.42E+00	8.11E+03	1.86E+07	1.08E+04	1.38E+04	8.00E+07	5.65E+03	2.25E+07	2.30E+04	9.01E+03	7.65E+04
	SEM	1.40E+00	3.31E+03	7.58E+06	4.41E+03	5.62E+03	3.27E+07	2.31E+03	9.19E+06	9.38E+03	3.68E+03	3.12E+04
	Rank	1	6	18	11	13	21	4	19	15	8	17
F14	Mean	1.42E+03	4.16E+03	5.74E+03	3.02E+03	2.38E+03	1.28E+06	2.39E+03	2.62E+04	5.80E+03	5.81E+03	2.17E+03
	Std	1.10E+01	2.09E+03	7.75E+03	2.19E+03	1.62E+03	1.81E+06	7.05E+02	5.02E+04	2.46E+02	3.06E+03	1.12E+03
	SEM	4.48E+00	8.53E+02	3.16E+03	8.92E+02	6.61E+02	7.40E+05	2.88E+02	2.05E+04	1.00E+02	1.25E+03	4.56E+02
	Rank	1	13	16	12	8	20	9	19	17	18	7
F15	Mean	1.50E+03	6.31E+03	1.21E+04	4.45E+03	4.65E+03	5.82E+06	4.42E+03	2.12E+04	1.14E+04	4.23E+04	7.99E+03
	Std	2.49E+00	2.74E+03	3.86E+03	1.70E+03	4.71E+03	1.15E+07	2.41E+03	3.90E+03	8.64E+03	4.37E+04	4.42E+03
	SEM	1.02E+00	1.12E+03	1.58E+03	6.95E+02	1.92E+03	4.71E+06	9.83E+02	1.59E+03	3.53E+03	1.78E+04	1.80E+03
	Rank	1	12	16	9	10	21	8	18	15	19	13

The consistent performance of FVIMDE across these benchmarks, including more challenging ones like F10 and F11, further cements its position as a top contender in the field of optimization. In F10, FVIMDE achieves the best mean value of 1.45E+03, surpassing FVIM (1.65E+03) and even sophisticated algorithms like MTDE (1.01E+04). Similarly, in F11, FVIMDE records a mean value of 1.11E+03, significantly outperforming GA (6.05E+03) and other algorithms like DOA (1.61E+03).

Table 7. Comparison results over CEC2017 benchmarks (F1–F30), run = 30, FES = 1000, agents No. = 30.

Function		WOA	PSO	MFO	SHIO	ZOA	MTDE	SCA	DOA	SCSO	GA	SA
F1	Mean	3.74E+06	2.54E+03	2.34E+07	7.84E+07	5.27E+08	1.80E+11	7.23E+08	2.31E+09	1.52E+07	4.94E+09	4.98E+07
	Std	1.89E+06	2.41E+03	3.62E+07	1.91E+08	7.65E+08	8.91E+09	2.26E+08	2.23E+09	2.17E+07	2.93E+09	2.29E+07
	Rank	5	2	8	10	13	22	14	16	7	18	9
F2	Mean	3.58E+06	2.00E+02	5.17E+07	3.39E+08	2.03E+07	3.47E+54	5.25E+07	6.87E+07	1.32E+07	9.90E+15	6.74E+05
	Std	8.62E+06	5.22E-05	1.23E+08	7.89E+08	2.20E+07	3.77E+54	4.37E+07	1.63E+08	2.05E+07	2.42E+16	4.18E+05
	Rank	5	1	12	15	9	22	13	14	7	21	4
F3	Mean	4.50E+03	3.01E+02	1.60E+04	7.13E+03	1.53E+03	1.68E+14	2.59E+03	3.92E+03	1.59E+03	4.88E+04	1.30E+04
	Std	5.00E+03	3.60E-14	9.91E+03	5.37E+03	1.72E+03	7.39E+13	1.11E+03	1.99E+03	1.62E+03	2.16E+04	1.59E+03
	Rank	12	2	19	14	5	22	8	11	6	21	16
F4	Mean	4.72E+02	4.02E+02	4.24E+02	4.39E+02	4.22E+02	3.18E+04	4.67E+02	5.15E+02	4.44E+02	1.01E+03	4.16E+02
	Std	8.45E+01	1.19E+00	3.76E+01	3.74E+01	2.83E+01	4.23E+03	4.51E+01	7.56E+01	4.83E+01	2.18E+02	5.51E+00
	Rank	14	2	8	9	7	22	12	15	10	18	5
F5	Mean	5.56E+02	5.42E+02	5.29E+02	5.32E+02	5.43E+02	1.26E+03	5.53E+02	5.54E+02	5.32E+02	6.01E+02	5.26E+02
	Std	2.11E+01	1.71E+01	7.81E+00	9.25E+00	2.58E+01	2.70E+01	8.07E+00	1.87E+01	1.45E+01	2.55E+01	7.20E+00
	Rank	14	10	7	8	11	22	12	13	9	19	6
F6	Mean	6.38E+02	6.15E+02	6.03E+02	6.05E+02	6.19E+02	7.24E+02	6.16E+02	6.28E+02	6.20E+02	6.73E+02	6.12E+02
	Std	1.27E+01	1.17E+01	3.05E+00	6.75E+00	8.09E+00	5.06E+00	2.27E+00	1.33E+01	9.41E+00	1.13E+01	2.33E+00
	Rank	15	9	3	4	11	22	10	14	12	21	5
F7	Mean	8.17E+02	7.36E+02	7.42E+02	7.49E+02	7.53E+02	3.65E+03	7.74E+02	8.00E+02	7.73E+02	8.97E+02	7.57E+02
	Std	3.74E+01	7.14E+00	1.34E+01	1.64E+01	1.51E+01	2.34E+02	5.34E+00	5.89E+01	3.11E+01	8.85E+01	1.39E+01
	Rank	18	3	4	5	7	22	12	14	11	20	9
F8	Mean	8.39E+02	8.23E+02	8.36E+02	8.28E+02	8.15E+02	1.46E+03	8.46E+02	8.43E+02	8.29E+02	8.77E+02	8.31E+02
	Std	1.88E+01	4.67E+00	1.59E+01	1.50E+01	7.91E+00	3.96E+01	8.15E+00	1.08E+01	6.67E+00	1.16E+01	6.38E+00
	Rank	13	4	12	7	3	22	16	15	9	20	10
F9	Mean	1.73E+03	9.78E+02	1.01E+03	1.15E+03	1.09E+03	3.33E+04	1.02E+03	1.39E+03	1.00E+03	2.61E+03	1.19E+03
	Std	7.62E+02	1.49E+02	1.79E+02	2.25E+02	1.03E+02	4.14E+03	3.14E+01	3.41E+02	1.33E+02	7.79E+02	1.47E+02
	Rank	17	3	7	11	10	22	8	13	6	20	12
F10	Mean	2.23E+03	1.75E+03	1.91E+03	2.04E+03	1.75E+03	1.01E+04	2.43E+03	2.66E+03	2.17E+03	2.95E+03	1.62E+03
	Std	2.51E+02	2.71E+02	1.53E+02	3.02E+02	2.07E+02	2.51E+02	2.15E+02	5.74E+02	2.02E+02	2.35E+02	1.71E+02
	Rank	12	4	7	9	5	22	14	16	11	20	2
F11	Mean	1.30E+03	1.13E+03	1.14E+03	1.17E+03	1.14E+03	1.88E+09	1.22E+03	1.61E+03	1.15E+03	6.05E+03	1.17E+03
	Std	7.05E+01	1.23E+01	3.55E+01	3.71E+01	2.07E+01	1.01E+09	3.19E+01	6.64E+02	2.55E+01	5.31E+03	2.96E+01
	Rank	14	2	4	6	3	22	9	15	5	20	7
F12	Mean	9.96E+06	1.75E+04	9.01E+06	6.50E+05	9.18E+05	2.57E+10	1.40E+07	4.50E+06	6.14E+05	1.87E+08	5.50E+05
	Std	8.01E+06	1.62E+04	8.91E+06	1.07E+06	6.61E+05	2.91E+09	7.47E+06	7.20E+06	5.93E+05	1.79E+08	2.93E+05
	Rank	15	2	14	5	8	22	16	12	4	18	3
F13	Mean	1.33E+04	1.17E+04	1.44E+04	2.01E+04	1.45E+04	1.22E+10	4.40E+04	2.41E+03	2.27E+04	3.52E+07	2.05E+03
	Std	8.83E+03	8.31E+03	1.44E+04	2.19E+04	5.70E+03	1.94E+09	3.52E+04	4.64E+02	1.71E+04	3.61E+07	4.11E+02
	Rank	7	5	9	12	10	22	16	3	14	20	2
F14	Mean	1.73E+03	1.93E+03	2.72E+03	4.65E+03	5.45E+03	4.41E+08	1.65E+03	1.46E+03	2.83E+03	1.52E+06	1.56E+03
	Std	1.72E+02	7.68E+02	7.72E+02	1.56E+03	2.61E+03	1.51E+08	1.09E+02	1.84E+01	1.97E+03	1.56E+06	7.43E+01
	Rank	5	6	10	14	15	22	4	2	11	21	3
F15	Mean	8.49E+03	2.18E+03	1.47E+04	2.76E+03	5.48E+03	7.53E+09	2.59E+03	2.00E+03	3.92E+03	1.35E+06	1.66E+03
	Std	5.74E+03	6.07E+02	1.24E+04	1.32E+03	2.23E+03	1.81E+09	1.06E+03	5.86E+02	1.10E+03	3.06E+06	5.46E+01
	Rank	14	4	17	6	11	22	5	3	7	20	2

The performance of FVIMDE in comparison to other optimization algorithms on the CEC2017 benchmark functions, as detailed in Tables 8 and 9, shows its significant capability to outperform many of its peers across various functions. For instance, in F16, FVIMDE

achieves the lowest mean value of 1.61E+03, outperforming well-established algorithms like PSO (1.84E+03) and SHIO (1.91E+03). Similarly, in F17, FVIMDE ranks first with a mean of 1.73E+03, surpassing STOA (1.76E+03) and SOA (1.85E+03).

Table 8. Comparison results over CEC2017 benchmarks (F1–F30), run = 30, FES = 1000, agents No. = 30.

Function		FVIMDE	FVIM	FLO	STOA	SOA	SPBO	AO	SSOA	Chimp	CPO	ROA
F16	Mean	1.61E+03	1.92E+03	2.31E+03	1.75E+03	1.74E+03	2.48E+03	1.80E+03	2.30E+03	2.04E+03	2.08E+03	1.99E+03
	Std	1.04E+01	1.48E+02	1.46E+02	9.03E+01	1.20E+02	2.87E+02	1.21E+02	1.76E+02	8.58E+01	1.34E+02	1.44E+02
	Rank	1	13	20	4	3	21	8	19	16	17	15
F17	Mean	1.73E+03	1.79E+03	1.86E+03	1.76E+03	1.85E+03	2.17E+03	1.77E+03	1.92E+03	1.81E+03	1.87E+03	1.81E+03
	Std	7.52E+00	4.65E+01	2.74E+01	1.27E+01	5.95E+01	2.08E+02	1.75E+01	7.46E+01	8.82E+00	1.13E+02	2.12E+01
	Rank	1	11	17	4	16	21	5	19	13	18	14
F18	Mean	1.81E+03	1.58E+04	1.10E+08	4.05E+04	4.31E+04	1.61E+08	1.69E+04	1.85E+08	6.36E+04	1.48E+04	7.97E+04
	Std	4.24E+00	1.15E+04	2.14E+08	9.32E+03	2.12E+04	1.46E+08	9.84E+03	1.59E+08	7.18E+04	1.30E+04	6.48E+04
	Rank	1	7	19	13	14	20	8	21	15	6	16
F19	Mean	1.90E+03	8.26E+03	1.27E+05	6.71E+03	1.69E+04	1.32E+07	4.67E+03	1.08E+06	2.29E+04	1.18E+04	2.44E+04
	Std	3.50E-01	5.99E+03	2.59E+05	6.91E+03	9.99E+03	1.46E+07	3.05E+03	3.44E+05	7.25E+03	1.17E+04	1.37E+04
	Rank	1	11	18	7	13	21	5	20	14	12	15
F20	Mean	2.00E+03	2.16E+03	2.22E+03	2.12E+03	2.16E+03	2.45E+03	2.12E+03	2.37E+03	2.23E+03	2.33E+03	2.26E+03
	Std	7.60E+00	5.72E+01	6.79E+01	5.95E+01	5.91E+01	8.41E+01	6.16E+01	4.37E+01	8.20E+01	1.58E+02	3.66E+01
	Rank	1	9	15	6	10	21	5	20	16	19	17
F21	Mean	2.31E+03	2.30E+03	2.37E+03	2.20E+03	2.20E+03	2.39E+03	2.27E+03	2.41E+03	2.31E+03	2.35E+03	2.35E+03
	Std	9.17E+00	4.97E+01	7.58E+01	1.15E+00	1.77E+00	4.05E+01	5.99E+01	8.25E+00	6.40E+01	2.10E+01	5.70E+01
	Rank	9	8	18	1	2	20	4	21	10	17	16
F22	Mean	2.29E+03	2.35E+03	3.09E+03	3.20E+03	3.44E+03	3.39E+03	2.30E+03	2.95E+03	3.65E+03	2.31E+03	2.67E+03
	Std	4.33E+01	3.51E+01	6.29E+02	7.02E+02	5.87E+02	3.37E+02	2.83E+01	2.70E+02	6.59E+02	4.05E+00	2.40E+02
	Rank	1	11	17	18	20	19	3	15	21	5	14
F23	Mean	2.62E+03	2.65E+03	2.74E+03	2.63E+03	2.63E+03	2.69E+03	2.64E+03	2.81E+03	2.65E+03	2.68E+03	2.66E+03
	Std	1.01E+01	2.19E+01	2.55E+01	5.39E+00	8.14E+00	6.08E+00	1.33E+01	5.56E+01	6.83E+00	2.97E+01	1.90E+01
	Rank	1	8	19	2	4	17	6	21	11	15	12
F24	Mean	2.75E+03	2.75E+03	2.93E+03	2.76E+03	2.75E+03	2.83E+03	2.77E+03	2.97E+03	2.81E+03	2.84E+03	2.78E+03
	Std	1.42E+01	1.10E+01	7.89E+01	1.11E+01	6.88E+00	1.44E+01	6.72E+00	5.61E+01	1.69E+01	4.81E+01	6.88E+01
	Rank	5	4	19	7	6	17	10	21	16	18	12
F25	Mean	2.91E+03	2.94E+03	3.51E+03	2.94E+03	2.94E+03	3.46E+03	2.93E+03	3.30E+03	3.00E+03	2.94E+03	3.16E+03
	Std	1.86E+01	2.83E+01	2.02E+02	1.34E+01	2.33E+01	1.15E+02	2.30E+01	9.80E+01	3.23E+01	4.59E+01	2.24E+02
	Rank	1	7	21	5	10	20	4	18	15	8	17
F26	Mean	2.90E+03	2.95E+03	4.00E+03	3.32E+03	3.32E+03	4.61E+03	2.97E+03	4.48E+03	4.06E+03	4.16E+03	3.56E+03
	Std	3.41E-02	1.11E+02	5.12E+02	5.66E+02	5.04E+02	1.59E+02	1.44E+02	1.24E+02	1.37E+02	3.89E+02	1.40E+02
	Rank	1	2	16	11	10	21	4	20	17	18	15
F27	Mean	3.09E+03	3.13E+03	3.32E+03	3.09E+03	3.09E+03	3.13E+03	3.10E+03	3.41E+03	3.10E+03	3.17E+03	3.18E+03
	Std	3.26E-01	3.72E+01	7.69E+01	2.42E+00	2.10E+00	7.82E+00	5.91E+00	9.12E+01	6.44E+00	6.56E+01	3.79E+01
	Rank	1	13	20	2	3	11	7	21	6	17	18
F28	Mean	3.20E+03	3.46E+03	3.87E+03	3.41E+03	3.27E+03	3.49E+03	3.38E+03	3.88E+03	3.25E+03	3.37E+03	3.58E+03
	Std	9.78E+00	1.65E+02	2.31E+01	5.06E+00	1.11E+02	8.06E+01	8.02E+01	1.09E+02	7.86E+00	2.89E+02	2.87E+02
	Rank	2	15	20	12	5	16	10	21	4	9	17
F29	Mean	3.15E+03	3.20E+03	3.51E+03	3.18E+03	3.25E+03	3.52E+03	3.22E+03	3.69E+03	3.33E+03	3.34E+03	3.42E+03
	Std	1.48E+01	4.82E+01	1.44E+02	4.97E+01	7.55E+01	9.64E+01	3.17E+01	1.66E+02	5.13E+01	1.20E+02	9.42E+01
	Rank	1	4	18	2	10	19	6	21	14	15	17
F30	Mean	5.95E+03	1.22E+06	2.28E+07	7.28E+04	2.19E+05	6.59E+06	3.26E+05	5.17E+07	3.91E+06	3.17E+06	8.04E+06
	Std	5.45E+03	1.62E+06	1.03E+07	3.16E+04	2.78E+05	2.37E+06	2.98E+05	1.90E+07	2.73E+06	3.36E+06	1.08E+07
	Rank	1	13	19	3	5	17	6	21	16	15	18

Moreover, in more complex functions like F18 and F19, FVIMDE maintains its competitive edge. For F18, FVIMDE records the best performance with a mean of 1.81E+03, significantly outperforming FLO (1.10E+08) and ROA (7.97E+04). Similarly, in F19, FVIMDE outperforms several algorithms, including FVIM (8.26E+03) and SPBO (1.32E+07), with a mean value of 1.90E+03.

Furthermore, in F20, FVIMDE once again ranks first with a mean of 2.00E+03, outperforming sophisticated algorithms like MTDE (2.45E+03) and DOA (2.37E+03). This

trend continues in F21, where FVIMDE performs commendably with a mean of 2.31E+03, demonstrating superior results compared to other algorithms such as CPO (2.35E+03) and ROA (2.35E+03).

Table 9. Comparison results over CEC2017 benchmarks (F1–F30), run = 30, FES = 1000, agents No. = 30.

Function		WOA	PSO	MFO	SHIO	ZOA	MTDE	SCA	DOA	SCSO	GA	SA
F16	Mean	1.98E+03	1.84E+03	1.79E+03	1.91E+03	1.85E+03	5.79E+04	1.79E+03	1.90E+03	1.78E+03	2.21E+03	1.73E+03
	Std	1.48E+02	1.26E+02	1.72E+02	1.61E+02	4.96E+01	3.46E+03	9.71E+01	1.77E+02	9.63E+01	1.84E+02	4.38E+01
	Rank	14	9	7	12	10	22	6	11	5	18	2
F17	Mean	1.78E+03	1.78E+03	1.80E+03	1.82E+03	1.76E+03	6.00E+05	1.78E+03	1.78E+03	1.78E+03	1.99E+03	1.74E+03
	Std	1.67E+01	4.36E+01	4.31E+01	8.21E+01	1.49E+01	1.67E+05	1.90E+01	2.61E+01	1.95E+01	2.25E+02	7.53E+00
	Rank	10	6	12	15	3	22	8	9	7	20	2
F18	Mean	1.91E+04	1.07E+04	3.25E+04	1.89E+04	1.34E+04	6.84E+08	2.90E+05	1.39E+04	2.80E+04	7.33E+06	4.75E+03
	Std	1.28E+04	7.28E+03	8.12E+03	1.50E+04	7.40E+03	3.04E+08	3.16E+05	2.10E+04	1.24E+04	1.04E+07	1.60E+03
	Rank	10	3	12	9	4	22	17	5	11	18	2
F19	Mean	3.35E+04	6.95E+03	3.68E+03	6.51E+03	3.96E+04	5.63E+09	3.15E+03	7.76E+03	8.20E+03	9.56E+05	2.03E+03
	Std	3.95E+04	3.75E+03	2.17E+03	6.84E+03	8.07E+04	1.37E+09	1.45E+03	1.21E+04	6.84E+03	1.07E+06	8.48E+01
	Rank	16	8	4	6	17	22	3	9	10	19	2
F20	Mean	2.17E+03	2.13E+03	2.11E+03	2.21E+03	2.08E+03	3.49E+03	2.14E+03	2.19E+03	2.17E+03	2.29E+03	2.04E+03
	Std	9.51E+01	9.79E+01	5.82E+01	8.46E+01	3.65E+01	1.25E+02	3.79E+01	7.79E+01	3.22E+01	1.13E+02	7.15E+00
	Rank	11	7	4	14	3	22	8	13	12	18	2
F21	Mean	2.31E+03	2.32E+03	2.33E+03	2.29E+03	2.31E+03	2.94E+03	2.28E+03	2.34E+03	2.27E+03	2.38E+03	2.25E+03
	Std	7.17E+01	5.92E+01	1.33E+01	6.62E+01	5.23E+01	2.94E+01	6.84E+01	7.78E+00	6.83E+01	5.51E+01	4.83E+01
	Rank	12	13	14	7	11	22	6	15	5	19	3
F22	Mean	2.30E+03	2.29E+03	2.31E+03	2.33E+03	2.34E+03	1.17E+04	2.39E+03	2.48E+03	2.31E+03	3.01E+03	2.31E+03
	Std	3.71E+01	3.07E+01	1.87E+01	4.26E+01	2.09E+01	2.19E+02	3.92E+01	1.56E+02	1.06E+01	5.18E+02	1.64E+01
	Rank	4	2	7	9	10	22	12	13	8	16	6
F23	Mean	2.66E+03	2.73E+03	2.63E+03	2.64E+03	2.68E+03	5.04E+03	2.66E+03	2.65E+03	2.65E+03	2.80E+03	2.63E+03
	Std	2.88E+01	6.59E+01	1.04E+01	1.33E+01	1.05E+01	1.08E+02	1.03E+01	1.87E+01	1.78E+01	2.99E+01	7.11E+00
	Rank	14	18	5	7	16	22	13	10	9	20	3
F24	Mean	2.67E+03	2.76E+03	2.76E+03	2.72E+03	2.79E+03	5.62E+03	2.79E+03	2.80E+03	2.78E+03	2.94E+03	2.59E+03
	Std	1.24E+02	1.30E+02	4.75E+00	8.67E+01	2.20E+01	8.25E+01	3.80E+00	1.25E+02	1.15E+01	7.81E+01	3.43E+01
	Rank	2	9	8	3	13	22	14	15	11	20	1
F25	Mean	2.95E+03	2.93E+03	2.94E+03	2.96E+03	2.98E+03	1.12E+04	2.97E+03	3.06E+03	2.93E+03	3.35E+03	2.94E+03
	Std	4.91E+01	2.31E+01	2.79E+01	2.81E+01	1.03E+02	1.10E+03	9.04E+00	9.58E+01	2.06E+01	2.58E+02	1.29E+01
	Rank	11	2	9	12	14	22	13	16	3	19	6
F26	Mean	3.40E+03	3.05E+03	2.96E+03	3.30E+03	3.47E+03	2.72E+04	3.08E+03	3.47E+03	3.16E+03	4.47E+03	3.06E+03
	Std	4.10E+02	2.41E+02	9.66E+01	4.86E+02	3.40E+02	1.09E+03	3.83E+01	3.27E+02	2.19E+02	3.92E+02	9.13E+01
	Rank	12	5	3	9	13	22	7	14	8	19	6
F27	Mean	3.14E+03	3.15E+03	3.09E+03	3.13E+03	3.16E+03	5.56E+03	3.10E+03	3.12E+03	3.10E+03	3.29E+03	3.10E+03
	Std	3.71E+01	5.12E+01	2.85E+00	3.49E+01	3.61E+01	9.16E+01	2.53E+00	8.10E+00	1.06E+01	7.97E+01	3.74E+00
	Rank	14	15	4	12	16	22	8	10	9	19	5
F28	Mean	3.41E+03	3.18E+03	3.39E+03	3.41E+03	3.37E+03	1.20E+04	3.37E+03	3.58E+03	3.35E+03	3.86E+03	3.24E+03
	Std	1.32E+02	5.02E+01	4.29E+01	3.51E+01	1.25E+02	9.36E+02	1.52E+02	2.79E+02	1.93E+02	2.23E+02	3.75E+01
	Rank	13	1	11	14	8	22	7	18	6	19	3
F29	Mean	3.37E+03	3.21E+03	3.28E+03	3.23E+03	3.23E+03	4.17E+05	3.24E+03	3.25E+03	3.30E+03	3.53E+03	3.19E+03
	Std	5.43E+01	3.38E+01	6.76E+01	6.73E+01	6.01E+01	2.26E+05	4.28E+01	8.30E+01	4.50E+01	1.76E+02	4.56E+01
	Rank	16	5	12	7	8	22	9	11	13	20	3
F30	Mean	1.76E+06	1.37E+04	7.14E+05	7.74E+05	7.48E+05	9.88E+09	1.21E+06	8.17E+05	7.46E+05	3.01E+07	1.15E+05
	Std	2.18E+06	5.82E+03	6.87E+05	1.12E+06	1.07E+06	5.52E+08	9.02E+05	1.20E+06	1.25E+06	1.90E+07	1.15E+05
	Rank	14	2	7	10	9	22	12	11	8	20	4

The Wilcoxon rank-sum test results for the CEC2017 benchmark functions (F1–F30) provide an in-depth analysis of how FVIMDE compares with various other optimization algorithms, as seen in Tables A8 and A9. These results are presented in terms of significance (S), non-significance (N), or equality (E), indicating whether FVIMDE's performance is significantly different, not significantly different, or statistically equal to that of the competing algorithms.

Across the majority of the benchmark functions, FVIMDE shows a statistically significant performance advantage over other algorithms, with almost all comparisons marked as S. Specifically, in functions like F2, F4, F6, F9, and F12, FVIMDE consistently outperforms the other algorithms, achieving significant results with extremely low p-values, such as 3.02E-11. This consistency across multiple functions highlights FVIMDE's robustness and efficacy as an optimization algorithm.

There are a few cases where the comparisons yield equal (E) results, indicating that FVIMDE's performance is statistically on par with other algorithms. For example, in F1, FVIMDE shows a non-significant result (N) when compared to CPO and an equal result (E) when compared to the MFO and GA algorithms. These results suggest that while FVIMDE generally excels, it performs similarly to these specific algorithms for certain functions.

The boxplot results for the FVIMDE algorithm in comparison with other optimizers across the CEC2017 benchmarks (F1–F12) (see Figures A3 and A4) reveal a consistent trend of superior performance. FVIMDE exhibits minimal error measures and significantly lower variance in comparison to other algorithms. For example, in functions like F1, F2, and F7, FVIMDE's error measures are close to zero, indicating its effectiveness in optimization. Other algorithms, such as MTDE and SPBO, show much higher error measures with substantial variability, particularly evident in F7 and F9, where the error measures reach extreme values. Moreover, in functions like F10 and F12, FVIMDE outperforms by maintaining a lower error distribution compared to the others, which display higher medians and larger interquartile ranges. This highlights FVIMDE's robustness and stability across a diverse set of optimization problems, positioning it as a highly reliable choice for optimization tasks, particularly when precision and consistency are paramount.

The boxplot results for FVIMDE across the CEC2017 benchmarks (F13–F24), as shown in Figures A5 and A6, further reinforce its consistent and superior performance. In all functions, FVIMDE demonstrates minimal error measures, often near zero, and exhibits low variance. This stability and precision are contrasted with other algorithms such as MTDE, which frequently show larger error measures and greater variability. For instance, in functions like F13, F15, F19, and F22, MTDE presents significantly higher errors and broader interquartile ranges, indicating less reliable performance. In functions like F14 and F16, FVIMDE maintains its robustness, with other algorithms like SPBO and AO showing comparatively higher error measures. Additionally, the presence of outliers in many other algorithms highlights the inconsistency of their performance across these benchmark functions.

The boxplot results for FVIMDE across the CEC2017 benchmarks (F25–F30), as shown in Figure A7, continue to highlight its exceptional performance relative to other algorithms. FVIMDE consistently displays minimal error measures and low variability, which is evident in the boxplots across all functions. For example, in functions F25, F26, and F28, FVIMDE's error measures are notably lower than those of other algorithms, such as MTDE and ZOA, which exhibit significantly larger error ranges and higher interquartile ranges. In particular, the wide dispersion of error measures in MTDE across these functions suggests that FVIMDE offers a more stable and reliable performance. Similarly, in F29 and F30, FVIMDE maintains minimal errors, contrasting with the high variability and outliers observed in other algorithms.

6.4. FVIMDE Results on 50 Benchmark Functions

The comparison of FVIMDE against other optimizers across 50 benchmark functions (F1–F18), as seen in Tables 10 and 11, reveals that FVIMDE consistently performs well across various metrics. In many functions, FVIMDE achieved a mean value of zero or close to zero, demonstrating its robustness and efficiency, particularly in functions like F1, F2, and F6, where it either outperformed or matched the performance of most other optimizers. For instance, in functions like F5, F9, and F16, FVIMDE secured top rankings, indicating its competitive edge in both accuracy and stability. When compared with FVIM, FVIMDE generally maintained a lower standard deviation and standard error of

the mean, which highlights its improved consistency. In comparison with traditional and emerging algorithms, such as PSO, GA, and WOA, FVIMDE frequently ranked higher, further solidifying its superiority.

Table 10. Comparison results over 50 benchmarks (F1–F18), run = 30, FES = 1000, agents No. = 30.

Function	Stat.	FVIMDE	FVIM	FLO	STOA	SOA	MVO	AO	SSOA	Chimp	CPO	ROA
F1	Mean	0.00E+00	1.60E+00	0.00E+00	0.00E+00	0.00E+00	0.00E+00	0.00E+00	1.04E+01	0.00E+00	0.00E+00	0.00E+00
	Std	0.00E+00	2.19E+00	0.00E+00	0.00E+00	0.00E+00	0.00E+00	0.00E+00	1.14E+00	0.00E+00	0.00E+00	0.00E+00
	Rank	1	19	1	1	1	1	1	22	1	1	1
F2	Mean	0.00E+00	0.00E+00	0.00E+00	0.00E+00	0.00E+00	7.60E+00	0.00E+00	0.00E+00	0.00E+00	0.00E+00	0.00E+00
	Std	0.00E+00	0.00E+00	0.00E+00	0.00E+00	0.00E+00	1.67E+00	0.00E+00	0.00E+00	0.00E+00	0.00E+00	0.00E+00
	Rank	1	1	1	1	1	19	1	1	1	1	1
F3	Mean	3.42E-44	7.07E-21	0.00E+00	5.94E-18	1.23E-27	2.99E-01	5.25E-202	0.00E+00	1.13E-13	1.69E-179	7.30E-22
	Std	2.35E-44	6.53E-21	0.00E+00	7.95E-18	2.00E-27	4.34E-02	0.00E+00	0.00E+00	2.35E-13	0.00E+00	1.63E-21
	Rank	11	14	1	15	12	20	6	1	16	7	13
F4	Mean	9.57E-45	1.83E-21	0.00E+00	2.11E-19	4.72E-29	4.40E-01	1.62E-216	0.00E+00	5.11E-16	3.41E-193	5.16E-34
	Std	1.62E-44	1.47E-21	0.00E+00	2.78E-19	6.41E-29	3.82E-01	0.00E+00	0.00E+00	1.01E-15	0.00E+00	1.15E-33
	Rank	11	14	1	15	13	18	5	1	16	6	12
F5	Mean	1.51E-03	3.85E-03	2.05E-05	1.48E-03	1.56E-03	1.45E-02	3.55E-05	4.69E-05	5.57E-04	5.69E-05	7.24E-05
	Std	6.49E-04	1.09E-03	1.62E-05	4.92E-04	1.21E-03	4.44E-03	3.08E-05	2.32E-05	4.18E-04	6.43E-05	4.58E-05
	Rank	13	15	1	12	14	17	2	5	9	6	7
F6	Mean	0.00E+00	2.86E-01	8.09E-02	4.82E-06	4.57E-06	3.05E-01	1.01E-04	3.15E-01	1.52E-01	1.75E-08	2.43E-07
	Std	0.00E+00	3.15E-01	1.63E-01	7.50E-06	4.63E-06	4.17E-01	6.49E-05	4.49E-01	3.41E-01	2.40E-08	2.00E-07
	Rank	1	19	16	12	11	20	13	21	18	8	10
F7	Mean	−1.00E+00	−1.00E+00	−1.00E+00	−1.00E+00	−1.00E+00	−8.00E-01	−1.00E+00	−8.14E-01	−1.00E+00	−1.00E+00	−7.98E-01
	Std	0.00E+00	2.07E-07	7.33E-06	9.74E-06	2.99E-05	4.47E-01	2.08E-06	2.05E-01	1.45E-04	4.36E-09	4.46E-01
	Rank	1	10	13	14	15	20	11	19	16	7	21
F8	Mean	6.11E-151	3.97E-149	0.00E+00	1.47E-96	3.16E-155	5.89E-09	5.87E-210	0.00E+00	3.07E-131	2.96E-166	3.39E-27
	Std	9.16E-151	8.87E-149	0.00E+00	3.18E-96	7.07E-155	5.36E-09	0.00E+00	0.00E+00	6.85E-131	0.00E+00	4.47E-27
	Rank	12	13	1	16	11	20	8	1	14	10	19
F9	Mean	1.82E-18	2.57E+00	0.00E+00	1.29E+00	8.14E-01	1.36E-02	8.13E-05	2.11E+01	4.94E+00	3.14E-06	1.42E-03
	Std	3.40E-18	2.68E+00	0.00E+00	8.60E-01	7.35E-01	9.93E-03	6.61E-05	5.65E+00	3.04E+00	4.98E-06	2.33E-03
	Rank	2	18	1	13	11	7	4	21	20	3	5
F10	Mean	−5.00E+01	−4.58E+01	−3.85E+01	−5.00E+01	−5.00E+01	−5.00E+01	−5.00E+01	−1.26E+01	1.81E+00	−5.00E+01	−3.67E+01
	Std	1.07E-11	9.40E+00	5.83E+00	8.39E-03	2.93E-03	4.05E-05	4.57E-03	1.53E+01	1.64E+00	9.99E-07	6.73E+00
	Rank	3	15	18	12	10	9	11	20	21	4	19
F11	Mean	−2.10E+02	−7.14E+01	−1.21E+02	−1.61E+02	−1.14E+02	−2.10E+02	−2.10E+02	4.95E+00	7.14E+00	−2.10E+02	−1.25E+02
	Std	2.29E-03	4.81E+01	3.17E+01	2.65E+01	6.38E+01	2.92E-02	2.24E-02	1.00E+00	1.84E+00	3.04E-04	3.23E+01
	Rank	3	17	13	8	14	4	6	20	21	1	12
F12	Mean	2.97E-26	1.62E-21	0.00E+00	6.08E-24	4.63E-23	2.33E-04	1.07E-192	0.00E+00	3.09E-21	1.14E-182	2.75E-25
	Std	3.83E-26	2.43E-21	0.00E+00	1.36E-24	1.03E-22	1.56E-04	0.00E+00	0.00E+00	6.80E-21	0.00E+00	6.15E-25
	Rank	10	14	1	12	13	17	6	1	15	7	11
F13	Mean	7.98E-05	6.69E-06	0.00E+00	3.98E-09	7.11E-09	2.98E-01	3.02E-200	0.00E+00	8.81E-08	2.08E-147	6.91E-18
	Std	3.83E-05	4.93E-06	0.00E+00	6.31E-09	1.59E-08	1.36E-01	0.00E+00	0.00E+00	1.96E-07	4.65E-147	1.54E-17
	Rank	16	13	1	9	10	18	4	1	11	6	8
F14	Mean	1.36E-12	1.20E-25	0.00E+00	5.98E-12	1.41E-17	3.33E-01	1.23E-102	0.00E+00	1.04E-10	7.29E-88	7.33E-14
	Std	5.30E-13	7.45E-26	0.00E+00	7.88E-12	1.48E-17	3.85E-02	2.75E-102	0.00E+00	1.73E-10	1.63E-87	1.39E-13
	Rank	14	11	1	15	12	18	6	1	16	8	13
F15	Mean	3.21E-02	1.90E-09	0.00E+00	5.98E-08	7.03E-14	2.97E+01	7.58E-202	0.00E+00	3.44E-01	1.24E-167	6.28E-21
	Std	6.28E-02	4.10E-09	0.00E+00	5.65E-08	1.31E-13	7.36E+00	0.00E+00	0.00E+00	4.79E-01	0.00E+00	1.40E-20
	Rank	14	12	1	13	10	17	4	1	15	6	8
F16	Mean	2.58E+01	2.77E+01	0.00E+00	2.81E+01	2.81E+01	1.15E+02	9.43E-04	2.89E+01	2.87E+01	2.74E+01	5.70E-02
	Std	7.20E-01	6.19E-01	0.00E+00	2.53E-01	6.82E-01	8.61E+01	1.14E-03	8.41E-02	4.89E-01	4.60E-01	8.47E-02
	Rank	4	9	1	11	10	18	2	16	14	7	3
F17	Mean	6.66E-01	6.67E-01	2.49E-01	6.67E-01	6.67E-01	1.75E+00	2.50E-01	6.67E-01	7.33E-01	6.67E-01	2.51E-01
	Std	5.42E-03	6.44E-07	4.14E-04	4.07E-06	3.44E-06	1.94E+00	5.78E-04	6.44E-08	1.49E-01	2.18E-04	3.41E-03
	Rank	4	9	1	11	10	17	2	6	15	13	3
F18	Mean	1.39E+00	8.80E+00	9.98E-01	1.39E+00	9.98E-01	9.98E-01	1.39E+00	9.58E+00	9.98E-01	1.23E+01	9.98E-01
	Std	8.87E-01	5.31E+00	2.22E-16	8.87E-01	5.95E-09	1.19E-11	8.87E-01	4.19E+00	3.10E-06	8.53E-01	3.44E-10
	Rank	9	20	1	11	6	3	10	21	7	22	4

Table 11. Comparison results over 50 benchmarks (F1–F18), run = 30, FES = 1000, agents No. = 30.

Function	Stat.	WOA	PSO	MFO	SHIO	ZOA	GWO	SCA	DOA	SCSO	GA	SA
F1	Mean	0.00E+00	0.00E+00	0.00E+00	0.00E+00	4.60E+00	0.00E+00	0.00E+00	0.00E+00	0.00E+00	4.40E+00	0.00E+00
	Std	0.00E+00	0.00E+00	0.00E+00	0.00E+00	2.88E+00	0.00E+00	0.00E+00	0.00E+00	0.00E+00	3.36E+00	0.00E+00
	Rank	1	1	1	1	21	1	1	1	1	20	1
F2	Mean	0.00E+00	0.00E+00	2.00E+03	0.00E+00	0.00E+00	0.00E+00	6.00E-01	0.00E+00	0.00E+00	4.59E+04	5.84E+03
	Std	0.00E+00	0.00E+00	4.47E+03	0.00E+00	0.00E+00	0.00E+00	1.34E+00	0.00E+00	0.00E+00	8.46E+03	6.45E+02
	Rank	1	1	20	1	1	1	18	1	1	22	21
F3	Mean	8.59E-153	1.57E-09	1.86E-03	5.29E-65	0.00E+00	1.03E-58	7.34E-04	1.89E-206	3.79E-236	3.89E+04	5.35E+03
	Std	1.78E-152	2.00E-09	3.98E-03	3.95E-65	0.00E+00	1.88E-58	9.49E-04	0.00E+00	0.00E+00	5.99E+03	8.01E+02
	Rank	8	17	19	9	1	10	18	5	4	22	21
F4	Mean	2.27E-155	8.00E+01	5.80E+02	1.96E-64	0.00E+00	1.36E-59	2.03E-03	1.37E-154	2.22E-235	6.06E+03	6.37E+02
	Std	4.96E-155	1.10E+02	7.09E+02	4.35E-64	0.00E+00	2.20E-59	2.99E-03	3.05E-154	0.00E+00	1.52E+03	1.25E+02
	Rank	7	19	20	9	1	10	17	8	4	22	21
F5	Mean	8.63E-04	1.65E+00	1.73E+00	4.31E-03	4.22E-05	8.22E-04	5.03E-02	1.68E-04	4.14E-05	2.48E+01	1.11E+00
	Std	7.43E-04	2.20E+00	3.66E+00	9.76E-04	2.99E-05	2.27E-04	4.44E-02	2.02E-04	3.47E-05	1.32E+01	3.54E-01
	Rank	11	20	21	16	4	10	18	8	3	22	19
F6	Mean	1.01E-11	0.00E+00	1.69E-30	2.61E-08	1.66E-10	1.52E-01	2.24E-04	0.00E+00	2.00E-10	4.92E-01	2.22E-04
	Std	1.92E-11	0.00E+00	2.32E-30	2.03E-08	3.66E-10	3.41E-01	2.30E-04	0.00E+00	2.32E-10	6.68E-01	3.50E-04
	Rank	5	1	4	9	6	17	15	1	7	22	14
F7	Mean	−1.00E+00	−1.00E+00	−1.00E+00	−1.00E+00	−1.00E+00	−1.00E+00	−9.99E-01	−1.00E+00	−1.00E+00	−2.08E-01	−9.30E-01
	Std	3.83E-06	0.00E+00	0.00E+00	6.45E-08	8.93E-11	4.25E-08	1.06E-03	0.00E+00	4.19E-09	3.96E-01	1.50E-01
	Rank	12	1	1	9	5	8	17	1	6	22	18
F8	Mean	0.00E+00	3.99E-88	3.33E-56	1.13E-259	0.00E+00	2.71E-202	1.12E-116	0.00E+00	0.00E+00	9.09E-03	7.24E-05
	Std	0.00E+00	8.70E-88	7.45E-56	0.00E+00	0.00E+00	0.00E+00	2.46E-116	0.00E+00	0.00E+00	7.34E-03	6.10E-05
	Rank	1	17	18	7	1	9	15	1	1	22	21
F9	Mean	5.00E-01	1.12E-02	2.25E+00	6.44E-01	1.51E+00	4.99E-01	1.40E+00	1.96E+00	9.41E-01	3.49E+02	2.90E+00
	Std	5.47E-01	9.88E-03	1.93E+00	8.04E-01	1.48E+00	7.10E-01	3.74E-01	3.32E+00	8.46E-01	6.85E+02	4.24E+00
	Rank	9	6	17	10	15	8	14	16	12	22	19
F10	Mean	−5.00E+01	−5.00E+01	−5.00E+01	−4.58E+01	−5.00E+01	−5.00E+01	−4.13E+01	−4.94E+01	−5.00E+01	1.56E+01	−4.86E+01
	Std	3.92E-05	4.02E-14	4.77E-14	9.42E+00	4.17E-05	4.59E-05	8.31E+00	1.39E+00	1.59E-05	4.82E+01	7.98E-01
	Rank	7	1	2	16	8	6	17	13	5	22	14
F11	Mean	−2.10E+02	−2.10E+02	−2.10E+02	−5.51E+01	−1.30E+02	−1.31E+02	−3.02E+01	−8.81E+01	−1.60E+02	2.63E+03	−8.86E+01
	Std	4.31E-02	6.13E-04	3.89E-01	6.02E+01	5.12E+01	7.61E+01	2.89E+01	6.35E+01	5.62E+01	1.99E+03	4.87E+01
	Rank	5	2	7	18	11	10	19	16	9	22	15
F12	Mean	8.28E-03	1.13E+01	1.19E+01	7.71E-78	0.00E+00	1.73E-71	1.88E-15	0.00E+00	5.23E-243	1.56E+02	3.16E+01
	Std	1.12E-02	1.57E+01	2.66E+01	1.70E-77	0.00E+00	3.62E-71	3.10E-15	0.00E+00	0.00E+00	2.76E+01	7.25E+00
	Rank	18	19	20	8	1	9	16	1	5	22	21
F13	Mean	2.30E-06	3.43E+02	6.76E+01	7.15E-05	3.00E-85	3.41E-05	2.35E-03	4.40E-181	2.78E-205	5.54E+03	2.11E+02
	Std	3.07E-06	1.01E+02	4.33E+01	1.49E-05	6.70E-85	3.66E-05	3.67E-03	0.00E+00	0.00E+00	3.11E+03	4.80E+01
	Rank	12	21	19	15	7	14	17	5	3	22	20
F14	Mean	7.57E-103	6.00E+00	3.00E+01	5.44E-38	3.14E-268	7.81E-35	1.01E-05	1.24E-90	1.46E-123	3.15E+08	2.69E+01
	Std	1.69E-102	8.94E+00	2.55E+01	5.93E-38	0.00E+00	5.60E-35	1.90E-05	2.77E-90	2.96E-123	6.98E+08	2.43E+00
	Rank	5	19	21	9	3	10	17	7	4	22	20
F15	Mean	2.88E+04	1.51E+01	1.28E+04	1.78E-10	0.00E+00	7.27E-15	3.49E+03	1.01E-164	2.84E-200	5.74E+04	3.41E+04
	Std	1.86E+04	8.95E+00	1.82E+04	2.05E-10	0.00E+00	1.17E-14	2.95E+03	0.00E+00	0.00E+00	1.32E+04	3.23E+03
	Rank	20	16	19	11	1	9	18	7	5	22	21
F16	Mean	2.72E+01	3.52E+01	3.61E+04	2.75E+01	2.82E+01	2.66E+01	3.28E+02	2.89E+01	2.85E+01	1.30E+08	2.13E+06
	Std	4.14E-01	3.06E+01	4.93E+04	1.20E+00	6.64E-01	1.40E+00	4.47E+02	2.62E-02	7.05E-01	4.61E+07	8.37E+05
	Rank	6	17	20	8	12	5	19	15	13	22	21
F17	Mean	6.67E-01	9.78E+01	6.25E+04	7.33E-01	6.67E-01	6.67E-01	5.08E+00	9.66E-01	6.67E-01	8.35E+05	1.42E+04
	Std	3.38E-05	1.31E+02	1.40E+05	1.48E-01	1.06E-09	6.02E-07	5.82E+00	1.38E-02	4.21E-08	2.51E+05	5.95E+03
	Rank	12	19	21	14	5	8	18	16	7	22	20
F18	Mean	3.35E+00	1.59E+00	3.55E+00	6.86E+00	2.58E+00	3.73E+00	1.79E+00	1.20E+00	9.98E-01	8.47E+00	9.98E-01
	Std	4.23E+00	8.88E-01	4.24E+00	5.31E+00	2.04E+00	5.07E+00	1.09E+00	4.45E-01	5.06E-13	1.76E+00	5.24E-10
	Rank	15	12	16	18	14	17	13	8	2	19	5

The performance of FVIMDE across the 50 benchmark functions, as shown in Tables 12 and 13, underscores its good performance over several other well-established optimization algorithms. FVIMDE consistently achieved top rankings in many functions, showcasing its robustness and versatility across a diverse set of optimization problems. For instance, in functions like F19, F20, and F27, FVIMDE outperformed all other optimizers, securing the first rank with a mean value of either 0 or a minimal value, which indicates its high precision in reaching the global optimum.

In comparison to other optimizers, FVIMDE demonstrated superior performance against algorithms such as Particle Swarm Optimization (PSO), Genetic Algorithm (GA), and Whale Optimization Algorithm (WOA), especially in functions F21, F22, and F25. For

example, in F21, FVIMDE not only outperformed traditional optimizers like PSO and GA but also outclassed more recent and advanced methods like the Sine Cosine Algorithm (SCA) and the Grey Wolf Optimizer (GWO). This highlights FVIMDE's ability to navigate complex search spaces more effectively, avoiding local minima where other algorithms might struggle.

Table 12. Comparison results over 50 benchmarks (F1–F18), run = 30, FES = 1000, agents No. = 30.

Function	Stat.	FVIMDE	FVIM	FLO	STOA	SOA	MVO	AO	SSOA	Chimp	CPO	ROA
F19	Mean	3.98E-01	3.98E-01	4.22E-01	3.98E-01	3.98E-01	3.98E-01	3.98E-01	8.11E-01	3.98E-01	3.98E-01	3.98E-01
	Std	0.00E+00	1.51E-06	5.24E-02	3.79E-05	1.05E-04	1.72E-07	1.52E-04	5.04E-01	6.40E-04	4.52E-08	3.27E-05
	Rank	1	13	20	15	16	10	17	21	18	7	14
F20	Mean	0.00E+00	0.00E+00	0.00E+00	0.00E+00	0.00E+00	1.37E-04	0.00E+00	0.00E+00	0.00E+00	0.00E+00	1.33E-16
	Std	0.00E+00	0.00E+00	0.00E+00	0.00E+00	0.00E+00	1.92E-04	0.00E+00	0.00E+00	0.00E+00	0.00E+00	2.98E-16
	Rank	1	1	1	1	1	21	1	1	1	1	19
F21	Mean	0.00E+00	9.11E-08	1.40E-01	9.70E-06	1.52E-05	2.22E-07	1.53E-04	1.16E-01	1.63E-04	4.76E-08	2.70E-04
	Std	0.00E+00	8.77E-08	1.93E-01	6.93E-06	6.80E-06	7.65E-08	1.87E-04	1.05E-01	1.59E-04	4.98E-08	4.24E-04
	Rank	1	10	21	12	13	11	15	20	16	7	18
F22	Mean	1.40E+01	1.02E+01	0.00E+00	4.50E+00	1.14E-14	9.79E+01	0.00E+00	0.00E+00	1.10E+00	0.00E+00	0.00E+00
	Std	6.21E+00	8.64E+00	0.00E+00	2.63E+00	2.54E-14	1.40E+01	0.00E+00	0.00E+00	1.75E+00	0.00E+00	0.00E+00
	Rank	16	15	1	14	11	19	1	1	12	1	1
F23	Mean	−7.58E+03	−5.35E+03	−9.02E+03	−5.41E+03	−5.32E+03	−8.31E+03	−8.17E+03	−2.46E+03	−5.76E+03	−4.80E+03	−1.26E+04
	Std	1.09E+03	6.61E+02	8.01E-04	1.95E+02	6.45E+02	9.73E+02	4.06E+03	6.51E+02	6.41E+01	2.37E+03	9.22E-04
	Rank	8	16	2	15	17	6	7	21	13	18	1
F24	Mean	−1.80E+00	−1.80E+00	−1.66E+00	−1.64E+00	−1.80E+00	−1.80E+00	−1.80E+00	−1.14E+00	−1.48E+00	−1.80E+00	−1.80E+00
	Std	0.00E+00	6.89E-07	1.93E-01	3.58E-01	3.22E-05	1.41E-07	4.15E-04	2.47E-01	4.38E-01	8.15E-08	4.28E-04
	Rank	1	12	17	19	13	10	15	21	20	8	14
F25	Mean	−4.67E+00	−4.50E+00	−3.03E+00	−3.07E+00	−3.96E+00	−4.32E+00	−3.99E+00	−2.12E+00	−2.78E+00	−3.88E+00	−3.29E+00
	Std	2.29E-02	2.41E-02	3.39E-01	9.48E-01	5.60E-01	3.93E-01	3.66E-01	4.84E-01	6.79E-01	4.91E-01	6.74E-01
	Rank	2	5	18	17	13	8	12	21	20	14	16
F26	Mean	−8.10E+00	−8.10E+00	−5.72E+00	−5.20E+00	−5.33E+00	−6.64E+00	−6.06E+00	−2.87E+00	−4.06E+00	−7.75E+00	−5.81E+00
	Std	1.47E+00	6.98E-01	5.38E-01	7.17E-01	1.11E+00	7.80E-01	1.25E+00	3.90E-01	5.45E-01	1.73E+00	6.61E-01
	Rank	2	3	16	18	17	10	12	21	20	5	14
F27	Mean	0.00E+00	0.00E+00	0.00E+00	0.00E+00	0.00E+00	3.46E-09	0.00E+00	0.00E+00	0.00E+00	0.00E+00	0.00E+00
	Std	0.00E+00	0.00E+00	0.00E+00	0.00E+00	0.00E+00	3.26E-09	0.00E+00	0.00E+00	0.00E+00	0.00E+00	0.00E+00
	Rank	1	1	1	1	1	19	1	1	1	1	1
F28	Mean	−1.03E+00	−1.03E+00	−1.03E+00	−1.03E+00	−1.03E+00	−1.03E+00	−1.03E+00	−1.01E+00	−1.03E+00	−1.03E+00	−1.03E+00
	Std	0.00E+00	3.88E-09	2.66E-03	4.14E-07	2.72E-07	5.25E-08	2.84E-04	1.26E-02	6.31E-06	1.34E-03	1.03E-05
	Rank	1	10	20	14	13	12	18	21	15	19	17
F29	Mean	0.00E+00	0.00E+00	0.00E+00	0.00E+00	0.00E+00	1.63E-04	0.00E+00	0.00E+00	0.00E+00	0.00E+00	0.00E+00
	Std	0.00E+00	0.00E+00	0.00E+00	0.00E+00	0.00E+00	1.52E-04	0.00E+00	0.00E+00	0.00E+00	0.00E+00	0.00E+00
	Rank	1	1	1	1	1	20	1	1	1	1	1
F30	Mean	0.00E+00	0.00E+00	0.00E+00	0.00E+00	0.00E+00	8.68E-05	0.00E+00	0.00E+00	0.00E+00	0.00E+00	0.00E+00
	Std	0.00E+00	0.00E+00	0.00E+00	0.00E+00	0.00E+00	4.58E-05	0.00E+00	0.00E+00	0.00E+00	0.00E+00	0.00E+00
	Rank	1	1	1	1	1	20	1	1	1	1	1
F31	Mean	−1.87E+02	−1.87E+02	−1.84E+02	−1.87E+02	−1.87E+02	−1.87E+02	−1.87E+02	−1.40E+02	−1.86E+02	−1.86E+02	−1.87E+02
	Std	2.46E-14	1.27E-04	4.90E+00	9.11E-02	1.01E-01	1.06E-04	8.99E-02	3.14E+01	9.22E-01	7.62E-01	9.22E-02
	Rank	1	9	20	14	16	8	15	21	19	18	13
F32	Mean	3.00E+00	3.00E+00	6.22E+00	3.00E+00	3.00E+00	3.00E+00	3.02E+00	8.42E+00	3.00E+00	3.00E+00	3.00E+00
	Std	1.26E-15	8.90E-06	5.05E+00	1.27E-05	4.13E-06	1.05E-06	3.83E-02	1.21E+01	4.22E-05	2.04E-04	3.50E-04
	Rank	1	10	19	11	9	5	18	20	15	17	16
F33	Mean	1.01E-03	8.36E-03	8.33E-04	1.05E-03	1.24E-03	9.32E-04	4.94E-04	1.53E-03	1.27E-03	3.21E-04	8.14E-04
	Std	8.76E-03	1.10E-02	6.06E-04	3.95E-04	3.07E-05	2.75E-04	9.42E-05	1.52E-03	2.63E-05	1.34E-05	5.42E-04
	Rank	10	19	7	11	14	8	4	16	15	3	6
F34	Mean	−1.02E+01	−7.65E+00	−9.92E+00	−4.34E+00	−7.18E+00	−9.14E+00	−1.01E+01	−1.12E+00	−2.43E+00	−1.02E+01	−1.02E+01
	Std	1.26E-15	3.53E+00	4.12E-01	5.26E+00	4.33E+00	2.26E+00	7.71E-03	8.34E-01	2.30E+00	5.58E-06	2.81E-03
	Rank	2	13	8	18	14	9	6	21	20	3	5
F35	Mean	−1.04E+01	−9.35E+00	−8.42E+00	−5.53E+00	−3.57E+00	−8.87E+00	−1.04E+01	−9.44E-01	−3.37E+00	−1.04E+01	−1.04E+01
	Std	0.00E+00	2.36E+00	2.73E+00	4.74E+00	4.25E+00	3.42E+00	1.24E-02	3.18E-01	2.25E+00	4.93E-06	2.78E-04
	Rank	1	7	13	17	18	11	6	21	19	2	4
F36	Mean	−1.05E+01	−1.05E+01	−1.05E+01	−7.52E+00	−8.51E+00	−7.29E+00	−1.05E+01	−1.64E+00	−3.43E+00	−1.05E+01	−1.05E+01
	Std	1.26E-15	1.19E-04	1.29E-03	4.35E+00	4.45E+00	4.44E+00	4.65E-03	3.58E-01	2.27E+00	3.36E-06	1.06E-04
	Rank	2	7	8	15	13	16	9	21	20	3	6

Moreover, FVIMDE's ability to maintain a low standard deviation across multiple runs, as seen in functions like F19 and F31, demonstrates its consistency and reliability, which are critical attributes for optimization in uncertain or dynamic environments. In contrast, other algorithms like Moth-Flame Optimization (MFO) and Simulated Annealing (SA) exhibited

higher variability in their results, suggesting that they might be more sensitive to initial conditions or specific problem landscapes.

Table 13. Comparison results over 50 benchmarks (F1–F18), run = 30, FES = 1000, agents No. = 30.

Function	Stat.	WOA	PSO	MFO	SHIO	ZOA	GWO	SCA	DOA	SCSO	GA	SA
F19	Mean	3.98E-01	3.98E-01	3.98E-01	3.98E-01	3.98E-01	3.98E-01	3.98E-01	3.98E-01	3.98E-01	6.83E+01	3.98E-01
	Std	2.21E-07	0.00E+00	0.00E+00	2.69E-07	3.86E-10	1.26E-06	5.25E-04	0.00E+00	6.17E-09	8.79E+00	1.50E-07
	Rank	8	1	1	11	5	12	19	1	6	22	9
F20	Mean	0.00E+00	0.00E+00	0.00E+00	0.00E+00	0.00E+00	0.00E+00	0.00E+00	0.00E+00	0.00E+00	1.29E+01	6.92E-05
	Std	0.00E+00	0.00E+00	0.00E+00	0.00E+00	0.00E+00	0.00E+00	0.00E+00	0.00E+00	0.00E+00	1.54E+01	1.45E-04
	Rank	1	1	1	1	1	1	1	1	1	22	20
F21	Mean	2.05E-04	0.00E+00	0.00E+00	8.26E-08	2.18E-13	6.65E-08	4.83E-04	0.00E+00	8.78E-10	3.42E-01	5.69E-05
	Std	5.55E-05	0.00E+00	0.00E+00	2.47E-08	4.88E-13	5.88E-08	2.62E-04	0.00E+00	1.36E-09	5.49E-01	6.64E-05
	Rank	17	1	1	9	5	8	19	1	6	22	14
F22	Mean	0.00E+00	8.89E+01	1.54E+02	4.12E+01	0.00E+00	0.00E+00	3.26E+00	0.00E+00	0.00E+00	3.23E+02	1.45E+02
	Std	0.00E+00	1.90E+01	6.20E+01	1.60E+01	0.00E+00	0.00E+00	5.98E+00	0.00E+00	0.00E+00	3.82E+01	8.18E+00
	Rank	1	18	21	17	1	1	13	1	1	22	20
F23	Mean	−8.78E+03	−6.58E+03	−8.66E+03	−5.72E+03	−6.99E+03	−6.38E+03	−3.97E+03	−4.57E+03	−6.88E+03	−2.21E+03	−8.64E+03
	Std	1.33E+03	5.45E+02	1.33E+03	4.34E+02	5.66E+02	5.77E+02	1.14E+02	1.98E+02	6.33E+02	6.28E+02	3.03E+02
	Rank	3	11	4	14	9	12	20	19	10	22	5
F24	Mean	−1.80E+00	−1.80E+00	−1.80E+00	−1.64E+00	−1.80E+00	−1.80E+00	−1.80E+00	−1.80E+00	−1.80E+00	−1.04E+00	−1.80E+00
	Std	1.62E-07	0.00E+00	0.00E+00	3.58E-01	2.79E-08	2.98E-07	1.90E-03	0.00E+00	4.82E-09	2.24E-01	2.74E-09
	Rank	9	1	1	18	7	11	16	1	5	22	6
F25	Mean	−4.32E+00	−4.11E+00	−4.38E+00	−4.51E+00	−4.64E+00	−4.35E+00	−2.98E+00	−4.05E+00	−3.76E+00	−1.51E+00	−4.67E+00
	Std	2.83E-01	8.04E-01	1.54E-01	1.68E-01	8.31E-02	4.77E-01	7.17E-01	6.51E-01	6.44E-01	2.99E-01	1.77E-02
	Rank	9	10	6	4	3	7	19	11	15	22	1
F26	Mean	−5.98E+00	−7.48E+00	−7.83E+00	−7.50E+00	−7.57E+00	−6.90E+00	−4.07E+00	−5.78E+00	−6.49E+00	−2.74E+00	−8.60E+00
	Std	4.85E-01	1.15E+00	7.97E-01	1.22E+00	4.68E-01	4.54E-01	5.77E-01	7.18E-01	3.23E-01	4.34E-01	9.26E-02
	Rank	13	8	4	7	6	9	19	15	11	22	1
F27	Mean	0.00E+00	0.00E+00	8.14E-04	0.00E+00	0.00E+00	0.00E+00	0.00E+00	0.00E+00	0.00E+00	6.47E-02	1.47E-05
	Std	0.00E+00	0.00E+00	1.82E-03	0.00E+00	0.00E+00	0.00E+00	0.00E+00	0.00E+00	0.00E+00	6.72E-02	2.79E-05
	Rank	1	1	21	1	1	1	1	1	1	22	20
F28	Mean	−1.03E+00	−1.03E+00	−1.03E+00	−1.03E+00	−1.03E+00	−1.03E+00	−1.03E+00	−1.03E+00	−1.03E+00	−8.69E-01	−1.03E+00
	Std	4.19E-12	0.00E+00	0.00E+00	1.86E-09	3.87E-11	1.17E-09	2.46E-05	1.92E-16	7.10E-11	1.73E-01	6.90E-08
	Rank	5	1	1	9	6	8	16	4	7	22	11
F29	Mean	0.00E+00	0.00E+00	0.00E+00	0.00E+00	0.00E+00	0.00E+00	0.00E+00	0.00E+00	0.00E+00	1.46E+00	1.93E-04
	Std	0.00E+00	0.00E+00	0.00E+00	0.00E+00	0.00E+00	0.00E+00	0.00E+00	0.00E+00	0.00E+00	2.61E+00	2.60E-04
	Rank	1	1	1	1	1	1	1	1	1	22	21
F30	Mean	2.44E-16	0.00E+00	0.00E+00	0.00E+00	0.00E+00	0.00E+00	0.00E+00	0.00E+00	0.00E+00	9.16E-01	1.92E-04
	Std	2.62E-16	0.00E+00	0.00E+00	0.00E+00	0.00E+00	0.00E+00	0.00E+00	0.00E+00	0.00E+00	1.87E+00	1.80E-04
	Rank	19	1	1	1	1	1	1	1	1	22	21
F31	Mean	−1.87E+02	−1.87E+02	−1.87E+02	−1.87E+02	−1.87E+02	−1.87E+02	−1.87E+02	−1.87E+02	−1.87E+02	−5.74E+01	−1.87E+02
	Std	8.11E-04	2.46E-14	1.42E-14	3.58E-02	8.29E-07	7.96E-02	4.10E-02	2.46E-14	6.57E-07	4.76E+01	1.87E-05
	Rank	10	3	1	11	5	12	17	3	6	22	7
F32	Mean	3.00E+00	3.00E+00	3.00E+00	3.00E+00	3.00E+00	1.92E+01	3.00E+00	3.00E+00	3.00E+00	2.25E+01	3.00E+00
	Std	6.77E-06	1.26E-15	1.31E-15	1.18E-05	1.99E-06	3.62E+01	3.87E-05	8.02E-15	2.02E-06	1.32E+01	1.72E-05
	Rank	8	1	1	12	6	21	14	4	7	22	13
F33	Mean	6.60E-04	4.69E-03	9.54E-04	8.59E-03	3.07E-04	8.36E-03	1.08E-03	8.52E-03	3.08E-04	2.29E-02	1.11E-03
	Std	3.35E-04	8.77E-03	3.92E-04	1.08E-02	5.63E-09	1.10E-02	4.31E-04	1.12E-02	3.13E-08	2.08E-02	2.89E-04
	Rank	5	17	9	21	1	18	12	20	2	22	13
F34	Mean	−7.09E+00	−8.12E+00	−1.02E+01	−7.65E+00	−1.02E+01	−9.13E+00	−5.02E+00	−6.08E+00	−4.22E+00	−7.45E-01	−1.01E+01
	Std	2.79E+00	2.78E+00	0.00E+00	3.53E+00	4.54E-05	2.28E+00	3.10E+00	2.27E+00	1.87E+00	4.94E-01	8.02E-03
	Rank	15	11	1	12	4	10	17	16	19	22	7
F35	Mean	−8.87E+00	−8.69E+00	−7.82E+00	−8.88E+00	−9.34E+00	−1.04E+01	−1.72E+00	−6.56E+00	−7.22E+00	−7.77E-01	−1.04E+01
	Std	3.41E+00	3.83E+00	3.64E+00	3.42E+00	2.38E+00	7.75E-05	1.82E+00	3.75E+00	2.90E+00	1.97E-01	1.28E-02
	Rank	10	12	14	9	8	3	20	16	15	22	5
F36	Mean	−5.20E+00	−1.05E+01	−5.94E+00	−8.91E+00	−1.05E+01	−1.05E+01	−4.03E+00	−9.08E+00	−8.37E+00	−9.00E-01	−1.05E+01
	Std	3.24E+00	8.88E-16	4.20E+00	3.63E+00	2.38E-05	8.65E-05	3.14E+00	2.33E+00	2.96E+00	8.38E-02	4.18E-02
	Rank	18	1	17	12	4	5	19	11	14	22	10

As we can see in Tables 14 and 15, the results over the 50 benchmark functions (F37–F50) highlight the strengths and occasional weaknesses of FVIMDE relative to these other approaches, showcasing where it excels and where it may need further refinement. For instance, in function F37, FVIMDE achieves a competitive mean value, ranking fourth among the 13 algorithms in the first table. This performance is noteworthy as it surpasses several well-known algorithms such as the Sine Cosine Algorithm (SCA), Ant Lion Optimizer (ALO), and the Chimp Optimizer. The result indicates FVIMDE's robustness in

dealing with this specific optimization problem, though it is slightly outperformed by PSO, MFO, and a few others.

Table 14. Comparison results over 50 benchmarks (F1–F18), run = 30, FES = 1000, agents No. = 30.

Function	Stat.	FVIMDE	FVIM	FLO	STOA	SOA	MVO	AO	SSOA	Chimp	CPO	ROA
F37	Mean	9.59E-02	1.46E+00	8.17E+00	1.30E+00	3.48E-01	1.18E-01	8.74E-01	1.36E+02	6.82E+00	2.15E+00	3.52E+00
	Std	2.10E-01	9.87E-01	6.22E+00	8.28E-01	3.02E-01	2.02E-01	5.92E-01	8.52E+01	4.63E+00	2.35E+00	2.00E+00
	Rank	4	13	19	12	7	6	9	21	18	15	16
F38	Mean	7.34E-04	2.21E-02	7.76E-01	8.64E+00	4.30E+01	6.89E-04	8.54E-02	5.48E+01	7.95E+00	2.70E-01	1.73E-01
	Std	1.48E-03	2.47E-02	1.10E+00	1.06E+01	6.22E+01	2.71E-04	5.26E-02	8.92E+01	9.78E+00	4.87E-01	2.49E-01
	Rank	2	8	15	19	21	1	10	22	18	14	12
F39	Mean	−3.86E+00	−3.86E+00	−3.72E+00	−3.86E+00	−3.86E+00	−3.86E+00	−3.86E+00	−3.29E+00	−3.85E+00	−3.86E+00	−3.84E+00
	Std	0.00E+00	3.30E-03	1.66E-01	3.50E-03	6.46E-04	1.59E-06	1.85E-03	4.57E-01	1.13E-03	7.69E-05	5.15E-02
	Rank	1	10	20	15	17	5	13	21	18	6	19
F40	Mean	−3.32E+00	−3.23E+00	−2.63E+00	−3.04E+00	−3.04E+00	−3.30E+00	−3.17E+00	−1.69E+00	−2.80E+00	−3.25E+00	−2.80E+00
	Std	1.46E-06	5.32E-02	8.85E-02	5.22E-02	5.23E-02	5.36E-02	7.57E-02	5.77E-01	5.38E-01	6.60E-02	5.89E-01
	Rank	1	12	20	17	16	5	13	21	19	10	18
F41	Mean	3.19E-03	4.34E-03	0.00E+00	7.96E-03	0.00E+00	5.71E-01	0.00E+00	0.00E+00	2.42E-02	0.00E+00	0.00E+00
	Std	5.28E-03	5.99E-03	0.00E+00	1.25E-02	0.00E+00	4.50E-02	0.00E+00	0.00E+00	3.74E-02	0.00E+00	0.00E+00
	Rank	12	14	1	15	1	19	1	1	17	1	1
F42	Mean	1.20E+01	4.59E-14	4.44E-16	2.00E+01	2.00E+01	1.59E+00	4.44E-16	4.44E-16	2.00E+01	4.44E-16	4.57E-13
	Std	1.09E+01	3.89E-15	0.00E+00	1.23E-03	3.28E-03	1.10E+00	0.00E+00	0.00E+00	8.03E-04	0.00E+00	9.98E-13
	Rank	16	11	1	20	19	14	1	1	21	1	12
F43	Mean	1.25E-01	1.32E-01	1.57E-32	1.66E-01	2.80E-01	2.79E+00	2.84E-07	9.12E-01	4.07E-01	1.40E-03	2.13E-06
	Std	8.35E-02	5.83E-02	0.00E+00	7.03E-02	9.86E-02	2.14E+00	3.37E-07	6.05E-02	2.30E-01	3.10E-03	2.64E-06
	Rank	10	11	1	12	13	19	3	18	15	5	4
F44	Mean	1.05E+00	1.13E+00	1.35E-32	1.98E+00	2.03E+00	6.51E-02	7.55E-06	2.92E+00	2.88E+00	1.55E-03	8.39E-05
	Std	1.82E-01	3.46E-01	0.00E+00	1.11E-01	2.28E-01	2.30E-02	7.16E-06	4.38E-02	1.25E-01	3.46E-03	1.29E-04
	Rank	9	10	1	13	14	6	2	17	16	4	3
F45	Mean	−1.08E+00	−1.08E+00	−5.06E-01	−9.31E-01	−9.31E-01	−1.08E+00	−1.08E+00	−1.82E-01	−7.80E-01	−9.86E-01	−1.08E+00
	Std	0.00E+00	7.33E-08	3.08E-01	3.36E-01	3.36E-01	7.82E-08	1.44E-04	7.30E-02	4.12E-01	6.09E-02	6.36E-06
	Rank	1	9	20	18	17	8	12	22	19	16	10
F46	Mean	−1.38E+00	−1.39E+00	−5.14E-01	−1.85E-01	−9.49E-01	−9.32E-01	−1.11E+00	−2.04E-01	−5.66E-01	−5.60E-01	−3.83E-01
	Std	2.65E-01	2.39E-01	2.68E-01	1.86E-01	5.11E-01	2.43E-02	3.59E-01	2.65E-01	9.52E-02	1.33E-01	3.01E-01
	Rank	3	2	17	21	11	12	5	20	15	16	19
F47	Mean	−5.76E-01	−5.18E-01	−1.32E-03	−4.73E-02	−3.77E-02	−4.23E-01	−4.59E-01	−5.91E-05	−7.45E-02	−2.22E-01	−1.47E-02
	Std	2.08E-01	1.85E-01	2.64E-03	4.93E-02	3.37E-02	8.49E-02	2.13E-01	1.02E-04	4.48E-02	1.43E-01	2.71E-02
	Rank	2	3	20	15	17	10	7	21	14	13	19
F48	Mean	0.00E+00	2.14E-04	3.99E+01	4.50E-02	5.87E-02	1.75E-05	7.93E-02	3.80E+01	1.41E+02	1.41E+00	3.72E-02
	Std	0.00E+00	1.16E-04	5.50E+01	3.45E-02	6.13E-02	1.04E-05	6.18E-02	1.02E+01	3.15E+02	3.16E+00	2.49E-02
	Rank	1	11	21	14	15	9	16	20	22	18	12
F49	Mean	9.66E+01	4.14E+01	1.84E+04	1.63E+03	9.51E+02	7.49E+02	7.01E+02	3.79E+04	1.51E+02	4.04E+02	8.02E+03
	Std	8.59E+01	8.20E+01	5.69E+03	1.49E+03	9.67E+02	9.36E+02	9.92E+02	2.71E+04	9.68E+01	6.29E+02	1.26E+04
	Rank	3	2	21	16	15	14	13	22	5	11	20
F50	Mean	1.79E+03	2.50E+04	1.63E+05	9.75E+03	6.96E+03	4.77E+02	4.93E+03	2.26E+05	3.47E+04	2.89E+04	1.01E+05
	Std	2.59E+03	1.58E+04	8.57E+04	7.48E+03	5.59E+03	8.69E+02	3.72E+03	3.44E+04	2.07E+04	2.46E+04	3.61E+04
	Rank	2	15	21	10	8	1	7	22	17	16	20

In function F38, FVIMDE ranks second, closely trailing behind the leading optimizer, which is a remarkable achievement given the challenging nature of this function. This shows that FVIMDE is particularly effective at finding near-optimal solutions quickly, outperforming many other methods, including STOA, ZOA, and DOA, which rank significantly lower in comparison. Function F39 further highlights FVIMDE's effectiveness, where it secures the top rank with a mean of −3.86, which matches the best-performing algorithms in this category. This outcome underscores FVIMDE's consistency and reliability in maintaining optimal or near-optimal performance across different trials. It also highlights its superiority over algorithms like MVO and AO, which rank lower in this function.

In function F40, FVIMDE also achieves the top rank with the best mean value, indicating its strength in solving optimization problems with complex landscapes. This performance is particularly impressive when compared to traditional algorithms like PSO, which ranked 14th, and GA, which ranked 22nd. FVIMDE's top ranking in this function suggests its superior ability to explore and exploit the search space effectively. On the other hand, there are functions where FVIMDE does not perform as strongly. For instance, in function F41, FVIMDE ranks 12th, which is relatively low compared to its usual per-

formance. This suggests that while FVIMDE is highly effective across many functions, there are still scenarios where other algorithms, such as PSO and GA, outperform it. This indicates potential areas for improvement or modifications to the algorithm to enhance its performance in such cases.

Functions F42 and F43 present mixed results for FVIMDE. In F42, FVIMDE achieves a mid-tier ranking, coming in at 16th. While it does not top the chart, it remains competitive, especially when considering that it outperforms several other advanced algorithms like STOA and Chimp Optimizer. In F43, however, FVIMDE ranks 10th, which indicates a solid performance but again shows room for improvement when compared to the top-performing algorithms in this function. Notably, in functions F44 and F45, FVIMDE ranks ninth and first, respectively. In the case of functions F46 to F50, FVIMDE continues to show competitive performance, particularly in F46 where it ranks third, and F50 where it ranks second. These results underscore FVIMDE's robustness and versatility across a wide range of optimization challenges. However, in functions like F47 and F49, FVIMDE's performance is somewhat less competitive, with rankings of 12th and 3rd, respectively, suggesting that while FVIMDE is generally strong, it may occasionally struggle with specific types of problems or landscapes.

Table 15. Comparison results over 50 benchmarks (F1–F18), run = 30, FES = 1000, agents No. = 30.

Function	Stat.	WOA	PSO	MFO	SHIO	ZOA	GWO	SCA	DOA	SCSO	GA	SA
F37	Mean	9.49E+00	4.16E-03	1.07E-01	5.65E+00	4.76E-02	5.63E-01	8.80E-01	1.53E+00	1.19E+00	1.86E+02	5.64E-02
	Std	6.97E+00	2.57E-03	2.15E-01	5.64E+00	6.53E-02	6.47E-01	4.80E-01	3.37E+00	8.37E-01	3.86E+02	5.81E-02
	Rank	20	1	5	17	2	8	10	14	11	22	3
F38	Mean	9.97E-01	7.47E-04	1.07E-02	4.74E-02	1.33E-03	4.65E-03	4.68E+00	1.13E-01	1.93E-01	1.43E+01	1.40E-02
	Std	1.13E+00	1.30E-03	1.15E-02	7.66E-02	1.08E-03	2.35E-03	8.74E+00	2.52E-01	3.86E-01	1.31E+01	1.29E-02
	Rank	16	3	6	9	4	5	17	11	13	20	7
F39	Mean	−3.86E+00	−3.86E+00	−3.86E+00	−3.86E+00	−3.86E+00	−3.86E+00	−3.86E+00	−3.86E+00	−3.86E+00	−3.12E+00	−3.86E+00
	Std	3.02E-03	3.52E-03	0.00E+00	1.16E-03	2.19E-04	2.28E-03	2.44E-03	3.85E-16	4.31E-03	5.32E-01	4.30E-07
	Rank	12	11	1	8	7	9	16	1	14	22	4
F40	Mean	−3.27E+00	−3.12E+00	−3.23E+00	−3.32E+00	−3.32E+00	−3.25E+00	−3.07E+00	−3.29E+00	−3.26E+00	−1.46E+00	−3.32E+00
	Std	1.07E-01	1.73E-01	5.32E-02	3.79E-06	5.87E-05	1.06E-01	7.40E-02	2.19E-02	8.64E-02	3.89E-01	6.43E-04
	Rank	7	14	11	2	3	9	15	6	8	22	4
F41	Mean	0.00E+00	1.87E-02	1.82E+01	3.72E-03	0.00E+00	0.00E+00	2.82E-01	0.00E+00	0.00E+00	4.19E+02	5.02E+01
	Std	0.00E+00	7.09E-03	4.06E+01	8.33E-03	0.00E+00	0.00E+00	1.34E-01	0.00E+00	0.00E+00	7.39E+01	6.94E+00
	Rank	1	16	20	13	1	1	18	1	1	22	21
F42	Mean	1.87E-15	3.42E-05	1.97E+01	7.55E-15	4.44E-16	1.61E-14	9.51E+00	4.44E-16	4.44E-16	2.01E+01	1.41E+01
	Std	1.95E-15	3.49E-05	3.37E-01	0.00E+00	0.00E+00	3.18E-15	9.31E+00	0.00E+00	0.00E+00	4.90E-01	1.26E+00
	Rank	8	13	18	9	1	10	15	1	1	22	17
F43	Mean	9.26E-03	6.00E-11	5.12E+07	2.96E-01	1.12E-01	4.72E-02	7.96E-01	7.05E-01	6.73E-02	1.56E+08	2.45E+05
	Std	9.51E-03	1.29E-10	1.14E+08	1.75E-01	3.24E-02	4.37E-02	3.52E-01	2.20E-01	3.75E-02	1.37E+08	2.79E+05
	Rank	6	2	21	14	9	7	17	16	8	22	20
F44	Mean	2.33E-01	2.20E-03	5.12E+07	1.62E+00	2.06E+00	5.21E-01	5.69E+00	2.93E+00	1.94E+00	2.12E+08	1.49E+05
	Std	8.93E-02	4.91E-03	1.14E+08	4.42E-01	3.38E-01	2.58E-01	4.74E+00	1.44E-01	5.06E-01	1.31E+08	1.81E+05
	Rank	7	5	21	11	15	8	19	18	12	22	20
F45	Mean	−1.08E+00	−1.08E+00	−1.08E+00	−1.08E+00	−1.01E+00	−1.08E+00	−1.08E+00	−1.07E+00	−1.08E+00	−4.06E-01	−1.08E+00
	Std	5.60E-13	0.00E+00	0.00E+00	8.05E-08	1.69E-01	2.63E-08	1.74E-04	3.38E-02	8.96E-10	3.49E-01	6.11E-06
	Rank	4	1	1	7	15	6	13	14	5	21	11
F46	Mean	−7.45E-01	−9.86E-01	−1.02E+00	−1.50E+00	−1.08E+00	−1.08E+00	−4.73E-01	−7.50E-01	−1.01E+00	−6.34E-03	−1.24E+00
	Std	2.24E-01	2.91E-01	4.60E-01	8.02E-06	3.85E-01	4.23E-01	1.36E-01	4.98E-01	2.87E-01	1.05E-02	3.39E-01
	Rank	14	10	8	1	6	7	18	13	9	22	4
F47	Mean	−2.35E-01	−4.86E-01	−3.46E-01	−4.56E-01	−4.25E-01	−5.06E-01	−4.11E-02	−1.70E-02	−5.02E-01	−4.65E-06	−6.01E-01
	Std	1.22E-01	2.82E-01	1.19E-01	2.16E-01	2.38E-01	1.88E-01	2.86E-02	1.29E-02	2.72E-01	6.34E-06	1.64E-01
	Rank	12	6	11	8	9	4	16	18	5	22	1
F48	Mean	2.12E-08	0.00E+00	0.00E+00	3.78E-02	3.36E-06	1.23E-04	5.45E-01	0.00E+00	2.77E-06	1.46E+00	6.06E-06
	Std	3.59E-08	0.00E+00	0.00E+00	7.75E-02	5.88E-06	8.29E-05	6.33E-01	0.00E+00	2.64E-06	1.70E+00	8.25E-06
	Rank	5	1	1	13	7	10	17	1	6	19	8
F49	Mean	5.79E+02	2.04E+02	1.03E+02	2.15E+02	1.88E+03	2.15E+02	2.10E+02	2.95E+03	2.02E+02	5.36E+03	2.95E+01
	Std	1.01E+03	1.09E+02	1.36E+02	2.33E+02	1.56E+03	2.30E+02	1.05E+02	3.49E+03	2.31E+02	7.59E+03	2.01E+01
	Rank	12	7	4	9	17	10	8	18	6	19	1
F50	Mean	1.24E+04	1.63E+04	3.00E+03	1.48E+04	1.57E+04	2.84E+03	8.25E+03	4.21E+04	4.55E+03	7.55E+04	2.38E+03
	Std	1.72E+04	1.73E+04	2.42E+03	2.38E+04	1.38E+04	2.78E+03	3.20E+03	2.56E+04	4.90E+03	2.90E+04	9.10E+02
	Rank	11	14	5	12	13	4	9	18	6	19	3

6.5. Experiments of Hybrid FVIM with DE Components

In this section, we present a series of experiments designed to evaluate the impact of different components of the Differential Evolution (DE) algorithm when combined with the hybrid FVIM (Four-Variable Inertia Method).

The DE algorithm is composed of three main operators: mutation, crossover, and selection, each contributing uniquely to the exploration and exploitation capabilities of the algorithm. By selectively removing or retaining these components in the hybrid approach, we aim to investigate their effects on optimization performance. These experiments provide valuable insights into how each DE component influences the solution quality in the hybrid FVIM framework.

Table 16 shows the results of the experiments comparing different DE components such as mutation only (FVIMMU), crossover only (FVIMCR), selection only (FVIMSE), and a combination of mutation and crossover (FVIMMUCR) across multiple benchmark functions (F1 to F12).

The results reveal that the full hybrid FVIMDE consistently outperforms the other configurations, securing the best rank across most functions. Configurations that exclude one or more DE components generally exhibit poorer performance, with FVIMMUCR (mutation and crossover) often ranking among the lowest, especially in more complex functions.

The results highlight the importance of integrating all DE components (mutation, crossover, and selection) to achieve better optimization outcomes, as evidenced by FVIMDE's superior results in terms of mean performance and ranking across the majority of the benchmark functions.

The experimental results demonstrate that including each DE component in isolation (mutation, crossover, or selection) generally led to worse optimization performance compared to the full integration of all components in the hybrid FVIMDE. This outcome can be attributed to the individual weaknesses of each component when applied alone.

Mutation only (FVIMMU): Mutation introduces diversity by perturbing existing solutions, which helps explore the search space. However, without crossover, mutation alone lacks the ability to effectively combine good traits from different solutions. This limitation can lead to slower convergence and an inability to escape local optima, as the algorithm relies solely on random variations rather than guided search.

Crossover only (FVIMCR): Crossover is designed to recombine existing solutions to explore new areas of the search space. However, when used in isolation, it tends to exploit the current population without introducing new diversity. Without mutation, crossover alone may quickly converge to suboptimal solutions, as it lacks the ability to explore beyond the recombined solutions' neighborhood.

Selection only (FVIMSE): Selection ensures that only the best solutions survive to the next generation, promoting convergence. However, without mutation or crossover, the algorithm has no mechanism to generate new solutions or explore the search space. Selection alone essentially preserves the best solutions from the initial population without improving them, leading to stagnation and poor optimization results.

Mutation and Crossover (FVIMMUCR): While combining mutation and crossover provides both exploration and recombination, the absence of selection weakens this configuration. Without selection, the algorithm lacks the necessary pressure to favor better solutions, leading to the retention of poor candidates and reducing the overall effectiveness of the search process.

The crossover plays a role in balancing between exploration, utilizing the diversity introduced by mutation, and exploitation; in addition, crossover does not directly introduce diversity but rather controls the level of diversity generated through mutation, striking a balance between exploration and intensification.

The results emphasize that each DE component plays a crucial role in balancing exploration and exploitation. The absence of any component limits the algorithm's ability to effectively optimize the search space, leading to worse performance. The full hybrid

FVIMDE, which integrates mutation, crossover, and selection, leverages the strengths of each component, resulting in better convergence and solution quality.

Table 16. Results of hybrid FVIM with DE components, FES = 1000, agents = 30.

Function	Statistics	FVIMDE	FVIMMU	FVIMCR	FVIMSE	FVIMMUCR
F1	Mean	3.01E+02	1.14E+04	9.12E+02	1.10E+03	1.39E+03
	Std	5.66E-01	5.46E+04	8.24E+02	1.15E+03	1.49E+03
	SEM	1.03E-01	9.98E+03	1.50E+02	2.09E+02	2.72E+02
	Rank	1	6	3	4	5
F2	Mean	4.06E+02	4.75E+02	4.18E+02	4.31E+02	6.98E+02
	Std	2.49E+00	3.10E+02	2.10E+01	2.86E+01	1.06E+03
	SEM	4.55E-01	5.67E+01	3.84E+00	5.23E+00	1.94E+02
	Rank	2	5	3	4	6
F3	Mean	6.00E+02	6.08E+02	6.06E+02	6.06E+02	6.10E+02
	Std	8.20E-02	6.66E+00	5.11E+00	3.95E+00	1.92E+01
	SEM	1.50E-02	1.22E+00	9.33E-01	7.22E-01	3.51E+00
	Rank	1	5	4	3	6
F4	Mean	8.11E+02	8.46E+02	8.25E+02	8.24E+02	8.26E+02
	Std	4.92E+00	4.02E+01	9.11E+00	8.66E+00	1.08E+01
	SEM	8.98E-01	7.34E+00	1.66E+00	1.58E+00	1.97E+00
	Rank	1	6	4	3	5
F5	Mean	9.00E+02	1.27E+03	9.62E+02	9.58E+02	9.51E+02
	Std	4.83E-02	8.89E+02	6.45E+01	5.38E+01	4.55E+01
	SEM	8.81E-03	1.62E+02	1.18E+01	9.83E+00	8.31E+00
	Rank	1	6	5	4	3
F6	Mean	1.80E+03	1.06E+07	6.32E+03	6.58E+03	1.23E+08
	Std	1.86E+00	4.26E+07	2.27E+03	2.07E+03	4.17E+08
	SEM	3.40E-01	7.78E+06	4.15E+02	3.79E+02	7.61E+07
	Rank	2	5	3	4	6
F7	Mean	2.02E+03	2.05E+03	2.04E+03	2.04E+03	2.04E+03
	Std	8.07E+00	5.92E+01	1.70E+01	1.09E+01	2.70E+01
	SEM	1.47E+00	1.08E+01	3.11E+00	1.98E+00	4.94E+00
	Rank	1	6	5	3	4
F8	Mean	2.21E+03	2.25E+03	2.23E+03	2.22E+03	2.23E+03
	Std	6.07E+00	8.62E+01	3.72E+00	3.96E+00	1.72E+01
	SEM	1.11E+00	1.57E+01	6.79E-01	7.23E-01	3.13E+00
	Rank	1	6	4	3	5
F9	Mean	2.53E+03	2.57E+03	2.55E+03	2.55E+03	2.55E+03
	Std	5.83E-09	1.19E+02	3.33E+01	1.98E+01	2.40E+01
	SEM	1.06E-09	2.18E+01	6.09E+00	3.61E+00	4.37E+00
	Rank	1	6	4	3	5
F10	Mean	2.51E+03	2.56E+03	2.56E+03	2.55E+03	2.60E+03
	Std	3.36E+01	1.06E+02	6.30E+01	6.43E+01	1.99E+02
	SEM	6.13E+00	1.94E+01	1.15E+01	1.17E+01	3.63E+01
	Rank	1	4	5	3	6
F11	Mean	2.60E+03	2.97E+03	2.84E+03	2.86E+03	2.84E+03
	Std	1.22E-01	4.92E+02	1.98E+02	2.08E+02	2.83E+02
	SEM	2.23E-02	8.98E+01	3.61E+01	3.79E+01	5.17E+01
	Rank	1	6	4	5	3
F12	Mean	2.86E+03	2.89E+03	2.86E+03	2.86E+03	2.90E+03
	Std	1.43E+00	6.91E+01	2.08E+00	1.74E+00	8.50E+01
	SEM	2.60E-01	1.26E+01	3.81E-01	3.18E-01	1.55E+01
	Rank	1	5	3	4	6

6.6. FVIMDE Convergence Diagram

The convergence curves for the CEC2022 benchmark Functions F1 through F6, as shown in Figure 2, illustrate how the FVIMDE optimizer performs across different types of optimization challenges. The curve for Function F1, a unimodal shifted and fully rotated Zakharov function, demonstrates a rapid initial decrease in the best value obtained. This behavior is typical for unimodal functions, where a direct approach can quickly lead to the global minimum. Function F2, a multimodal shifted and fully rotated Rosenbrock

function, shows a steep initial drop followed by a slower, more gradual descent. Moreover, Function F3, the shifted and fully rotated expanded Schaffer F6 Function, displays a more consistent and gradual descent, reflecting its multimodal landscape filled with numerous local optima that challenge FVIMDE's differentiation between local and global minima. Similarly, Function F4, the shifted and fully rotated non-continuous Rastrigin function, shows rapid early improvements that slows as the search continues, which is characteristic of a function landscape dotted with many local optima and the added complexity of non-continuity.

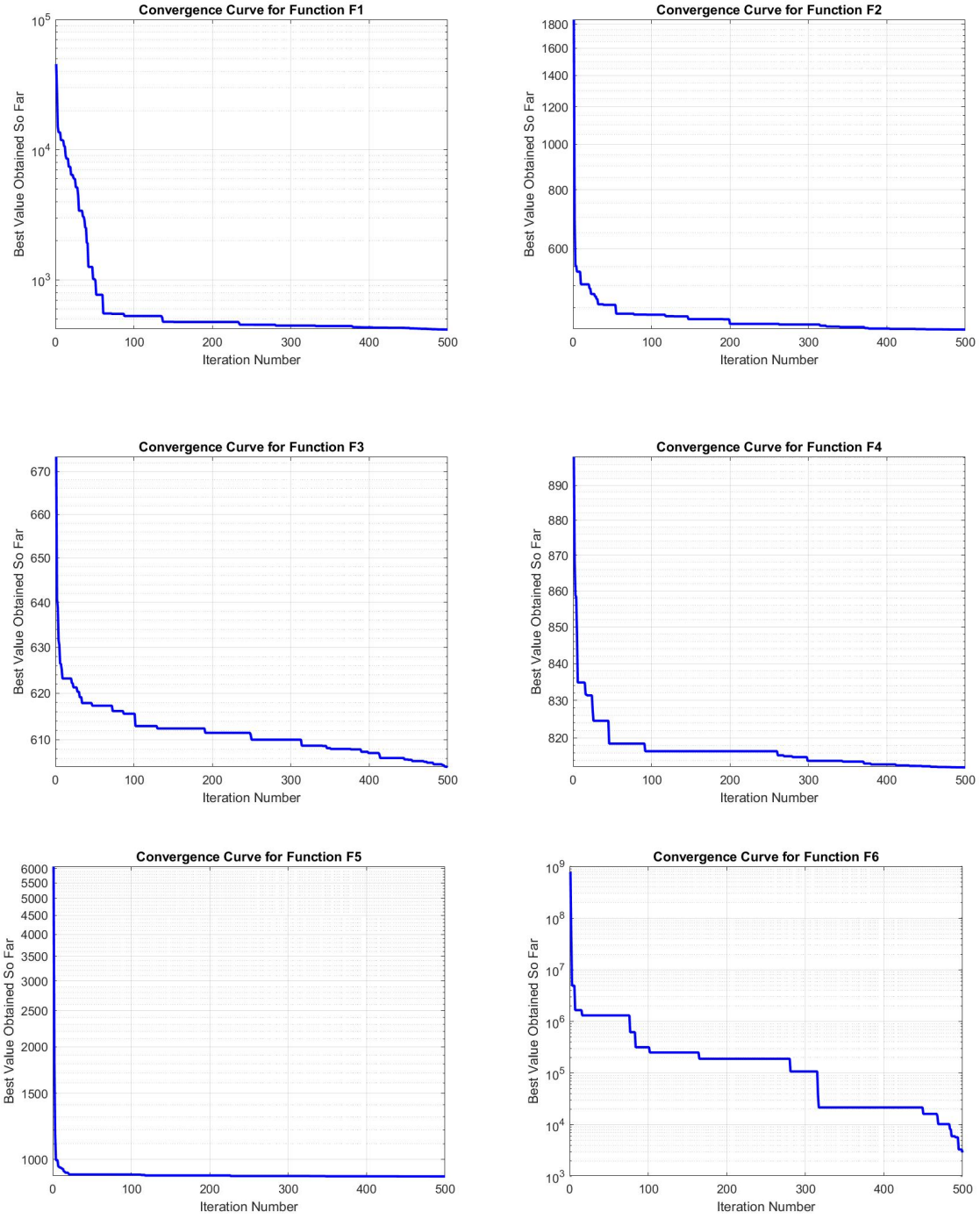

Figure 2. Convergence diagram over CEC2022 benchmark functions (F1–F6).

Function F5, the shifted and fully rotated Levy function, presents a very sharp initial improvement that plateaus—a pattern resulting from the function's long, narrow valleys, which require precise movements to reach the global minimum. Moreover, Function F6's curve, representing a hybrid function, shows several plateaus indicative of the diverse function landscape it comprises, testing both the exploitation and exploration capabilities of FVIMDE.

The convergence curves for Functions F7 to F12, as shown in Figure 3, illustrate how FVIMDE performs across hybrid and composition functions. The curve for Function F7, a hybrid function, showcases a sharp initial descent and subsequent gradual improvements, suggesting that FVIMDE quickly locates a promising region but then switches to a more cautious approach to refine its search towards the global optimum. This indicates a balanced capability in exploring new areas and exploiting known good solutions.

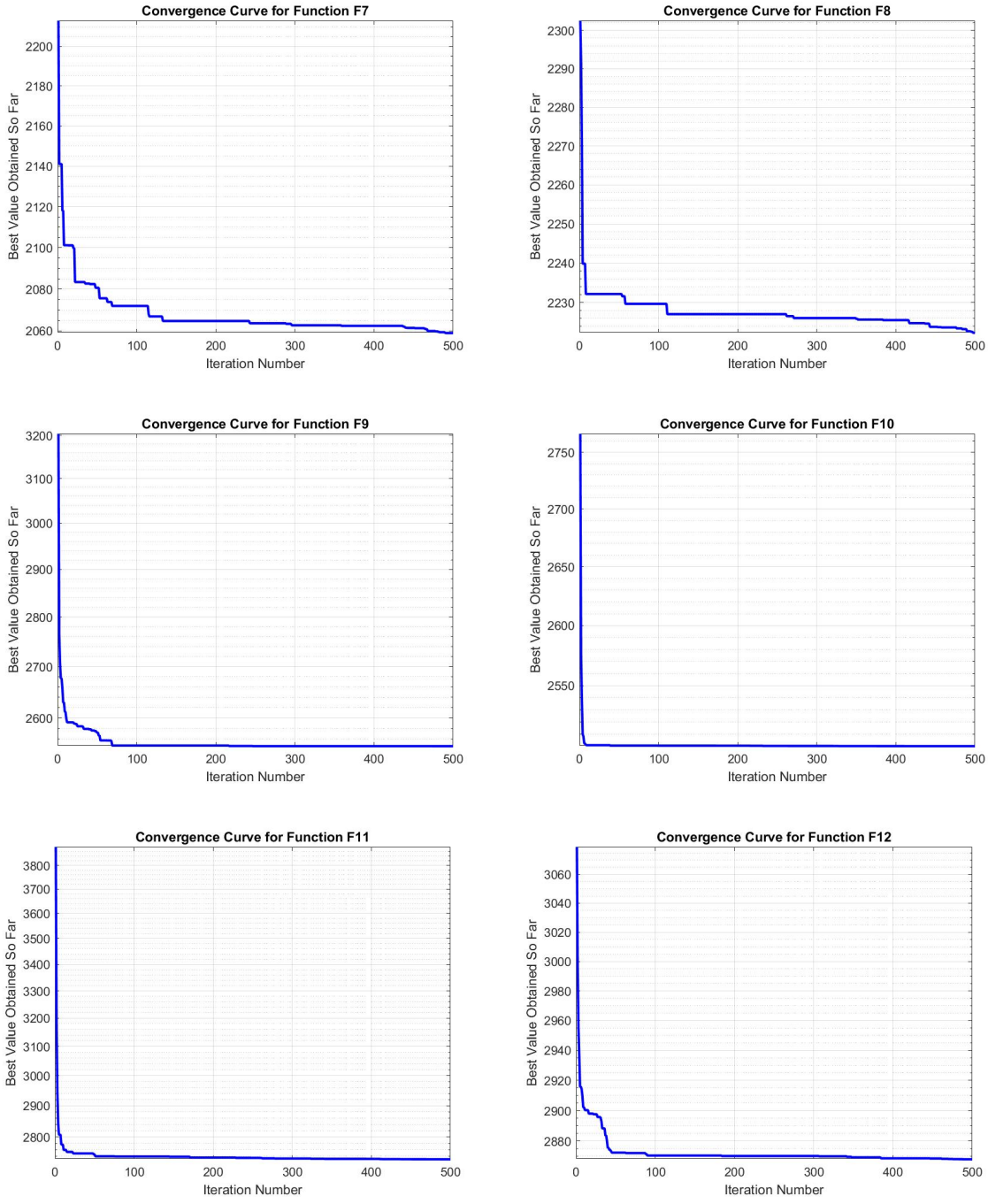

Figure 3. Convergence diagram over CEC2022 benchmark functions (F7–F12).

Similarly, Function F8's convergence curve also begins with a steep drop but features fewer pronounced steps, which might point to a smoother landscape or more effective navigation strategies employed by FVIMDE. The relative flatness after the initial improvement might reflect fewer local optima or a more unified region drawing the optimizer toward the global optimum.

For Function F9, a composition function, the curve displays a rapid initial decline followed by a prolonged, slow convergence, reflecting FVIMDE's ability to quickly identify viable paths to the optimum. However, the complexity of the composition, likely involving multiple overlapping functions, necessitates meticulous adjustments to fine-tune the solution.

Function F10's curve, similar to F9, shows a steep initial descent that transitions into a steady, albeit slower, progression towards the minimum. This pattern underlines FVIMDE's proficiency in managing simultaneous optimization challenges presented by composition functions, effectively handling the layered landscapes.

The convergence behavior for Function F11 mirrors that of Function F10 with a sharp initial drop. However, the extended plateau in the later stages of the iterations suggests a demanding optimization landscape where further improvements become increasingly difficult as FVIMDE approaches the vicinity of the global optimum.

Moreover, the curve for Function F12 depicts a gradual but consistent decline throughout the iterations, suggesting continuous, incremental improvements. This indicates either a complex but navigable landscape or that FVIMDE consistently makes small gains that cumulatively bring it closer to the optimum without major disruptions.

7. Solving Engineering Design Optimization Problems Using FVIMDE

In the realm of structural engineering, the design optimization issues are typically categorized as Constrained Optimization Problems (COPs), which exhibit a high degree of nonlinearity and involve numerous design variables under complex constraints. This nonlinearity often leads to a multimodal response landscape. To address this, metaheuristic global optimization algorithms are often employed to find optimal solutions.

Constrained Optimization

A COP generally involves an objective function in conjunction with various equality and inequality constraints. It also often includes specified lower and upper bounds for the design variables. For a situation involving n design variables, the COP can be expressed in the following manner:

The objective function $f(\mathbf{X})$ is the target for minimization. Here, $g_i(\mathbf{X})$ and $h_k(\mathbf{X})$ represent the inequality and equality constraint functions, respectively, with m inequality constraints and p equality constraints. The problem becomes a nonlinear optimization problem if at least one of the functions $f(\mathbf{X})$, $g_i(\mathbf{X})$, or $h_k(\mathbf{X})$ is nonlinear.

$$\begin{aligned} &\text{Minimize:} \quad f(\mathbf{X}) \\ &\text{Subject to:} \\ &g_i(\mathbf{X}) \leq 0, \quad i = 1, 2, \ldots, m \\ &h_k(\mathbf{X}) = 0, \quad k = 1, 2, \ldots, p \\ &a_j \leq x_j \leq b_j, \quad j = 1, \ldots, n \\ &\mathbf{X} = (x_1, x_2, \ldots, x_n) \end{aligned} \tag{19}$$

Metaheuristic algorithms are generally devised for both constrained and unconstrained search spaces. However, to apply these algorithms to COPs, additional mechanisms are required to integrate the constraints into their objective function. In addressing COPs, it becomes essential to manage both feasible and infeasible solutions, with greater emphasis on the latter. Although completely ignoring infeasible solutions could simplify the process, such an approach might lead to the loss of potentially valuable information

about certain promising areas within the function landscape. To circumvent this issue, a traditional method involves imposing a penalty for infeasible solutions. This method includes a constraint violation in the penalized candidate solutions, effectively transforming them into an unconstrained objective function, which is then optimized using techniques suited for unconstrained optimization.

The measure of how much a candidate solution $\mathbf{X}$ deviates from the given constraints is defined as the constraint violation $V(\mathbf{X})$, as shown in Equations (20) and (21). The evaluation of this violation in the COP typically utilizes the (22) equations.

$$V(\mathbf{X}) = \begin{cases} 0, & \text{if } \mathbf{X} \in F \\ > 0, & \text{if } \mathbf{X} \notin F \end{cases}, \text{where } F \text{ is the feasible region} \tag{20}$$

$$V(\mathbf{X}) = \max\left(\max_i\{0, g_i(\mathbf{X})\}, \max_k\{|h_k(\mathbf{X})|\}\right) \tag{21}$$

$$V(\mathbf{X}) = \sum_i \max\{0, g_i(\mathbf{X})\}^m + \sum_k |h_k(\mathbf{X})|^m \tag{22}$$

In COP, the technique of constraint handling is a critical criterion to achieve the optimal solution within the feasible region, if such a region exists. This approach primarily aims to exploit infeasible candidate solutions and extract useful information for the stochastic search process. For managing constraints, Deb's rules [58] are employed, considering both the constraint violation and the value of the objective function.

Handling active constraints in COPs presents significant challenges. All equality constraints are inherently active, and for inequality constraints, those which satisfy $g_i(\mathbf{X}) = 0$ at the global optimum are deemed active constraints. Hence, issues involving equality constraints require cautious handling to ensure high-quality solutions. A common practice is to transform equality constraints into inequality constraints. This transformation often involves a variety of techniques, one of which is the use of a tolerance parameter (tp). This parameter assists in converting equality constraints into their inequality counterparts. Thus, the constraints of Equation (19) can be expressed as follows. Let G_{ineq} denote the set of constraints, where the set is defined as:

$$G_{\text{ineq}} = \{\mathbf{X} \in \mathbb{R}^n : g_i(\mathbf{X}) \leq 0,\ i = 1, \ldots, m \text{ and } |h_i(\mathbf{X}) - tp| \leq 0,\ i = 1, \ldots, p\} \tag{23}$$

where tp is the tolerance parameter for the equality constraints represented by function h_i. The objective is to minimize the fitness function $f(\mathbf{X})$ subject to the constraints in G_{ineq}:

$$\min_{\mathbf{X}} f(\mathbf{X}) \quad \text{subject to} \quad \mathbf{X} \in G_{\text{ineq}} \tag{24}$$

8. Application FVIM to Solve Structural Engineering Design Problems

This section demonstrates the effectiveness of FVIMDE algorithms through the resolution of five structural engineering design problems. The performance is compared with state-of-the-art and metaheuristic algorithms.

8.1. Experimental Setup

The parameter settings for all engineering problems are shown in Table 17.

Table 17. Evaluation parameters summary.

Parameter	Details
Stopping criterion	Maximum of 1000 function evaluations
Runs	30 independent runs
Statistical results	Best (BEST), mean (MEAN), worst (WORST), and standard deviation (SD)

In the engineering design problems, the FVIMDE has been compared with various optimization algorithms. The algorithms evaluated encompass: Moth-Flame Optimization (MFO) [53], Whale Optimization Algorithm (WOA) [51], Multi-Verse Optimizer (MVO) [50], Sine Cosine Algorithm (SCA) [52], Equilibrium Optimizer (EO) [59], Henry Gas Solubility Optimization (FOX) [60], Sea-Horse optimizer (SHO) [61], Artificial hummingbird algorithm [35], Reptile Search Algorithm (RSA) [62], and Dragonfly algorithm [63].

8.1.1. Tension/Compression Spring Design Problem

The Tension/Compression Spring Design Problem (See Figure 4)is a pivotal optimization challenge in mechanical engineering, aiming to minimize the spring's weight while adhering to various physical and geometric constraints [64]. This entails optimizing key design variables such as wire diameter, mean coil diameter, and the number of active coils, which influence the spring's mechanical properties. The choice of material also plays a critical role in determining the spring's strength and resilience, with manufacturing considerations impacting the feasibility and cost-effectiveness of the design. Engineers tackle this problem using a blend of analytical methods, empirical formulas, and computational techniques like finite element analysis to simulate the spring's performance under load, and optimization algorithms to efficiently navigate the design space. The ultimate goal is to develop a spring that meets specific load-bearing requirements, durability standards, and application-specific conditions, embodying the integration of theoretical principles, practical constraints, and advanced optimization strategies in engineering design.

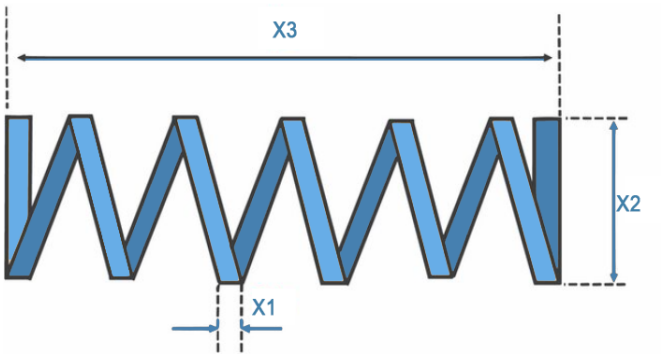

Figure 4. Tension/compression spring design problem.

The primary goal is to minimize the fabrication cost of a spring, governed by three parameters and four constraints. These include wire diameter (x_1), spring coil diameter (x_2), number of active coils (x_3), and constraints related to deflection ($g_1(\mathbf{X})$), shear stress ($g_2(\mathbf{X})$), surge frequency ($g_3(\mathbf{X})$), and outer diameter limit ($g_4(\mathbf{X})$).

The mathematical formulation of the problem is as follows:

Let $LB = [lb_1, lb_2, lb_3]$ and $UB = [ub_1, ub_2, ub_3]$ denote the lower and upper bounds of the design variables, respectively. Here, lb_i and ub_i represent the lower and upper bounds of the ith design variable. Vio denotes any violation conditions, and Obj represents the objective function to be minimized. The global minimum achieved is denoted by $GloMin$.

The objective function, denoted as z, is defined as:

$$z = x_1^2 \cdot x_2 \cdot (x_3 + 2)$$

where x_1, x_2, and x_3 are the design variables representing certain characteristics of the spring.

Constraints g are defined as follows:

$$g_1(x) = 1 - \frac{x_2^3 \cdot x_3}{71785 \cdot x_1^4} \geq 0$$
$$g_2(x) = \frac{4 \cdot x_2^2 - x_1 \cdot x_2}{12566 \cdot (x_2 \cdot x_1^3 - x_1^4)} + \frac{1}{5108 \cdot x_1^2} - 1 \geq 0$$
$$g_3(x) = 1 - \frac{140.45 \cdot x_1}{x_2^2 \cdot x_3} \geq 0$$
$$g_4(x) = \frac{x_1 + x_2}{1.5} - 1 \geq 0$$

where $g_i(x)$ represents the ith constraint function, and x_1, x_2, and x_3 are the design variables.

The lower and upper bounds for the design variables are defined by LB and UB, respectively, and any other conditions such as violation conditions are defined by Vio.

As can be seen in Table 18 for the Tension/Compression Spring Design Problem, the FVIMDE optimizer resulted in efficient outcomes. An analysis of the results demonstrates that the mean objective function value obtained by FVIMDE is 1.2665E-02, the most competitive across all optimizers considered in this study. The consistency of the FVIMDE algorithm is validated by an exceedingly low standard deviation of 1.4363E-09, indicative of a high level of result repeatability and algorithmic robustness. This suggests that the variability in the quality of solutions across different executions is negligible, signifying a stable convergence towards the global optimum.

Table 18. Results of tension/compression spring design problem, run = 30, FES = 1000, agents No. = 50.

Optimizer	Mean	Std	Max	Min Value	X1	X2	X3
FVIMDE	1.2665E-02	1.4363E-09	1.2665E-02	1.2665E-02	5.1686E-02	3.5663E-01	1.1294E+01
GWO	1.3401E-02	3.4570E-04	1.4014E-02	1.3009E-02	5.4997E-02	4.3879E-01	7.8022E+00
HHO	1.3186E-02	6.4970E-05	1.3258E-02	1.3051E-02	5.00E-02	3.1378E-01	1.4637E+01
MVO	1.8210E-01	1.5741E-01	5.2245E-01	2.1680E-02	6.0214E-02	5.2439E-01	9.4024E+00
CPO	1.4828E-02	1.8026E-03	1.8760E-02	1.3051E-02	5.5594E-02	4.5532E-01	7.2742E+00
FOX	5.4527E-02	4.7292E-02	1.4619E-01	1.0625E-02	5.00E-02	2.5000E-01	1.5000E+01
ZOA	2.9691E-02	9.0947E-03	4.4030E-02	1.8975E-02	5.7850E-02	4.0690E-01	1.1935E+01
FOX	1.3122E-02	1.5122E-04	1.3220E-02	1.2747E-02	5.00E-02	3.1725E-01	1.4072E+01
AVOA	1.3466E-02	6.6278E-04	1.5278E-02	1.2804E-02	5.0140E-02	3.2034E-01	1.3899E+01
SCA	1.3106E-02	1.6643E-04	1.3248E-02	1.2798E-02	5.00E-02	3.1728E-01	1.4134E+01
MFO	1.2709E-02	1.9473E-05	1.2720E-02	1.2666E-02	5.1787E-02	3.5907E-01	1.1153E+01
WOA	1.3323E-02	1.2549E-04	1.3498E-02	1.3077E-02	5.00E-02	3.1683E-01	1.4510E+01

Further scrutiny reveals that the differences between the maximum values and the minimum values are small, which solidifies the assertion of FVIMDE's steadfast performance in each independent run. The parameters corresponding to the optimal design dimensions, denoted as X1, X2, and X3, are identified as 5.1686E-02, 3.5663E-01, and 1.1294E+01, respectively. These parameter values specify the dimensions that yield the minimum objective value, which in the context of engineering design, translates to an optimal spring configuration. However, the number of active coils $P = x1$, the diameter of the winding $D = x2$, and the diameter of the wire $d = x3$. FVIMDE has converged to a set of dimensions given by $x1 =$ 5.1686E-02, $x2 =$ 3.5663E-01, and $x3 =$ 1.1294E+01, which lie within the physical ranges of [0.05,2], [0.25,1.3], and [2,15], respectively.

Comparatively, FVIMDE outperforms the other algorithms, which exhibit higher means and standard deviations, suggesting a less optimal mean performance and a higher variability in their search outcomes.

8.1.2. The Welded Beam Design Problem

The Welded Beam Design Optimization Problem is a fundamental engineering challenge that focuses on designing an optimal welded beam structure under specific constraints while minimizing costs [65]. The problem involves determining the optimal dimensions of the beam, such as the length, width, height, and thickness of the weld, to ensure the structure's safety and functionality. Engineers must balance various factors, including material strength, beam deflection, shear stress, and bending stress, ensuring the design adheres to industry standards and safety regulations. The objective often includes minimizing the cost associated with the material and fabrication while maximizing the beam's performance under expected loads. This optimization problem is typically addressed using computational methods, including numerical optimization techniques and finite element analysis, to explore the design space efficiently and identify the most cost-effective and reliable beam design. Through this problem, engineers enhance their understanding of how different design variables impact the structural integrity and cost-efficiency of welded beams, contributing to more effective and economical structural design practices in engineering.

The objective here is to minimize the manufacturing cost of a welded beam, involving four optimized variables and seven constraints. These include the thickness of the weld (x_1), the length of the clamped bar (x_2), the height of the bar (x_3), and the thickness of the bar (x_4) and constraints like shear stress, bending stress in the beam, buckling load, end deflection of the beam, normal stress, and boundary considerations. The design of the welded beam is depicted in Figure 5.

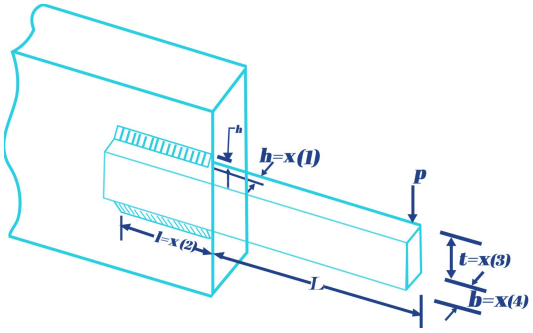

Figure 5. The welded beam design problem.

The mathematical formulation of the problem is as follows:

Let $LB = [lb_1, lb_2, lb_3, lb_4]$ and $UB = [ub_1, ub_2, ub_3, ub_4]$ denote the lower and upper bounds of the design variables, respectively. Here, lb_i and ub_i represent the lower and upper bounds of the ith design variable. Vio denotes any violation conditions, and Obj represents the objective function to be minimized. The global minimum achieved is denoted by $GloMin$.

The objective function, denoted as z, is defined as:

$$z = 1.10471 \cdot x_1^2 \cdot x_2 + 0.04811 \cdot x_3 \cdot x_4 \cdot (14 + x_2)$$

where x_1, x_2, x_3, and x_4 are the design variables representing certain characteristics of the welded beam.

Constraints g are defined as follows:

$$
\begin{aligned}
g_1(x) &= x_2 \cdot x_3 - x_1 \geq 0 \\
g_2(x) &= \frac{p}{\sqrt{2} \cdot x_1 \cdot x_2} - 1.5 \geq 0 \\
g_3(x) &= \frac{p}{\sqrt{2} \cdot x_1 \cdot x_2} - 1.5 \geq 0 \\
g_4(x) &= \frac{6 \cdot p \cdot l}{x_4 \cdot x_3^2} - 30000 \geq 0 \\
g_5(x) &= \frac{4 \cdot p \cdot l^3}{E \cdot x_3^3 \cdot x_4} - 10000 \geq 0 \\
g_6(x) &= \frac{p}{2 \cdot \sqrt{2} \cdot x_1 \cdot x_2} - 13600 \geq 0 \\
g_7(x) &= \sqrt{(\frac{p}{2 \cdot \sqrt{2} \cdot x_1 \cdot x_2})^2 + \frac{m \cdot x_2}{2 \cdot r} + (\frac{m}{j})^2} - 30000 \geq 0 \\
g_8(x) &= \frac{p \cdot l}{x_4 \cdot x_3^2} - 30000 \geq 0 \\
g_9(x) &= p - p_c \geq 0 \\
g_{10}(x) &= \sqrt{(\frac{p}{2 \cdot \sqrt{2} \cdot x_1 \cdot x_2})^2 + \frac{m \cdot x_2}{2 \cdot r} + (\frac{m}{j})^2} - 30000 \geq 0
\end{aligned}
$$

where $g_i(x)$ represents the ith constraint function, and x_1, x_2, x_3, and x_4 are the design variables. p represents the load, l represents the length, E represents the modulus of elasticity, m represents the bending moment, r represents the radius of gyration, and j represents the section modulus. p_c represents the critical load.

The lower and upper bounds for the design variables are defined by LB and UB, respectively, and any other conditions such as violation conditions are defined by Vio.

As can be seen in Table 19, the results presented indicate that FVIMDE achieves a mean value of 1.724948, a maximum of 1.725806, and an impressively low standard deviation of 0.000302, showcasing its strong performance consistency and reliability in converging towards optimal solutions.

Table 19. Results of the weld beam design problem, run = 30, agents = 50, FES = 1000.

Optimizer	Mean	Max	Std	Best	X1	X2	X3	X4
FVIMDE	1.724948	1.725806	0.000302	1.724852	0.20573	3.470489	9.036624	0.20573
FVIM	1.726068	1.726818	0.00049	1.725337	0.205748	3.47167	9.036949	0.205761
WSO	1.724852	1.724852	2.44E-11	1.724852	0.20573	3.470489	9.036624	0.20573
ZOA	1.803883	1.887076	0.06735	1.725173	0.205635	3.471647	9.03894	0.205718
SCA	1.816392	1.856325	0.03809	1.725198	0.205717	3.470253	9.03908	0.205726
RTH	1.724852	1.724852	1.01E-14	1.745062	0.199505	3.619743	9.094364	0.205716
PSO	1.726374	1.727971	0.000855	1.724852	0.20573	3.470489	9.036624	0.20573
POA	1.724852	1.724852	1.78E-09	1.724852	0.20573	3.470489	9.036624	0.20573
MVO	1.735975	1.771371	0.013881	1.726231	0.205337	3.482284	9.035197	0.205814
AVOA	1.724852	1.724853	1.85E-07	1.724852	0.20573	3.470489	9.036624	0.20573
FOX	1.731082	1.758473	0.01269	1.724852	0.20573	3.470489	9.036624	0.20573
MFO	1.724852	1.724852	4.66E-11	1.724852	0.20573	3.470489	9.036624	0.20573
HOA	2.365591	2.562652	0.14433	2.067993	0.287823	2.784202	7.682421	0.292287
BBO	1.872117	2.319204	0.175173	1.727696	0.203668	3.515431	9.036619	0.20573
GWO	1.726062	1.728523	0.000917	1.725133	0.205712	3.471168	9.037725	0.205733
ROA	1.724852	1.724853	1.3E-07	1.724852	0.20573	3.470489	9.036624	0.20573
CPO	1.729198	1.735134	0.002661	1.726255	0.20513	3.483531	9.03688	0.205799
COA	1.725016	1.725156	8.17E-05	1.724925	0.205697	3.471248	9.036709	0.20573
Chimp	2.273522	2.564183	0.209989	1.982986	0.204561	4.149214	10	0.205138
HHO	1.724852	1.724852	1.42E-12	1.724852	0.20573	3.470489	9.036624	0.20573

FVIMDE's best value aligns closely with the lowest values obtained by other high-performing algorithms such as WSO, POA, AVOA, MFO, ROA, and HHO. These algorithms exhibit minimal variations in their performance metrics, especially in terms of standard deviation, which suggests a robustness similar to that of FVIMDE. In contrast, other algorithms such as ZOA and SCA show higher mean and maximum values, coupled with larger standard deviations. This indicates variability in their performance, which may lead to less reliable outcomes in similar optimization tasks. Moreover, algorithms like HOA and Chimp demonstrate poorer metrics with much higher mean and standard deviations, underscoring their unsuitability for this particular problem under the tested conditions.

8.1.3. Cantilever Beam Design Problem

The Cantilever Beam Design Problem constitutes a pivotal aspect of structural engineering, focusing on the optimal design of a beam fixed at one end, known as a cantilever [15]. Engineers aim to determine the most efficient dimensions and material properties for the beam to withstand specified loads while adhering to various constraints. Key considerations include minimizing deflection, stress, and material usage while maximizing strength and stability. The design variables typically encompass beam length, cross-sectional dimensions, material properties, and support conditions. Engineers leverage analytical methods, empirical equations, and computational simulations to address this optimization problem effectively. Finite element analysis and optimization algorithms facilitate the exploration of the design space, enabling engineers to identify the most suitable beam configuration that balances performance, safety, and cost-effectiveness. Through the Cantilever Beam Design Problem, engineers advance their understanding of structural behavior and develop strategies to create robust and efficient beam designs for a wide range of applications, from bridges and buildings to mechanical components and aerospace structures. The Cantilever Beam Design Problem involves a structure composed of five hollow square cross-sections, as illustrated in Figure 6.

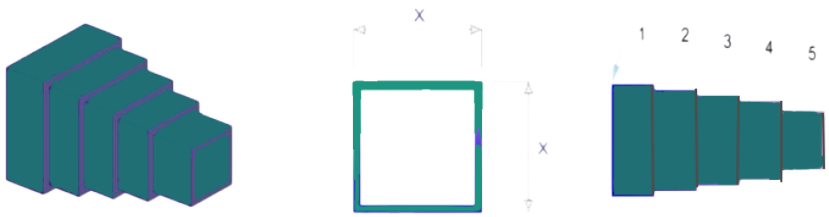

Figure 6. Cantilever beam design problem.

The mathematical formulation of the problem is as follows:

Let $LB = [lb_1, lb_2, lb_3, lb_4, lb_5]$ and $UB = [ub_1, ub_2, ub_3, ub_4, ub_5]$ denote the lower and upper bounds of the design variables, respectively. Here, lb_i and ub_i represent the lower and upper bounds of the ith design variable. *Vio* denotes any violation conditions, and *Obj* represents the objective function to be minimized. The global minimum achieved is denoted by *GloMin*.

The objective function, denoted as z, is defined as:

$$z = 0.0624 \cdot (x_1 + x_2 + x_3 + x_4 + x_5)$$

where x_1, x_2, x_3, x_4, and x_5 are the design variables representing certain characteristics of the cantilever beam.

Constraints g are defined as follows:

$$g_1(x) = \frac{61}{x_1^3} + \frac{37}{x_2^3} + \frac{19}{x_3^3} + \frac{7}{x_4^3} + \frac{1}{x_5^3} - 1 \geq 0$$

where $g_i(x)$ represents the ith constraint function, and x_1, x_2, x_3, x_4, and x_5 are the design variables.

The lower and upper bounds for the design variables are defined by LB and UB, respectively, and any other conditions such as violation conditions are defined by Vio.

As can be seen in Table 20, in the evaluation of optimization techniques for the Cantilever Beam Design Problem, the FVIMDE algorithm has demonstrated a highly effective performance. The statistical measurements for FVIMDE reveal a mean objective function value of 1.340, with an exceedingly narrow standard deviation of 1.765×10^{-7}, indicating an extraordinary level of precision in FVIMDE's outcomes across various computational iterations. This precision is complemented by the consistency of the maximum value, which precisely matches the mean and best values, denoting a good stability in reaching the optimal solution.

Table 20. Results of the cantilever beam design problem, run = 30, agents = 50, FES = 1000.

	Statistical Measurements				(X1–X4) for Minimum Value				
Sheet Name	**Mean**	**Std**	**Max**	**Best**	**X1**	**X2**	**X3**	**X4**	**X5**
FVIMDE	1.340E+00	1.765E-07	1.340E+00	1.340E+00	6.017E+00	5.306E+00	4.498E+00	3.501E+00	2.152E+00
SNS	1.340E+00	6.326E-07	1.340E+00	1.340E+00	6.018E+00	5.307E+00	4.495E+00	3.504E+00	2.150E+00
GWO	2.062E+00	6.002E-01	3.217E+00	1.511E+00	8.534E+00	4.145E+00	5.071E+00	4.510E+00	1.962E+00
HHO	3.796E+00	5.335E-01	4.712E+00	2.969E+00	7.249E+00	7.984E+00	1.058E+01	1.179E+01	9.974E+00
MVO	6.371E+00	1.449E+00	8.901E+00	4.017E+00	2.630E+01	6.630E+00	3.912E+00	1.197E+01	1.556E+01
CPO	2.805E+00	1.710E+00	5.983E+00	1.399E+00	7.231E+00	5.051E+00	3.861E+00	4.319E+00	1.951E+00
FOX	7.552E+00	1.139E+00	9.611E+00	6.061E+00	1.550E+01	5.194E+01	2.087E+01	4.175E+00	4.650E+00
ZOA	4.532E+00	9.627E-01	5.712E+00	2.931E+00	7.721E+00	3.787E+00	2.553E+01	5.680E+00	4.249E+00
FOX	5.668E+00	8.355E-01	6.703E+00	4.446E+00	2.396E+01	1.483E+01	5.848E+00	1.304E+01	1.358E+01
AVOA	3.229E+00	1.315E+00	5.863E+00	1.625E+00	5.697E+00	8.405E+00	4.295E+00	4.685E+00	2.954E+00
SCA	3.098E+00	1.933E+00	7.983E+00	1.756E+00	1.052E+01	7.122E+00	4.686E+00	2.823E+00	2.988E+00
MFO	1.341E+00	4.005E-04	1.341E+00	1.340E+00	5.976E+00	5.352E+00	4.506E+00	3.500E+00	2.142E+00
WOA	3.574E+00	8.699E-01	5.001E+00	1.749E+00	4.906E+00	9.387E+00	6.039E+00	5.316E+00	2.387E+00

The design variables for the minimum value solution, denoted by X1 through X5, have been optimized to 6.017, 5.306, 4.498, 3.501, and 2.152, respectively. These values represent critical dimensions or properties in the cantilever beam design that adhere to the constraints and objectives set forth in the problem.

When comparing with the other algorithms, FVIMDE's performance is not only consistent but also indicates a significant margin of superiority in locating the minimum value solution. For instance, algorithms like the GWO and WOA present higher standard deviations and maximum values, which suggest a less consistent approach towards optimization and potential difficulty in reliably identifying the global optimum.

The data evidently position the FVIMDE algorithm as an efficient and reliable optimization tool for the Cantilever Beam Design Problem, manifesting an impressive capability to navigate the search space and converge towards an optimal solution with a high degree of accuracy and repeatability. Such characteristics are indispensable in engineering design optimization, where the reliability of the computational tool directly impacts the feasibility and performance of the designed structure.

8.1.4. Three-Bar Truss Design Problem

The Three-Bar Truss Design Problem is a classic optimization challenge in structural engineering, focusing on optimizing the design of a truss system composed of three bars [66]. The goal is to minimize the weight or maximize the strength of the truss while satisfying certain constraints. Typically, the design variables include dimensions such as the lengths or cross-sectional areas of the bars, which influence the truss's behavior under load. The constraints often involve limits on stresses, deflections, or geometric properties to ensure the truss meets performance requirements and remains structurally stable. This problem serves as a fundamental example in structural optimization, demonstrating the trade-offs between different design objectives and constraints in engineering design. It has applications in various fields such as civil engineering, aerospace engineering, and mechanical engineering, where lightweight and efficient structural designs are crucial for performance and safety.

The objective of the Three-Bar Truss Design Problem is to design a truss with minimum weight without violating any constraints (see Figure 7).

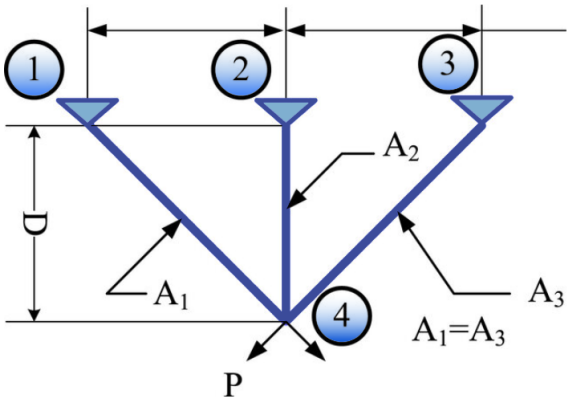

Figure 7. Three-bar truss design problem.

The mathematical formulation of the problem is as follows:

Let $LB = [lb_1, lb_2, \ldots, lb_n]$ and $UB = [ub_1, ub_2, \ldots, ub_n]$ denote the lower and upper bounds of the design variables, respectively. Here, lb_i and ub_i represent the lower and upper bounds of the ith design variable. *Vio* denotes any violation conditions, and *Obj* represents the objective function to be minimized. The global minimum achieved is denoted by *GloMin*.

The objective function, denoted as z, is defined as:

$$z = 100 \cdot (2\sqrt{2}x_1 + x_2)$$

where x_1 and x_2 are the design variables representing certain characteristics of the three-bar truss.

Constraints g are defined as follows:

$$g_1(x) = \frac{\sqrt{2}x_1 + x_2}{\sqrt{2}x_1^2 + 2x_1x_2} \cdot 2 - 2 \geq 0$$
$$g_2(x) = \frac{x_2}{\sqrt{2}x_1^2 + 2x_1x_2} \cdot 2 - 2 \geq 0$$
$$g_3(x) = \frac{1}{\sqrt{2}x_2 + x_1} \cdot 2 - 2 \geq 0$$

where $g_i(x)$ represents the ith constraint function, and x_1 and x_2 are the design variables.

The lower and upper bounds for the design variables are defined by LB and UB, respectively, and any other conditions such as violation conditions are defined by *Vio*.

Table 21 shows that the statistical measurements yield a mean objective function value of 252.3, accompanied by a standard deviation of 12.72, signifying the average and variability of performance across multiple runs. The maximum value achieved by FVIMDE is 265.6, with the best-recorded value being lower at 232.0, reflecting the optimizer's capacity to identify highly effective solutions, albeit with a notable range of outcomes.

The design variables X1 and X2, corresponding to the optimized parameters of the truss design, attained values of 0.69 and 0.3688, respectively, at the best solution. These values are critical as they directly influence the structural integrity and weight of the truss, which are pivotal considerations in engineering design.

When comparing with the results of other optimizers, FVIMDE's performance manifests as competitive, specifically in terms of achieving the lowest 'best' value, which is indicative of the potential to reach superior design solutions. Notwithstanding the broad standard deviation, which suggests a greater variability in solution quality, the ability of

FVIMDE to reach a notably lower 'best' value may be advantageous in practical applications where the optimal design is paramount, despite the variability.

Table 21. Results of the three-bar truss design problem, run = 30, agents = 50, FES = 1000.

	Statistical Measurements				(X1–X2) for Best Value	
Optimizer	**Mean**	**Std**	**Max**	**Best**	**X1**	**X2**
FVIMDE	2.523E+02	1.272E+01	2.656E+02	2.320E+02	6.900E-01	3.688E-01
GWO	2.639E+02	1.921E-07	2.639E+02	2.639E+02	7.887E-01	4.083E-01
HHO	2.598E+02	5.064E+00	2.640E+02	2.498E+02	7.681E-01	3.257E-01
MVO	2.636E+02	3.371E-01	2.639E+02	2.628E+02	7.831E-01	4.135E-01
CPO	2.598E+02	4.458E+00	2.643E+02	2.515E+02	7.236E-01	4.688E-01
FOX	2.636E+02	8.884E-01	2.651E+02	2.620E+02	7.819E-01	4.086E-01
ZOA	2.639E+02	6.783E-08	2.639E+02	2.639E+02	7.887E-01	4.082E-01
FOX	2.636E+02	7.599E-01	2.640E+02	2.615E+02	7.833E-01	3.996E-01
AVOA	2.632E+02	5.715E-01	2.639E+02	2.620E+02	7.768E-01	4.227E-01
SCA	2.633E+02	1.660E+00	2.650E+02	2.601E+02	8.002E-01	3.376E-01
MFO	2.586E+02	4.265E+00	2.641E+02	2.524E+02	7.962E-01	2.722E-01
WOA	2.639E+02	1.376E-04	2.639E+02	2.639E+02	7.885E-01	4.088E-01
MFO	2.635E+02	3.574E-01	2.639E+02	2.628E+02	7.898E-01	3.940E-01

Other optimizers, such as the Grey Wolf Optimizer (GWO) and the Whale Optimization Algorithm (WOA), exhibit lower standard deviations, reflecting a more consistent approach to the solution space exploration, albeit potentially at the cost of not reaching as optimal a solution, as indicated by their 'best' values. This analysis underscores the significance of FVIMDE's strategy in navigating the search space, striking a balance between exploration and exploitation, and exhibiting a noteworthy proficiency in discerning high-quality solutions for the Three-Bar Truss Design Problem.

8.1.5. Tabular Column Design Problem

The Tabular Column Design Problem is a crucial engineering optimization challenge aiming to determine the optimal dimensions of a tubular column while considering various constraints and objectives [67]. In this problem, the goal is to minimize the weight of the column while ensuring it meets specific strength and stability requirements. Key parameters include the outer diameter of the column (x_1) and the thickness of its wall (x_2). The objective function seeks to minimize the weight of the column while adhering to constraints such as maintaining a minimum aspect ratio, limiting the maximum stress the column can endure, and ensuring geometric feasibility. By optimizing these parameters, engineers can design tubular columns that are both structurally sound and efficient in terms of material usage.

The objective of the Tabular Column Design Problem is to minimize the cost of designing a uniform column of the tabular section, incorporating material and construction costs. The column, made of material with a length (L), yield stress (S), modulus of elasticity (E), and density (D), is designed to carry a compressive load (P). This problem is characterized by two optimized variables: the mean diameter of the column (x_1) and the tube thickness (x_2). It includes six constraints: ensuring the stress in the column is less than the buckling stress ($g_1(\mathbf{X})$) and the yield stress ($g_2(\mathbf{X})$); restricting the mean diameter between 2 and 14 cm ($g_3(\mathbf{X})$ and $g_4(\mathbf{X})$); and limiting the column thickness to the commercially available range of 0.2–0.8 cm ($g_5(\mathbf{X})$ and $g_6(\mathbf{X})$).

The Tubular Column Design Problem involves optimizing the design of a tubular column subjected to specific constraints and objectives. Let x_1 represent the outer diameter of the column and x_2 represent the thickness of the column's wall. The objective function z aims to minimize the weight of the column while meeting strength requirements and is expressed as:

$$z = 9.8x_1x_2 + 2x_1$$

Subject to the following constraints:

$$g_1 = 1.59 - x_1 x_2 \geq 0$$
$$g_2 = 47.4 - x_1 x_2 (x_1^2 + x_2^2) \geq 0$$
$$g_3 = \frac{2}{x_1} - 1 \geq 0$$
$$g_4 = \frac{x_1}{14} - 1 \geq 0$$
$$g_5 = \frac{2}{x_1} - 1 \geq 0$$
$$g_6 = \frac{x_1}{8} - 1 \geq 0$$

Here, g_1 illustrates that the column's dimensions maintain a minimum aspect ratio, g_2 imposes a limit on the maximum stress the column can withstand, and g_3, g_4, g_5, and g_6 are additional geometric constraints on the column's dimensions to ensure stability and feasibility.

Table 22 shows that FVIMDE has good performance over the Tabular Column Design Problem, where the mean objective function value achieved by FVIMDE is 26.49, which is reflective of its robust optimization capability across various trials. The astoundingly low standard deviation of 2.160E-09 points to an unparalleled level of precision and consistency in the results—a characteristic that is paramount in engineering design applications where reliability and predictability are of utmost significance.

Table 22. Results of the tabular column design problem, run = 30, agents = 50, FES = 1000.

	Statistical Measurements				**(X1–X4) for Minimum Value**	
Sheet Name	**Mean**	**Std**	**Max**	**Best**	**K**	**L**
FVIMDE	2.649E+01	2.160E-09	2.649E+01	2.649E+01	5.452E+00	2.916E-01
SNS	2.649E+01	3.413E-09	2.649E+01	2.649E+01	5.452E+00	2.916E-01
GWO	2.655E+01	3.984E-02	2.661E+01	2.649E+01	5.460E+00	2.910E-01
HHO	2.663E+01	8.973E-02	2.676E+01	2.653E+01	5.444E+00	2.931E-01
MVO	2.931E+01	1.346E+00	3.119E+01	2.693E+01	5.232E+00	3.211E-01
CPO	2.664E+01	9.296E-02	2.682E+01	2.654E+01	5.417E+00	2.959E-01
FOX	3.032E+01	1.989E+00	3.310E+01	2.698E+01	5.234E+00	3.220E-01
ZOA	2.663E+01	8.878E-02	2.679E+01	2.649E+01	5.428E+00	2.939E-01
FOX	2.762E+01	1.409E+00	3.111E+01	2.653E+01	5.473E+00	2.906E-01
AVOA	2.681E+01	1.914E-01	2.706E+01	2.650E+01	5.419E+00	2.950E-01
SCA	2.664E+01	1.049E-01	2.681E+01	2.651E+01	5.457E+00	2.916E-01
MFO	2.659E+01	6.546E-02	2.672E+01	2.651E+01	5.462E+00	2.912E-01
WOA	2.649E+01	4.410E-04	2.649E+01	2.649E+01	5.452E+00	2.916E-01

The congruity between the mean, maximum, and 'best' values, all recorded at 26.49, further substantiates the FVIMDE algorithm's steadfast performance in arriving at the most favorable solution. The reported parameter values for K and L, at 5.452 and 0.2916 respectively, which correspond to the minimum objective value, indicate specific design dimensions for the tabular column that are optimized for performance.

The distinguished performance of the FVIMDE algorithm can presumably be ascribed to its adept exploitation of the search space and the subtle fine-tuning of solutions. This is facilitated by FVIMDE's structured approach to maintaining a hierarchy of potential solutions and dynamically updating their positions, which is likely to attributed to its superior convergence characteristics.

9. Conclusions

This study introduced the Hybrid FVIMDE Algorithm, ingeniously combining the Finite Volume Integration Method (FVIM) with Differential Evolution (DE) to tackle complex optimization challenges across engineering design domains. Our extensive evaluations, conducted over a diverse set of benchmarks, including CEC2017, CEC2022, and an ad-

ditional 50 benchmark functions, demonstrate the robustness and superior performance of FVIMDE against traditional optimization algorithms. FVIMDE showed outperformed results in benchmark tests and also showcased remarkable proficiency in addressing real-world structural engineering problems. We compared its efficacy in solving five complex structural engineering tasks against other established algorithms, revealing its potential to outperform in terms of both efficiency and outcome quality. The FVIMDE hybrid algorithm combines the strengths of FVIM for precise exploitation and DE for dynamic exploration, maintaining an effective balance that enhances convergence rates and solution accuracy. The algorithm's design ensures adaptability and robustness across various optimization scenarios.

The success of FVIMDE invites further exploration into its applications and enhancements, particularly in expanding its utility to other types of engineering challenges and exploring adaptive parameter tuning mechanisms to further its efficacy. Future studies may also explore diverse hybridization methods for FVIM and tackle clustering or classification problems, large-scale optimizations, and multiobjective optimizations.

Author Contributions: Conceptualization, H.N.F., A.S.A.-S., A.I., S.N.F., F.H. and S.N.M.; methodology, H.N.F., A.S.A.-S., A.I., S.N.F., F.H. and S.N.M.; validation, H.N.F., A.S.A.-S., A.I., S.N.F., F.H. and S.N.M.; formal analysis, H.N.F., A.S.A.-S., A.I., S.N.F., F.H. and S.N.M.; investigation, H.N.F., A.S.A.-S., A.I., S.N.F., F.H. and S.N.M.; resources, H.N.F., A.S.A.-S., A.I., S.N.F., F.H. and S.M.; data curation, H.N.F., A.S.A.-S., A.I., S.N.F., F.H. and S.N.M.; writing—original draft preparation, H.N.F., A.S.A.-S., A.I., S.N.F., F.H. and S.N.M.; writing—review and editing, H.N.F., A.S.A.-S., A.I., S.N.F., F.H. and S.N.M.; visualization, H.N.F., A.S.A.-S., A.I., S.N.F., F.H. and S.N.M. All authors have read and agreed to the published version of the manuscript.

Funding: This research received no external funding.

Data Availability Statement: Data are available upon request from the authors.

Conflicts of Interest: The authors declare no conflicts of interest.

Appendix A. 2022 IEEE Congress on Evolutionary Computation (CEC2022) Benchmark Functions

Table A1. The 2022 IEEE Congress on Evolutionary Computation (CEC2022) benchmark functions.

No.	Category	Function Description	f_{min}
Unimodal functions			
F1	Unimodal function	Shifted and fully rotated Zakharov function	300
Multimodal functions			
F2		Shifted and fully rotated Rosenbrock function	400
F3		Shifted and fully rotated Expanded Schaffer f6 function	600
F4		Shifted and fully rotated non-continuous Rastrigin function	800
F5		Shifted and fully rotated Levy function	900
Hybrid functions			
F6		Hybrid function 1 (N = 3)	1800
F7		Hybrid function 2 (N = 6)	2000
F8		Hybrid function 3 (N = 5)	2200
Composition functions			
F9		Composition function 1 (N = 5)	2300
F10		Composition function 2 (N = 4)	2400
F11		Composition function 3 (N = 5)	2600
F12		Composition function 4 (N = 6)	2700

Appendix B. 2017 IEEE Congress on Evolutionary Computation (CEC2017) Benchmark Suites

Table A2. 2017 IEEE Congress on Evolutionary Computation (CEC2017) benchmark suites.

	F No.	Functions	Fi(x*)
Unimodal functions	1	Shifted and rotated Bent Cigar function	100
	2	Shifted and rotated Zakharov function	200
	3	Shifted and rotated Rosenbrock's function	300
	4	Shifted and rotated Rastrigin's function	400
	5	Shifted and rotated expanded Scaffer's F6 function	500
Simple multimodal functions	6	Shifted and rotated Lunacek Bi_Rastrigin function	600
	7	Shifted and rotated Non-Continuous Rastrigin's function	700
	8	Shifted and rotated Levy function	800
	9	Shifted and rotated Schwefel's function	900
	10	Hybrid function 1 (N = 3)	1000
	11	Hybrid function 2 (N = 3)	1100
	12	Hybrid function 3 (N = 3)	1200
	13	Hybrid function 4 (N = 4)	1300
Hybrid functions	14	Hybrid function 5 (N = 4)	1400
	15	Hybrid function 6 (N = 5)	1500
	16	Hybrid function 6 (N = 5)	1600
	17	Hybrid function 6 (N = 5)	1700
	18	Hybrid function 6 (N = 6)	1800
	19	Hybrid function 6 (N = 6)	1900
	20	Composition function 1 (N = 3)	2000
	21	Composition function 2 (N = 3)	2100
	22	Composition function 3 (N = 4)	2200
	23	Composition function 4 (N = 4)	2300
Composition functions	24	Composition function 5 (N = 5)	2400
	25	Composition function 6 (N = 5)	2500
	26	Composition function 7 (N = 6)	2600
	27	Composition function 8 (N = 6)	2700
	28	Composition function 9 (N = 3)	2800
	29	Composition function 10 (N = 3)	2900

Appendix C. 50 Benchmark Functions

Table A3. Fifty benchmark functions: D: dimensions; C: characteristics; U: unimodal; M: multimodal; S: separable; N: non-separable.

Name	Characteristics	Function	Dimension Range, f_{opt}
Steptint	U, S	$f_1(x) = 25 + \sum_{i=1}^{n} \lfloor x_i \rfloor$	$5, [-5.12, 5.12], 0$
Step	U, S	$f_2(x) = \sum_{i=1}^{n} (\lfloor x_i + 0.5 \rfloor)^2$	$30, [-100, 100], 0$
Sphere	U, S	$f_3(x) = \sum_{i=1}^{n} x_i^2$	$30, [-100, 100], 0$
SumSquares	U, S	$f_4(x) = \sum_{i=1}^{n} i \cdot x_i^2$	$30, [-10, 10], 0$
Quartic	U, S	$f_5(x) = \sum_{i=1}^{n} i \cdot x_i^4 + \text{random}[0, 1)$	$30, [-1.28, 1.28], 0$
Beale	U, N	$f_6(x) = (1.5 - x_1 + x_1x_2)^2 + (2.25 - x_1 + x_1x_2^2)^2 + (2.625 - x_1 + x_1x_3^2)^2$	$2, [-4.5, 4.5], 0$
Easom	U, N	$f_7(x) = -\cos(x_1)\cos(x_2)e^{-(x_1-\pi)^2-(x_2-\pi)^2}$	$2, [-100, 100], -1$
Matyas	U, N	$f_8(x) = 0.26(x_1^2 + x_2^2) - 0.48x_1x_2$	$2, [-10, 10], 0$
Colville	U, N	$f_9(x) = 100(x_1 - x_2^2)^2 + (x_1 - 1)^2 + 90(x_3 - x_4^2)^2 + 10.1((x_2 - 1)^2 + (x_4 - 1)^2) + 19.8(x_2 - 1)(x_4 - 1)$	$4, [-10, 10], 0$
Trid6	U, N	$f_{10}(x) = \sum_{i=1}^{6} (x_i - 1)^2 - \sum_{i=2}^{6} x_i x_{i-1}$	$6, [-D^2, D^2], -50$
Trid10	U, N	$f_{11}(x) = \sum_{i=1}^{10} (x_i - 1)^2 - \sum_{i=2}^{10} x_i x_{i-1}$	$10, [-D^2, D^2], -210$
Zakharov	U, N	$f_{12}(x) = \sum_{i=1}^{n} x_i^2 + (\sum_{i=1}^{n} 0.5ix_i)^2 + (\sum_{i=1}^{n} 0.5ix_i)^4$	$10, [-5, 10], 0$
Powell	U, N	$f_{13}(x) = \sum_{i=1}^{n/4} (x_{4i-3} + 10x_{4i-2})^2 + 5(x_{4i-1} - x_{4i})^2 + (x_{4i-2} - 2x_{4i-1})^4 + 10(x_{4i-3} - x_{4i})^4$	$24, [-4, 5], 0$
Schwefel 2.22	U, N	$f_{14}(x) = \sum_{i=1}^{n} \lvert x_i \rvert + \prod_{i=1}^{n} \lvert x_i \rvert$	$30, [-10, 10], 0$
Schwefel 1.2	U, N	$f_{15}(x) = \sum_{i=1}^{n} \left(\sum_{j=1}^{i} x_j\right)^2$	$30, [-100, 100], 0$
Rosenbrock	U, N	$f_{16}(x) = \sum_{i=1}^{n-1} (100(x_{i+1} - x_i^2)^2 + (x_i - 1)^2)$	$30, [-30, 30], 0$
Dixon-Price	U, N	$f_{17}(x) = (x_1 - 1)^2 + \sum_{i=2}^{n} i(2x_i^2 - x_{i-1})^2$	$30, [-10, 10], 0$
Foxholes	M, S	$f_{18}(x) = \left[\frac{1}{500} + \sum_{j=1}^{25} \frac{1}{j + \sum_{i=1}^{2} (x_i - a_{ij})^6}\right]^{-1}$	$2, [-65.536, 65.536], 0.998$
Branin	M, S	$f_{19}(x) = \left(x_2 - \frac{5.1}{4\pi^2}x_1^2 + \frac{5}{\pi}x_1 - 6\right)^2 + 10\left(1 - \frac{1}{8\pi}\right)\cos(x_1) + 10$	$2, [-5, 10] \times [0, 15], 0.398$
Bohachevsky 1	M, S	$f_{20}(x) = x_1^2 + 2x_2^2 - 0.3\cos(3\pi x_1) - 0.4\cos(4\pi x_2) + 0.7$	$2, [-100, 100], 0$

Table A4. Benchmark functions; D: dimensions; C: characteristics; U: unimodal; M: multimodal; S: separable; N: non-separable.

Name	Characteristics	Function	Dimension Range, f_{opt}
Booth	M, S	$f_{21}(x) = (x_1 + 2x_2 - 7)^2 + (2x_1 + x_2 - 5)^2$	$2, [-10, 10], 0$
Rastrigin	M, S	$f_{22}(x) = 10n + \sum_{i=1}^{n}[x_i^2 - 10\cos(2\pi x_i)]$	$30, [-5.12, 5.12], 0$
Schwefel	M, S	$f_{23}(x) = 418.9829n - \sum_{i=1}^{n}[x_i \sin(\sqrt{\lvert x_i \rvert})]$	$30, [-500, 500], -12569.5$
Michalewicz2	M, S	$f_{24}(x) = -\sum_{i=1}^{2} \sin(x_i) \sin^{20}\left(\frac{ix_i^2}{\pi}\right)$	$2, [0, \pi], -1.8013$
Michalewicz5	M, S	$f_{25}(x) = -\sum_{i=1}^{5} \sin(x_i) \sin^{20}\left(\frac{ix_i^2}{\pi}\right)$	$5, [0, \pi], -4.6877$
Michalewicz10	M, S	$f_{26}(x) = -\sum_{i=1}^{10} \sin(x_i) \sin^{20}\left(\frac{ix_i^2}{\pi}\right)$	$10, [0, \pi], -9.6602$
Schaffer	M, N	$f_{27}(x) = 0.5 + \frac{\sin^2(\sqrt{x_1^2+x_2^2})-0.5}{(1+0.001(x_1^2+x_2^2))^2}$	$2, [-100, 100], 0$
Six Hump Camel Back	M, N	$f_{28}(x) = (4 - 2.1x_1^2 + \frac{x_1^4}{3})x_1^2 + x_1x_2 - 4(x_2^2 - x_2^4)x_2^2$	$2, [-5, 5], -1.03163$
Bohachevsky2	M, N	$f_{29}(x) = x_1^2 + 2x_2^2 - 0.3\cos(3\pi x_1)\cos(4\pi x_2) + 0.3$	$2, [-100, 100], 0$
Bohachevsky3	M, N	$f_{30}(x) = x_1^2 + 2x_2^2 - 0.3\cos(3\pi x_1 + 4\pi x_2) + 0.3$	$2, [-100, 100], 0$
Shubert	M, N	$f_{31}(x) = \sum_{i=1}^{5} i\cos((i+1)x_1 + i)\sum_{j=1}^{5} j\cos((j+1)x_2 + j)$	$2, [-10, 10], -186.7309$
Goldstein-Price	M, N	$f_{32}(x) = [1 + (x_1 + x_2 + 1)^2(19 - 14x_1 + 3x_1^2 - 14x_2 + 6x_1x_2 + 3x_2^2)] \times [30 + (2x_1 - 3x_2)^2(18 - 32x_1 + 12x_1^2 + 48x_2 - 36x_1x_2 + 27x_2^2)]$	$2, [-2, 2], 3$
Kowalik	M, N	$f_{33}(x) = \sum_{i=1}^{11} \frac{a_i - \frac{x_1(b_i^2+b_ix_2)}{b_i^2+b_ix_3+x_4}}{a_i^2}$	$4, [-5, 5], 0.00031$
Shekel5	M, N	$f_{34}(x) = -\sum_{i=1}^{5} \frac{1}{(x_i-a_i)^TC(x_i-a_i)+c_i}$	$4, [0, 10], -10.1532$
Shekel7	M, N	$f_{35}(x) = -\sum_{i=1}^{7} \frac{1}{(x_i-a_i)^TC(x_i-a_i)+c_i}$	$4, [0, 10], -10.4028$
Shekel10	M, N	$f_{36}(x) = -\sum_{i=1}^{10} \frac{1}{(x_i-a_i)^TC(x_i-a_i)+c_i}$	$4, [0, 10], -10.5363$
Perm	M, N	$f_{37}(x) = \sum_{k=1}^{n}\left(\sum_{i=1}^{n}(i^k + \beta)((x_i/i)^k - 1)\right)^2$	$4, [-D, D], 0$
PowerSum	M, N	$f_{38}(x) = \sum_{k=1}^{4}\left(\sum_{i=1}^{n}(x_i^k) - b_k\right)^2$	$4, [0, D], 0$
Hartman3	M, N	$f_{39}(x) = -\sum_{i=1}^{4} c_i \exp\left(-\sum_{j=1}^{3} a_{ij}(x_j - p_{ij})^2\right)$	$3, [0, 1], -3.86$
Hartman6	M, N	$f_{40}(x) = -\sum_{i=1}^{4} c_i \exp\left(-\sum_{j=1}^{6} a_{ij}(x_j - p_{ij})^2\right)$	$6, [0, 1], -3.32$

Table A5. Benchmark functions: D: dimensions, C: characteristics, U: unimodal, M: multimodal, S: separable, N: non-separable.

Name	C	Function	D	Range	f_{opt}
Griewank	MN	$f_{41}(x) = \frac{1}{4000}\sum_{i=1}^{n} x_i^2 - \prod_{i=1}^{n}\cos\left(\frac{x_i}{\sqrt{i}}\right) + 1$	30	$[-600, 600]$	0
Ackley	MN	$f_{42}(x) = -20\exp\left(-0.2\sqrt{\frac{1}{n}\sum_{i=1}^{n} x_i^2}\right) - \exp\left(\frac{1}{n}\sum_{i=1}^{n}\cos 2\pi x_i\right) + 20 + e$	30	$[-32, 32]$	0
Penalized	MN	$f_{43}(x) = \pi n\left[10\sin^2(\pi y_1) + \sum_{i=1}^{n-1}(y_i - 1)^2[1 + 10\sin^2(\pi y_{i+1})] + (y_n - 1)^2\right] + \sum_{i=1}^{n} u(x_i, 10, 100, 4)$	30	$[-50, 50]$	0
Penalized2	MN	$f_{44}(x) = 0.1\left[\sin^2(3\pi x_1) + \sum_{i=1}^{n-1}(x_i - 1)^2[1 + \sin^2(3\pi x_{i+1})] + (x_n - 1)^2[1 + \sin^2(2\pi x_n)]\right] + \sum_{i=1}^{n} u(x_i, 5, 100, 4)$	30	$[-50, 50]$	0
Langerman2	MN	$f_{45}(x) = -c\exp\left(-\frac{1}{\pi}\sum_{j=1}^{n}(x_j - a_{ij})^2\right)\cos\left(\pi\sum_{j=1}^{n}(x_j - a_{ij})^2\right)$	2	$[0, 10]$	1.08
Langerman5	MN	$f_{46}(x)$ similar to f_5	5	$[0, 10]$	1.5
Langerman10	MN	$f_{47}(x)$ similar to f_5	10	$[0, 10]$	-
FletcherPowell2	MN	$f_{48}(x) = \sum_{i=1}^{n}(A_i - B_i)^2$ where $A_i = \sum_{j=1}^{n}(a_{ij}\sin\alpha_j + b_{ij}\cos\alpha_j)$, $B_i = \sum_{j=1}^{n}(a_{ij}\sin x_j + b_{ij}\cos x_j)$	2	$[-\pi, \pi]$	0
FletcherPowell5	MN	$f_{49}(x)$ similar to f_8	5	$[-\pi, \pi]$	0
FletcherPowell10	MN	$f_{50}(x)$ similar to f_8	0	$[-\pi, \pi]$	0

Appendix D. Wilcoxon Rank Sum Results over CEC2022 Benchmarks

Table A6. Wilcoxon rank sum results over CEC2022 benchmarks (F1–F12), run = 30, FES = 1000, agents No. = 30.

Function	FVIM	FLO	STOA	SOA	SPBO	AO	SSOA	Chimp	CPO	ROA
F1	4.07716E-11 U: 468.00 S	3.02E-11 U: 465.00 S	1.78E-10 U: 483.00 S	7.39E-11 U: 474.00 S	3.02E-11 U: 465.00 S	3.69E-11 U: 467.00 S	3.02E-11 U: 465.00 S	3.02E-11 U: 465.00 S	3.02E-11 U: 465.00 S	3.02E-11 U: 465.00 S
F2	1.10234E-08 U: 528.00 S	3.02E-11 U: 465.00 S	1.61E-10 U: 482.00 S	4.98E-11 U: 470.00 S	3.02E-11 U: 465.00 S	8.89E-10 U: 500.00 S	3.02E-11 U: 465.00 S	3.02E-11 U: 465.00 S	4.11E-07 U: 572.00 S	3.02E-11 U: 465.00 S
F3	3.68973E-11 U: 467.00 S	3.02E-11 U: 465.00 S	3.02E-11 U: 465.00 S	3.02E-11 U: 465.00 S	3.02E-11 U: 465.00 S	3.02E-11 U: 465.00 S	3.02E-11 U: 465.00 S	3.02E-11 U: 465.00 S	3.02E-11 U: 465.00 S	3.02E-11 U: 465.00 S
F4	0.000189162 U: 1168.00 N	4.5E-11 U: 469.00 S	0.001174 U: 695.00 S	9.26E-09 U: 526.00 S	3.02E-11 U: 465.00 S	0.325527 U: 848.00 E	3.02E-11 U: 465.00 S	1.07E-09 U: 502.00 S	6.01E-08 U: 548.00 S	5.49E-11 U: 471.00 S
F5	3.01986E-11 U: 465.00 S	3.02E-11 U: 465.00 S	3.02E-11 U: 465.00 S	3.02E-11 U: 465.00 S	3.02E-11 U: 465.00 S	3.02E-11 U: 465.00 S	3.02E-11 U: 465.00 S	3.02E-11 U: 465.00 S	3.02E-11 U: 465.00 S	3.02E-11 U: 465.00 S
F6	1.77691E-10 U: 483.00 S	3.02E-11 U: 465.00 S	3.02E-11 U: 465.00 S	3.02E-11 U: 465.00 S	3.02E-11 U: 465.00 S	3.02E-11 U: 465.00 S	3.02E-11 U: 465.00 S	3.02E-11 U: 465.00 S	2.03E-09 U: 509.00 S	3.34E-11 U: 466.00 S
F7	9.26029E-09 U: 526.00 S	3.02E-11 U: 465.00 S	3.02E-11 U: 465.00 S	3.02E-11 U: 465.00 S	3.02E-11 U: 465.00 S	3.02E-11 U: 465.00 S	3.02E-11 U: 465.00 S	3.02E-11 U: 465.00 S	3.02E-11 U: 465.00 S	3.02E-11 U: 465.00 S
F8	4.80107E-07 U: 574.00 S	3.02E-11 U: 465.00 S	2.37E-10 U: 486.00 S	3.02E-11 U: 465.00 S	3.02E-11 U: 465.00 S	4.08E-11 U: 468.00 S	3.02E-11 U: 465.00 S	3.02E-11 U: 465.00 S	2.39E-08 U: 537.00 S	3.02E-11 U: 465.00 S
F9	3.01986E-11 U: 465.00 S	3.02E-11 U: 465.00 S	3.02E-11 U: 465.00 S	3.02E-11 U: 465.00 S	3.02E-11 U: 465.00 S	3.02E-11 U: 465.00 S	3.02E-11 U: 465.00 S	3.02E-11 U: 465.00 S	3.02E-11 U: 465.00 S	3.02E-11 U: 465.00 S
F10	0.000421751 U: 676.00 S	2.92E-09 U: 513.00 S	1.73E-06 U: 591.00 S	4.8E-07 U: 574.00 N	1.73E-07 U: 561.00 S	3.65E-08 U: 542.00 S	9.76E-10 U: 501.00 S	2.39E-08 U: 537.00 S	2.92E-09 U: 513.00 S	2.92E-09 U: 513.00 S
F11	2.0338E-09 U: 509.00 S	4.5E-11 U: 469.00 S	2.03E-09 U: 509.00 S	5E-09 U: 519.00 S	3.02E-11 U: 465.00 S	7.12E-09 U: 523.00 S	3.69E-11 U: 467.00 S	4.5E-11 U: 469.00 S	8.1E-10 U: 499.00 S	1.21E-10 U: 479.00 S
F12	0.002958985 U: 632.00	3.02E-11 U: 465.00	0.08771 U: 1031.00	0.673495 U: 886.00	3.02E-11 U: 465.00	2.83E-08 U: 539.00	3.02E-11 U: 465.00	8.99E-11 U: 476.00	3.02E-11 U: 465.00	3.02E-11 U: 465.00
Total	S:11, N:1, E:0	S:12, N:0, E:0	S:11, N:0, E:1	S:10, N:1, E:1	S:12, N:0, E:0	S:11, N:0, E:1	S:12, N:0, E:0	S:12, N:0, E:0	S:12, N:0, E:0	S:12, N:0, E:0

Table A7. Continue Wilcoxon rank sum results over CEC2022 benchmarks (F1–F12), run = 30, FES = 1000, agents No. = 30.

WOA	PSO	MFO	SHIO	ZOA	MTDE	SCA	DOA	SCSO	GA	SA
3.02E-11 U: 465.00 S	1.96E-10 U: 484.00 S	3.82E-10 U: 491.00 S	4.98E-11 U: 470.00 S	4.62E-10 U: 493.00 S	2.96E-11 U: 465.00 S	4.98E-11 U: 470.00 S	3.82E-10 U: 491.00 S	1.61E-10 U: 482.00 S	3.02E-11 U: 465.00 S	3.02E-11 U: 465.00 S
3.82E-09 U: 516.00 S	1.69E-09 U: 507.00 S	9.49E-07 U: 583.00 S	1.6E-07 U: 560.00 S	8.1E-10 U: 499.00 S	2.99E-11 U: 465.00 S	3.02E-11 U: 465.00 S	6.72E-10 U: 497.00 S	5.07E-10 U: 494.00 S	3.02E-11 U: 465.00 S	3.02E-11 U: 465.00 S
3.02E-11 U: 465.00 S	3.69E-11 U: 467.00 S	0.200949 U: 1002.00 E	2.44E-09 U: 511.00 S	3.02E-11 U: 465.00 S	3E-11 U: 465.00 S	3.02E-11 U: 465.00 S	3.02E-11 U: 465.00 S	3.02E-11 U: 465.00 S	3.02E-11 U: 465.00 S	3.02E-11 U: 465.00 S
1.41E-09 U: 505.00 S	0.340288 U: 980.00 E	0.082357 U: 797.00 E	0.982307 U: 917.00 E	0.023243 U: 1069.00 N	2.98E-11 U: 465.00 S	4.5E-11 U: 469.00 S	0.025101 U: 763.00 S	2.78E-07 U: 567.00 S	3.02E-11 U: 465.00 S	3.02E-11 U: 465.00 S
3.02E-11 U: 465.00 S	3.02E-11 U: 465.00 S	1.03E-06 U: 584.00 S	3.02E-11 U: 465.00 S	3.02E-11 U: 465.00 S	2.99E-11 U: 465.00 S	3.02E-11 U: 465.00 S	3.02E-11 U: 465.00 S	3.02E-11 U: 465.00 S	3.02E-11 U: 465.00 S	3.02E-11 U: 465.00 S
4.2E-10 U: 492.00 S	8.99E-11 U: 476.00 S	2.15E-10 U: 485.00 S	2.03E-09 U: 509.00 S	1.29E-09 U: 504.00 S	2.99E-11 U: 465.00 S	3.02E-11 U: 465.00 S	0.000141 U: 657.00 S	9.76E-10 U: 501.00 S	3.02E-11 U: 465.00 S	3.02E-11 U: 465.00 S
3.02E-11 U: 465.00 S	2.03E-09 U: 509.00 S	1.43E-08 U: 531.00 S	3.02E-11 U: 465.00 S	3.16E-10 U: 489.00 S	2.97E-11 U: 465.00 S	3.02E-11 U: 465.00 S	1.09E-10 U: 478.00 S	3.02E-11 U: 465.00 S	3.02E-11 U: 465.00 S	3.02E-11 U: 465.00 S
3.02E-11 U: 465.00 S	0.00238 U: 709.00 S	0.1809 U: 824.00 E	1.03E-06 U: 584.00 S	0.000309 U: 599.00 S	2.97E-11 U: 465.00 S	3.02E-11 U: 465.00 S	2.57E-07 U: 566.00 S	2.39E-08 U: 537.00 S	3.02E-11 U: 465.00 S	9.26E-09 U: 526.00 S
3.02E-11 U: 465.00 S	3.02E-11 U: 465.00 S	0.000282 U: 1155.00 S	3.02E-11 U: 465.00 S	3.02E-11 U: 465.00 S	2.96E-11 U: 465.00 S	3.02E-11 U: 465.00 S	0.001249 U: 619.00 S	3.02E-11 U: 465.00 S	3.02E-11 U: 465.00 S	3.02E-11 U: 465.00 S
2.03E-09 U: 509.00 S	0.012732 U: 746.00 S	1.19E-06 U: 586.00 N	0.011228 U: 743.00 S	5E-09 U: 519.00 S	1.69E-08 U: 533.00 S	4.44E-07 U: 573.00 S	8.48E-09 U: 525.00 S	1.16E-07 U: 556.00 S	1.7E-08 U: 533.00 S	1.11E-06 U: 585.00 -
9.76E-10 U: 501.00 S	3.5E-09 U: 515.00 S	0.000149 U: 658.00 S	8.1E-10 U: 499.00 S	8.1E-10 U: 499.00 S	3E-11 U: 465.00 S	8.48E-09 U: 525.00 S	1.69E-09 U: 507.00 S	2.44E-09 U: 511.00 S	4.5E-11 U: 469.00 S	8.48E-09 U: 525.00 S
4.62E-10 U: 493.00	0.233989 U: 834.00	0.00081 U: 1142.00	2.03E-07 U: 563.00	3.02E-11 U: 465.00	2.99E-11 U: 465.00	3.02E-11 U: 465.00	7.12E-09 U: 523.00	0.001004 U: 692.00	3.02E-11 U: 465.00	2.37E-10 U: 486.00
S:12, N:0, E:0	S:10, N:0, E:2	S:7, N:2, E:3	S:11, N:0, E:1	S:11, N:1, E:0	S:12, N:0, E:0	S:12, N:0, E:0	S:12, N:0, E:0	S:12, N:0, E:0	S:12, N:0, E:0	S:11, N:1, E:0

Appendix E. Wilcoxon Sum Rank Test Results over 50 Benchmarks

Table A8. Wilcoxon results over CEC2017 benchmarks (F1–F12), run = 30, FES = 1000, agents No. = 30.

Function	FVIM	FLO	STOA	SOA	SPBO	AO	SSOA	Chimp	CPO	ROA
F1	1.17E-05 U: 618.00 S	3.02E-11 U: 465.00 S	3.02E-11 U: 465.00 S	3.02E-11 U: 465.00 S	3.02E-11 U: 465.00 S	3.02E-11 U: 465.00 S	3.02E-11 U: 465.00 S	3.02E-11 U: 465.00 S	1.73E-07 U: 1269.00 N	3.02E-11 U: 465.00 S
F2	3.02E-11 U: 465.00 S	3.02E-11 U: 465.00 S	3.02E-11 U: 465.00 S	3.02E-11 U: 465.00 S	3.02E-11 U: 465.00 S	3.02E-11 U: 465.00 S	3.02E-11 U: 465.00 S	3.02E-11 U: 465.00 S	4.2E-10 U: 492.00 S	3.02E-11 U: 465.00 S
F3	3.02E-11 U: 465.00 S	3.02E-11 U: 465.00 S	4.08E-11 U: 468.00 S	3.02E-11 U: 465.00 S	3.02E-11 U: 465.00 S	7.77E-09 U: 524.00 S	3.02E-11 U: 465.00 S	3.02E-11 U: 465.00 S	3.82E-09 U: 1314.00 N	3.02E-11 U: 465.00 S
F4	3.02E-11 U: 465.00 S	3.02E-11 U: 465.00 S	3.02E-11 U: 465.00 S	3.02E-11 U: 465.00 S	3.02E-11 U: 465.00 S	1.09E-10 U: 478.00 S	3.02E-11 U: 465.00 S	3.02E-11 U: 465.00 S	1.07E-07 U: 555.00 S	3.02E-11 U: 465.00 S
F5	8.15E-05 U: 648.00 S	3.02E-11 U: 465.00 S	3.2E-09 U: 514.00 S	7.69E-08 U: 551.00 S	3.02E-11 U: 465.00 S	8.1E-10 U: 499.00 S	3.02E-11 U: 465.00 S	3.02E-11 U: 465.00 S	4.98E-11 U: 470.00 S	3.02E-11 U: 465.00 S
F6	0.019883 U: 757.00 S	3.02E-11 U: 465.00 S	3.02E-11 U: 465.00 S	3.02E-11 U: 465.00 S	3.02E-11 U: 465.00 S	3.02E-11 U: 465.00 S	3.02E-11 U: 465.00 S	3.02E-11 U: 465.00 S	3.02E-11 U: 465.00 S	3.02E-11 U: 465.00 S
F7	0.245814 U: 994.00 E	3.02E-11 U: 465.00 S	5.46E-09 U: 520.00 S	1.31E-08 U: 530.00 S	3.02E-11 U: 465.00 S	3.52E-07 U: 570.00 S	3.02E-11 U: 465.00 S	3.02E-11 U: 465.00 S	7.39E-11 U: 474.00 S	3.02E-11 U: 465.00 S
F8	0.000201 U: 663.00 S	3.02E-11 U: 465.00 S	1.78E-10 U: 483.00 S	5.07E-10 U: 494.00 S	3.02E-11 U: 465.00 S	4.2E-10 U: 492.00 S	3.02E-11 U: 465.00 S	3.02E-11 U: 465.00 S	3.34E-11 U: 466.00 S	3.02E-11 U: 465.00 S
F9	2.23E-09 U: 510.00 S	3.02E-11 U: 465.00 S	3.02E-11 U: 465.00 S	3.02E-11 U: 465.00 S	3.02E-11 U: 465.00 S	6.07E-11 U: 472.00 S	3.02E-11 U: 465.00 S	3.02E-11 U: 465.00 S	3.02E-11 U: 465.00 S	3.02E-11 U: 465.00 S
F10	1.29E-06 U: 587.00 S	3.02E-11 U: 465.00 S	7.69E-08 U: 551.00 S	2.32E-06 U: 595.00 S	3.02E-11 U: 465.00 S	4.11E-07 U: 572.00 S	3.02E-11 U: 465.00 S	3.02E-11 U: 465.00 S	9.92E-11 U: 477.00 S	4.08E-11 U: 468.00 S
F11	8.89E-10 U: 500.00 S	3.02E-11 U: 465.00 S	4.5E-11 U: 469.00 S	7.39E-11 U: 474.00 S	3.02E-11 U: 465.00 S	3.02E-11 U: 465.00 S	3.02E-11 U: 465.00 S	3.02E-11 U: 465.00 S	2.15E-10 U: 485.00 S	3.02E-11 U: 465.00 S
F12	3.02E-11 U: 465.00	3.02E-11 U: 465.00	3.02E-11 U: 465.00	3.02E-11 U: 465.00	3.02E-11 U: 465.00	3.02E-11 U: 465.00	3.02E-11 U: 465.00	3.02E-11 U: 465.00	3.02E-11 U: 465.00	3.02E-11 U: 465.00
Total	S:11, N:0, E:1	S:12, N:0, E:0	S:12, N:0, E:0	S:12, N:0, E:0	S:12, N:0, E:0	S:12, N:0, E:0	S:12, N:0, E:0	S:12, N:0, E:0	S:10, N:2, E:0	S:12, N:0, E:0

Table A9. Continued Wilcoxon results over CEC2017 benchmarks (F1–F12), run = 30, FES = 1000, agents No. = 30.

Function	WOA	PSO	MFO	SHIO	ZOA	MTDE	SCA	DOA	SCSO	GA	SA
F1	3.02E-11 U: 465.00 S	5.09E-06 U: 606.00 S	0.970491 U: 912.00 E	2.67E-09 U: 512.00 S	7.6E-07 U: 580.00 S	2.9E-11 U: 465.00 S	3.02E-11 U: 465.00 S	2.37E-10 U: 486.00 S	0.222573 U: 832.00 E	3.02E-11 U: 465.00 S	3.02E-11 U: 465.00 S
F2	3.02E-11 U: 465.00 S	3.02E-11 U: 465.00 S	5.97E-05 U: 643.00 S	3.02E-11 U: 465.00 S	3.02E-11 U: 465.00 S	2.89E-11 U: 465.00 S	3.02E-11 U: 465.00 S	3.02E-11 U: 465.00 S	3.34E-11 U: 466.00 S	3.02E-11 U: 465.00 S	3.02E-11 U: 465.00 S
F3	3.34E-11 U: 466.00 S	4.98E-11 U: 470.00 S	0.251881 U: 837.00 E	3.02E-11 U: 465.00 S	1.46E-10 U: 481.00 S	2.86E-11 U: 465.00 S	3.02E-11 U: 465.00 S	9.76E-10 U: 501.00 S	4.98E-11 U: 470.00 S	3.02E-11 U: 465.00 S	3.02E-11 U: 465.00 S
F4	3.02E-11 U: 465.00 S	3.02E-11 U: 465.00 S	5.99E-11 U: 472.00 S	5.07E-10 U: 494.00 S	3.02E-11 U: 465.00 S	2.89E-11 U: 465.00 S	3.02E-11 U: 465.00 S	2.87E-10 U: 488.00 S	3.02E-11 U: 465.00 S	3.02E-11 U: 465.00 S	3.02E-11 U: 465.00 S
F5	6.07E-11 U: 472.00 S	7.2E-05 U: 646.00 S	1.69E-09 U: 507.00 S	2.03E-09 U: 509.00 S	2.23E-09 U: 510.00 S	2.91E-11 U: 465.00 S	3.02E-11 U: 465.00 S	2.61E-10 U: 487.00 S	2.15E-10 U: 485.00 S	3.02E-11 U: 465.00 S	1.17E-09 U: 503.00 S
F6	3.02E-11 U: 465.00 S	0.000422 U: 676.00 S	0.045063 U: 779.00 S	5.49E-11 U: 471.00 S	3.02E-11 U: 465.00 S	3.01E-11 U: 465.00 S	3.02E-11 U: 465.00 S	3.02E-11 U: 465.00 S	3.02E-11 U: 465.00 S	3.02E-11 U: 465.00 S	3.02E-11 U: 465.00 S
F7	1.78E-10 U: 483.00 S	0.662735 U: 885.00 E	0.013832 U: 748.00 S	0.000812 U: 688.00 S	0.000132 U: 656.00 S	2.94E-11 U: 465.00 S	3.02E-11 U: 465.00 S	1.85E-08 U: 534.00 S	1.29E-09 U: 504.00 S	3.02E-11 U: 465.00 S	3.47E-10 U: 490.00 S
F8	3.34E-11 U: 466.00 S	0.000201 U: 663.00 S	1.54E-09 U: 506.00 S	9.06E-08 U: 553.00 S	0.000399 U: 675.00 S	2.88E-11 U: 465.00 S	3.02E-11 U: 465.00 S	6.12E-10 U: 496.00 S	2.15E-10 U: 485.00 S	3.02E-11 U: 465.00 S	3.02E-11 U: 465.00 S
F9	3.02E-11 U: 465.00 S	4.44E-07 U: 573.00 S	0.104666 U: 805.00 E	3.34E-11 U: 466.00 S	3.02E-11 U: 465.00 S	2.95E-11 U: 465.00 S	3.02E-11 U: 465.00 S	3.02E-11 U: 465.00 S	3.34E-11 U: 466.00 S	3.02E-11 U: 465.00 S	3.02E-11 U: 465.00 S
F10	9.76E-10 U: 501.00 S	0.137323 U: 814.00 E	2.02E-08 U: 535.00 S	2.68E-06 U: 597.00 S	0.025101 U: 763.00 S	2.99E-11 U: 465.00 S	1.09E-10 U: 478.00 S	1.09E-10 U: 478.00 S	1.43E-08 U: 531.00 S	3.69E-11 U: 467.00 S	0.006097 U: 729.00 S
F11	8.99E-11 U: 476.00 S	2.92E-09 U: 513.00 S	1.25E-07 U: 557.00 S	8.99E-11 U: 476.00 S	3.34E-11 U: 466.00 S	2.89E-11 U: 465.00 S	3.02E-11 U: 465.00 S	3.02E-11 U: 465.00 S	3.47E-10 U: 490.00 S	3.02E-11 U: 465.00 S	3.02E-11 U: 465.00 S
F12	3.02E-11 U: 465.00	3.02E-11 U: 465.00	3.02E-11 U: 465.00	3.02E-11 U: 465.00	3.02E-11 U: 465.00	2.94E-11 U: 465.00	3.02E-11 U: 465.00	3.69E-11 U: 467.00	3.02E-11 U: 465.00	3.02E-11 U: 465.00	3.02E-11 U: 465.00
Total	S:12, N:0, E:0	S:10, N:0, E:2	S:9, N:0, E:3	S:12, N:0, E:0	S:12, N:0, E:0	S:12, N:0, E:0	S:12, N:0, E:0	S:12, N:0, E:0	S:11, N:0, E:1	S:12, N:0, E:0	S:12, N:0, E:0

Table A10. Wilcoxon Sum rank test results over 50 benchmarks (F1–F25), run = 30, FES = 1000, agents No. = 30.

Function	FVIM	FLO	STOA	SOA	MVO	AO	SSOA	Chimp	CPO	ROA
F1	3.02E-11 U: 915.0000 E	1.21E-12 U: 915.0000 E	3.02E-11 U: 915.0000 E	4.08E-11 U: 915.0000 E	3.02E-11 U: 915.0000 E	3.02E-11 U: 915.0000 E	1.01E-12 U: 465.0000 S	3.02E-11 U: 915.0000 E	3.02E-11 U: 915.0000 E	3.02E-11 U: 915.0000 E
F2	0.160802 U: 945.0000 E	0.160802 U: 945.0000 E	0.160802 U: 945.0000 E	0.160802 U: 945.0000 E	2.27E-12 U: 465.0000 S	0.160802 U: 945.0000 E	0.160802 U: 945.0000 E	1 U: 915.0000 E	0.160802 U: 945.0000 E	0.160802 U: 945.0000 E
F3	3.02E-11 U: 1365.0000 N	1.21E-12 U: 1365.0000 N	3.02E-11 U: 465.0000 S	4.08E-11 U: 1362.0000 N	3.02E-11 U: 465.0000 S	3.02E-11 U: 1365.0000 N	1.21E-12 U: 1365.0000 N	0.000132 U: 656.0000 S	3.02E-11 U: 1365.0000 N	3.02E-11 U: 1365.0000 N
F4	3.02E-11 U: 1365.0000 N	1.21E-12 U: 1365.0000 N	3.02E-11 U: 465.0000 S	4.08E-11 U: 1362.0000 N	3.02E-11 U: 465.0000 S	3.02E-11 U: 1365.0000 N	1.21E-12 U: 1365.0000 N	8.88E-06 U: 614.0000 S	3.02E-11 U: 1365.0000 N	3.02E-11 U: 1365.0000 N
F5	3.65E-08 U: 1288.0000 N	3.02E-11 U: 1365.0000 N	0.026077 U: 1066.0000 N	1.07E-09 U: 1328.0000 N	1.09E-10 U: 478.0000 S	3.02E-11 U: 1365.0000 N	3.02E-11 U: 1365.0000 N	8.48E-09 U: 1305.0000 N	3.02E-11 U: 1365.0000 N	3.02E-11 U: 1365.0000 N
F6	1.21E-12 U: 465.0000 S	1.21E-12 U: 465.0000 S	1.21E-12 U: 465.0000 S	1.21E-12 U: 465.0000 S	1.21E-12 U: 465.0000 S	1.21E-12 U: 465.0000 S	1.21E-12 U: 465.0000 S	1.21E-12 U: 465.0000 S	1.21E-12 U: 465.0000 S	1.21E-12 U: 465.0000 S
F7	1.21E-12 U: 465.0000 S	0.00137 U: 780.0000 S	1.21E-12 U: 465.0000 S	1.21E-12 U: 465.0000 S	1.21E-12 U: 465.0000 S	1.21E-12 U: 465.0000 S	1.21E-12 U: 465.0000 S	1.21E-12 U: 465.0000 S	1.21E-12 U: 465.0000 S	1.21E-12 U: 465.0000 S
F8	3.02E-11 U: 1365.0000 N	1.21E-12 U: 1365.0000 N	8.35E-08 U: 552.0000 S	3.02E-11 U: 1365.0000 N	3.02E-11 U: 465.0000 S	3.02E-11 U: 1365.0000 N	1.21E-12 U: 1365.0000 N	3.02E-11 U: 1365.0000 N	3.02E-11 U: 1365.0000 N	3.02E-11 U: 465.0000 S
F9	3.02E-11 U: 465.0000 S	1.21E-12 U: 1365.0000 N	3.02E-11 U: 465.0000 S	3.02E-11 U: 465.0000 S	3.02E-11 U: 465.0000 S	6.01E-08 U: 548.0000 S	3.02E-11 U: 465.0000 S	3.02E-11 U: 465.0000 S	0.009069 U: 738.0000 N	5.07E-10 U: 494.0000 S
F10	6.7E-11 U: 473.0000 S	3.02E-11 U: 465.0000 S	3.02E-11 U: 465.0000 S	3.02E-11 U: 465.0000 S	6.7E-11 U: 473.0000 S	3.02E-11 U: 465.0000 S	3.02E-11 U: 465.0000 S	3.02E-11 U: 465.0000 S	2.96E-05 U: 1198.0000 N	3.02E-11 U: 465.0000 S
F11	0.001518 U: 700.0000 S	3.02E-11 U: 465.0000 S	3.02E-11 U: 465.0000 S	3.02E-11 U: 465.0000 S	0.311188 U: 984.0000 E	1.25E-07 U: 557.0000 S	3.02E-11 U: 465.0000 S	3.02E-11 U: 465.0000 S	1.46E-10 U: 1349.0000 N	3.02E-11 U: 465.0000 S
F12	3.02E-11 U: 1365.0000 N	1.72E-12 U: 1365.0000 N	0.011711 U: 744.0000 S	3.02E-11 U: 1365.0000 N	3.02E-11 U: 465.0000 S	3.02E-11 U: 1365.0000 N	1.72E-12 U: 1365.0000 N	0.304177 U: 845.0000 E	3.02E-11 U: 1365.0000 N	1.43E-05 U: 1209.0000 N
F13	3.47E-10 U: 1340.0000 N	1.21E-12 U: 1365.0000 N	3.02E-11 U: 1365.0000 N	3.02E-11 U: 1365.0000 N	3.02E-11 U: 465.0000 S	3.02E-11 U: 1365.0000 N	1.21E-12 U: 1365.0000 N	3.02E-11 U: 1365.0000 N	3.02E-11 U: 1365.0000 N	3.02E-11 U: 1365.0000 N
F14	3.02E-11 U: 1365.0000 N	3.02E-11 U: 1365.0000 N	2.23E-09 U: 510.0000 S	3.02E-11 U: 1365.0000 N	3.02E-11 U: 465.0000 S	3.02E-11 U: 1365.0000 N	3.02E-11 U: 1365.0000 N	0.028129 U: 766.0000 S	3.02E-11 U: 1365.0000 N	3.02E-11 U: 1365.0000 N
F15	3.02E-11 U: 1365.0000 N	9.4E-12 U: 1365.0000 N	4.5E-11 U: 1361.0000 N	3.02E-11 U: 1365.0000 N	3.02E-11 U: 465.0000 S	3.02E-11 U: 1365.0000 N	1.72E-12 U: 1365.0000 N	0.011228 U: 743.0000 S	3.02E-11 U: 1365.0000 N	3.02E-11 U: 1365.0000 N
F16	0.610008 U: 950.0000 E	1.21E-12 U: 1365.0000 N	0.001597 U: 701.0000 S	0.000856 U: 689.0000 S	3.02E-11 U: 465.0000 S	3.02E-11 U: 1365.0000 N	1.61E-10 U: 482.0000 S	4.62E-10 U: 493.0000 S	0.3871 U: 856.0000 E	3.02E-11 U: 1365.0000 N
F17	0.003034 U: 1116.0000 S	3.02E-11 U: 1365.0000 N	0.001442 U: 699.0000 N	5.19E-07 U: 1255.0000 N	6.7E-11 U: 473.0000 S	3.02E-11 U: 1365.0000 N	3.02E-11 U: 1365.0000 N	2.32E-06 U: 595.0000 S	9.53E-07 U: 583.0000 N	5.07E-10 U: 1336.0000 N
F18	1.94E-11 U: 471.0000 S	0.520149 U: 878.5000 E	1.21E-10 U: 489.0000 S	7.35E-11 U: 484.0000 S	2.2E-10 U: 495.0000 N	9.93E-11 U: 487.0000 S	1.28E-11 U: 467.0000 S	2.2E-10 U: 495.0000 N	1.28E-11 U: 467.0000 S	1.63E-10 U: 492.0000 S
F19	1.21E-12 U: 465.0000 S	4.57E-12 U: 480.0000 S	1.21E-12 U: 465.0000 S	1.21E-12 U: 465.0000 S	1.21E-12 U: 465.0000 S	1.21E-12 U: 465.0000 S	1.21E-12 U: 465.0000 S	1.21E-12 U: 465.0000 S	1.21E-12 U: 465.0000 S	1.21E-12 U: 465.0000 S
F20	1.21E-12 U: 915.0000 E	4.57E-12 U: 915.0000 E	1.21E-12 U: 915.0000 E	1.21E-12 U: 915.0000 E	1.21E-12 U: 465.0000 S	1.21E-12 U: 915.0000 E	1.21E-12 U: 915.0000 E	1.21E-12 U: 915.0000 E	1.21E-12 U: 915.0000 E	0.041911 U: 855.0000 S
F21	1.21E-12 U: 465.0000 S	1.21E-12 U: 465.0000 S	1.21E-12 U: 465.0000 S	1.21E-12 U: 465.0000 S	1.21E-12 U: 465.0000 S	1.21E-12 U: 465.0000 S	1.21E-12 U: 465.0000 S	1.21E-12 U: 465.0000 S	1.21E-12 U: 465.0000 S	1.21E-12 U: 465.0000 S
F22	0.000253 U: 1163.0000 N	1.21E-12 U: 1365.0000 N	4.44E-07 U: 1257.0000 N	4.2E-10 U: 1338.0000 N	1.78E-10 U: 483.0000 S	1.21E-12 U: 1365.0000 N	1.21E-12 U: 1365.0000 N	2E-06 U: 1237.0000 N	1.21E-12 U: 1365.0000 N	1.21E-12 U: 1365.0000 N
F23	0.099258 U: 1027.0000 E	1.59E-10 U: 1344.0000 N	0.258051 U: 992.0000 E	0.652044 U: 946.0000 E	8.48E-09 U: 1305.0000 N	0.020681 U: 1072.0000 N	3.02E-11 U: 465.0000 S	3.32E-06 U: 1230.0000 N	5.97E-05 U: 643.0000 S	3.02E-11 U: 1365.0000 N
F24	1.21E-12 U: 465.0000 S	1.21E-12 U: 465.0000 S	1.21E-12 U: 465.0000 S	1.21E-12 U: 465.0000 S	1.21E-12 U: 465.0000 S	1.21E-12 U: 465.0000 S	1.21E-12 U: 465.0000 S	1.21E-12 U: 465.0000 S	1.21E-12 U: 465.0000 S	1.21E-12 U: 465.0000 S
F25	6.12E-10 U: 496.0000 S	3.02E-11 U: 465.0000 S	4.5E-11 U: 469.0000 S	3.02E-11 U: 465.0000 S	3.96E-08 U: 543.0000 S	3.02E-11 U: 465.0000 S	3.02E-11 U: 465.0000 S	3.02E-11 U: 465.0000 S	1.96E-10 U: 484.0000 S	3.02E-11 U: 465.0000 S

Table A11. Wilcoxon Sum rank test results over 50 benchmarks (F26–F50), run = 30, FES = 1000, agents No. = 30.

Function	FVIM	FLO	STOA	SOA	MVO	AO	SSOA	Chimp	CPO	ROA
F26	0.019112 U: 1074.0000 N	1.29E-09 U: 504.0000 S	2.15E-10 U: 485.0000 S	2.23E-09 U: 510.0000 S	6.36E-05 U: 644.0000 S	2.03E-09 U: 509.0000 S	3.02E-11 U: 465.0000 S	3.02E-11 U: 465.0000 S	0.464273 U: 865.0000 E	5.57E-10 U: 495.0000 S
F27	1.21E-12 U: 915.0000 E	1.21E-12 U: 915.0000 E	1.21E-12 U: 915.0000 E	1.21E-12 U: 915.0000 E	1.21E-12 U: 465.0000 S	1.21E-12 U: 915.0000 E	1.21E-12 U: 915.0000 E	1.21E-12 U: 915.0000 E	1.21E-12 U: 915.0000 E	1.21E-12 U: 915.0000 E
F28	2.36E-12 U: 465.0000 S	2.64E-12 U: 466.0000 S	2.36E-12 U: 465.0000 S	2.36E-12 U: 465.0000 S	2.36E-12 U: 465.0000 S	2.36E-12 U: 465.0000 S	2.36E-12 U: 465.0000 S	2.36E-12 U: 465.0000 S	2.36E-12 U: 465.0000 S	2.36E-12 U: 465.0000 S
F29	1.21E-12 U: 915.0000 E	1.21E-12 U: 915.0000 E	1.21E-12 U: 915.0000 E	1.21E-12 U: 915.0000 E	1.21E-12 U: 465.0000 S	1.21E-12 U: 915.0000 E	1.21E-12 U: 915.0000 E	1.21E-12 U: 915.0000 E	1.21E-12 U: 915.0000 E	1.21E-12 U: 825.0000 S
F30	1.21E-12 U: 915.0000 E	1.21E-12 U: 915.0000 E	1.21E-12 U: 915.0000 E	1.21E-12 U: 915.0000 E	1.21E-12 U: 465.0000 S	1.21E-12 U: 915.0000 E	1.21E-12 U: 915.0000 E	1.21E-12 U: 915.0000 E	1.21E-12 U: 915.0000 E	1.21E-12 U: 765.0000 S
F31	1.36E-07 U: 558.0000 S	0.000433 U: 676.5000 S	4.08E-11 U: 468.0000 S	3.02E-11 U: 465.0000 S	1.7E-08 U: 533.0000 S	3.02E-11 U: 465.0000 S	3.02E-11 U: 465.0000 S	3.02E-11 U: 465.0000 S	6.52E-09 U: 522.0000 S	3.69E-11 U: 467.0000 S
F32	2.08E-11 U: 465.0000 S	2.08E-11 U: 465.0000 S	2.08E-11 U: 465.0000 S	2.08E-11 U: 465.0000 S	2.08E-11 U: 465.0000 S	2.08E-11 U: 465.0000 S	2.08E-11 U: 465.0000 S	2.08E-11 U: 465.0000 S	2.08E-11 U: 465.0000 S	2.08E-11 U: 465.0000 S
F33	1.87E-05 U: 625.0000 S	3.83E-05 U: 636.0000 S	3.82E-09 U: 516.0000 S	3.02E-11 U: 465.0000 S	5.19E-07 U: 575.0000 S	0.000132 U: 656.0000 N	4.12E-06 U: 603.0000 S	3.02E-11 U: 465.0000 S	0.000213 U: 664.0000 N	0.000125 U: 655.0000 S
F34	3.02E-11 U: 465.0000 S	3.02E-11 U: 465.0000 S	3.02E-11 U: 465.0000 S	3.02E-11 U: 465.0000 S	3.02E-11 U: 465.0000 S	3.02E-11 U: 465.0000 S	3.02E-11 U: 465.0000 S	3.02E-11 U: 465.0000 S	3.02E-11 U: 465.0000 S	3.02E-11 U: 465.0000 S
F35	3.02E-11 U: 465.0000 S	3.02E-11 U: 465.0000 S	3.02E-11 U: 465.0000 S	3.02E-11 U: 465.0000 S	3.02E-11 U: 465.0000 S	3.02E-11 U: 465.0000 S	3.02E-11 U: 465.0000 S	3.02E-11 U: 465.0000 S	3.02E-11 U: 465.0000 S	3.02E-11 U: 465.0000 S
F36	3.02E-11 U: 465.0000 S	3.02E-11 U: 465.0000 S	3.02E-11 U: 465.0000 S	3.02E-11 U: 465.0000 S	3.02E-11 U: 465.0000 S	3.02E-11 U: 465.0000 S	3.02E-11 U: 465.0000 S	3.02E-11 U: 465.0000 S	3.02E-11 U: 465.0000 S	3.02E-11 U: 465.0000 S
F37	2.32E-06 U: 595.0000 S	1.21E-10 U: 479.0000 S	4.31E-08 U: 544.0000 S	1.2E-08 U: 529.0000 S	0.211561 U: 1000.0000 E	2.15E-10 U: 485.0000 S	3.02E-11 U: 465.0000 S	3.02E-11 U: 465.0000 S	2.6E-08 U: 538.0000 S	2.23E-09 U: 510.0000 S
F38	0.325527 U: 848.0000 E	1.86E-09 U: 508.0000 S	5.57E-10 U: 495.0000 S	1.61E-10 U: 482.0000 S	9.83E-08 U: 1276.0000 N	2.19E-08 U: 536.0000 S	3.02E-11 U: 465.0000 S	3.02E-11 U: 465.0000 S	0.001302 U: 697.0000 S	4.98E-11 U: 470.0000 S
F39	1.01E-11 U: 465.0000 S	1.01E-11 U: 465.0000 S	1.01E-11 U: 465.0000 S	1.01E-11 U: 465.0000 S	1.01E-11 U: 465.0000 S	1.01E-11 U: 465.0000 S	1.01E-11 U: 465.0000 S	1.01E-11 U: 465.0000 S	1.01E-11 U: 465.0000 S	1.01E-11 U: 465.0000 S
F40	0.455297 U: 966.0000 E	3.82E-10 U: 491.0000 S	3.02E-11 U: 465.0000 S	3.02E-11 U: 465.0000 S	0.10547 U: 805.0000 E	0.005084 U: 725.0000 S	3.02E-11 U: 465.0000 S	3.96E-08 U: 543.0000 S	0.145319 U: 1014.0000 E	3.02E-11 U: 465.0000 S
F41	0.014872 U: 1078.0000 N	1.21E-12 U: 1365.0000 N	1.39E-06 U: 588.0000 S	0.141278 U: 1015.0000 E	3.02E-11 U: 465.0000 S	1.21E-12 U: 1365.0000 N	1.21E-12 U: 1365.0000 N	0.015014 U: 750.0000 S	1.21E-12 U: 1365.0000 N	5.22E-12 U: 1365.0000 N
F42	2.96E-11 U: 1365.0000 N	1.21E-12 U: 1365.0000 N	3.02E-11 U: 465.0000 S	3.02E-11 U: 465.0000 S	3.02E-11 U: 465.0000 S	1.21E-12 U: 1365.0000 N	1.21E-12 U: 1365.0000 N	3.02E-11 U: 465.0000 S	1.21E-12 U: 1365.0000 N	3.34E-11 U: 1364.0000 N
F43	0.021506 U: 1071.0000 N	1.21E-12 U: 1365.0000 N	0.093341 U: 801.0000 E	1.17E-05 U: 618.0000 S	8.1E-10 U: 499.0000 S	3.02E-11 U: 1365.0000 N	3.02E-11 U: 465.0000 S	2.2E-07 U: 564.0000 S	3.02E-11 U: 1365.0000 N	3.02E-11 U: 1365.0000 N
F44	0.032651 U: 1060.0000 N	1.21E-12 U: 1365.0000 N	2.19E-08 U: 536.0000 S	3.69E-11 U: 467.0000 S	3.02E-11 U: 1365.0000 N	3.02E-11 U: 1365.0000 N	3.02E-11 U: 465.0000 S	3.02E-11 U: 465.0000 S	3.02E-11 U: 1365.0000 N	3.02E-11 U: 1365.0000 N
F45	1.21E-12 U: 465.0000 S	1.21E-12 U: 465.0000 S	1.21E-12 U: 465.0000 S	1.21E-12 U: 465.0000 S	1.21E-12 U: 465.0000 S	1.21E-12 U: 465.0000 S	1.21E-12 U: 465.0000 S	1.21E-12 U: 465.0000 S	1.21E-12 U: 465.0000 S	1.21E-12 U: 465.0000 S
F46	0.000213 U: 664.0000 S	4.08E-11 U: 468.0000 S	3.34E-11 U: 466.0000 S	3.02E-11 U: 465.0000 S	0.739399 U: 938.0000 E	1.41E-09 U: 505.0000 S	3.02E-11 U: 465.0000 S	3.02E-11 U: 465.0000 S	5.49E-11 U: 471.0000 S	5.49E-11 U: 471.0000 S
F47	0.195791 U: 827.0000 E	3.02E-11 U: 465.0000 S	3.02E-11 U: 465.0000 S	2.87E-10 U: 488.0000 S	0.695215 U: 888.0000 E	0.000284 U: 669.0000 S	3.02E-11 U: 465.0000 S	1.33E-10 U: 480.0000 S	1.16E-07 U: 556.0000 S	3.02E-11 U: 465.0000 S
F48	1.27E-11 U: 465.0000 S	1.27E-11 U: 465.0000 S	1.27E-11 U: 465.0000 S	1.27E-11 U: 465.0000 S	1.27E-11 U: 465.0000 S	1.27E-11 U: 465.0000 S	1.27E-11 U: 465.0000 S	1.27E-11 U: 465.0000 S	1.27E-11 U: 465.0000 S	1.27E-11 U: 465.0000 S
F49	0.000587 U: 682.0000 S	3.02E-11 U: 465.0000 S	2.83E-08 U: 539.0000 S	3.5E-09 U: 515.0000 S	0.000655 U: 684.0000 S	1.11E-06 U: 585.0000 S	3.02E-11 U: 465.0000 S	8.88E-06 U: 614.0000 S	0.000117 U: 654.0000 S	8.89E-10 U: 500.0000 S
F50	3.81E-07 U: 571.0000	3.02E-11 U: 465.0000	2.61E-10 U: 487.0000	2.37E-10 U: 486.0000	0.19073 U: 826.0000	7.38E-10 U: 498.0000	3.02E-11 U: 465.0000	3.02E-11 U: 465.0000	4.18E-09 U: 517.0000	3.02E-11 U: 465.0000
Total	S:25, N:14, E:11	S:26, N:17, E:7	S:37, N:5, E:8	S:32, N:10, E:8	S:39, N:4, E:7	S:27, N:17, E:6	S:33, N:12, E:5	S:37, N:6, E:7	S:23, N:18, E:9	S:32, N:15, E:3

Table A12. Wilcoxon sum rank test results over 50 benchmarks (F1–F25), run = 30, FES = 1000, agents No. = 30.

Function	WOA	PSO	MFO	SHIO	ZOA	GWO	SCA	DOA	SCSO	GA	SA
F1	3.02E-11 U: 915.0000 E	3.02E-11 U: 915.0000 E	3.02E-11 U: 915.0000 E	3.02E-11 U: 915.0000 E	5.87E-10 U: 540.0000 S	3.02E-11 U: 915.0000 E	3.02E-11 U: 915.0000 E	3.02E-11 U: 915.0000 E	3.02E-11 U: 915.0000 E	5.07E-09 U: 570.0000 S	3.02E-11 U: 915.0000 E
F2	0.557056 U: 930.5000 E	0.160802 U: 945.0000 E	5.89E-11 U: 500.5000 S	0.160802 U: 945.0000 E	0.160802 U: 945.0000 E	0.160802 U: 945.0000 E	2.06E-08 U: 572.5000 S	0.160802 U: 945.0000 E	0.160802 U: 945.0000 E	2.37E-12 U: 465.0000 S	2.37E-12 U: 465.0000 S
F3	3.02E-11 U: 1365.0000 N	3.02E-11 U: 465.0000 S	3.02E-11 U: 465.0000 S	3.02E-11 U: 1365.0000 N	3.02E-11 U: 1365.0000 N	3.02E-11 U: 1365.0000 N	3.02E-11 U: 465.0000 S	3.01E-11 U: 1365.0000 N	3.02E-11 U: 1365.0000 N	3.02E-11 U: 465.0000 S	3.02E-11 U: 465.0000 S
F4	3.02E-11 U: 1365.0000 N	3.02E-11 U: 465.0000 S	3.02E-11 U: 465.0000 S	3.02E-11 U: 1365.0000 N	3.02E-11 U: 1365.0000 N	3.02E-11 U: 1365.0000 N	3.02E-11 U: 465.0000 S	3.02E-11 U: 1365.0000 N	3.02E-11 U: 1365.0000 N	3.02E-11 U: 465.0000 S	3.02E-11 U: 465.0000 S
F5	4.11E-07 U: 1258.0000 N	3.02E-11 U: 465.0000 S	3.02E-11 U: 465.0000 S	0.011228 U: 1087.0000 N	3.02E-11 U: 1365.0000 N	3.47E-10 U: 1340.0000 N	3.02E-11 U: 465.0000 S	3.69E-11 U: 1363.0000 N	3.02E-11 U: 1365.0000 N	3.02E-11 U: 465.0000 S	3.02E-11 U: 465.0000 S
F6	1.21E-12 U: 465.0000 S	U: 915.0000 E	0.160802 U: 885.0000 E	1.21E-12 U: 465.0000 S	4.57E-12 U: 480.0000 S	1.21E-12 U: 465.0000 S	1.21E-12 U: 465.0000 S	8.87E-07 U: 645.0000 S	1.21E-12 U: 465.0000 S	1.21E-12 U: 465.0000 S	1.21E-12 U: 465.0000 S
F7	1.21E-12 U: 465.0000 S	1.21E-12 U: 915.0000 E	1.21E-12 U: 915.0000 E	1.21E-12 U: 465.0000 S	8.87E-07 U: 645.0000 S	1.21E-12 U: 465.0000 S	1.21E-12 U: 465.0000 S	1.21E-12 U: 915.0000 E	1.21E-12 U: 465.0000 S	1.21E-12 U: 465.0000 S	1.21E-12 U: 465.0000 S
F8	3.02E-11 U: 1365.0000 N	3.02E-11 U: 465.0000 S	0.000399 U: 1155.0000 S	3.02E-11 U: 1365.0000 N	1.21E-12 U: 1365.0000 N	3.02E-11 U: 1365.0000 N	0.403538 U: 858.0000 E	3E-11 U: 1365.0000 N	3.02E-11 U: 1365.0000 N	3.02E-11 U: 465.0000 S	3.02E-11 U: 465.0000 S
F9	3.02E-11 U: 465.0000 S	7.39E-11 U: 474.0000 S	3.02E-11 U: 465.0000 S	6.07E-11 U: 472.0000 S	3.02E-11 U: 465.0000 S	3.69E-11 U: 467.0000 S	3.02E-11 U: 465.0000 S	0.000399 U: 1155.0000 S	3.02E-11 U: 465.0000 S	3.02E-11 U: 465.0000 S	3.02E-11 U: 465.0000 S
F10	0.000132 U: 656.0000 S	2.13E-11 U: 1365.0000 N	3.02E-11 U: 1365.0000 N	0.001174 U: 695.0000 S	0.437641 U: 862.0000 E	1.6E-07 U: 560.0000 S	3.02E-11 U: 465.0000 S	0.001836 U: 1125.0000 S	0.559231 U: 875.0000 E	3.02E-11 U: 465.0000 S	3.02E-11 U: 465.0000 S
F11	0.074827 U: 794.0000 E	8.99E-11 U: 1354.0000 N	5.19E-07 U: 575.0000 S	0.000587 U: 682.0000 S	2.87E-10 U: 488.0000 S	0.761828 U: 936.0000 E	3.02E-11 U: 465.0000 S	3.02E-11 U: 465.0000 S	2.78E-07 U: 567.0000 S	3.02E-11 U: 465.0000 S	3.02E-11 U: 465.0000 S
F12	3.02E-11 U: 465.0000 S	3.02E-11 U: 465.0000 S	3.02E-11 U: 465.0000 S	3.02E-11 U: 1365.0000 N	3.02E-11 U: 1365.0000 N	3.02E-11 U: 1365.0000 N	3.02E-11 U: 465.0000 S	2.95E-11 U: 1365.0000 N	3.02E-11 U: 1365.0000 N	3.02E-11 U: 465.0000 S	3.02E-11 U: 465.0000 S
F13	4.98E-11 U: 1360.0000 N	3.02E-11 U: 465.0000 S	3.02E-11 U: 465.0000 S	0.00062 U: 1147.0000 N	3.02E-11 U: 1365.0000 N	4.08E-11 U: 1362.0000 N	3.02E-11 U: 465.0000 S	3.01E-11 U: 1365.0000 N	3.02E-11 U: 1365.0000 N	3.02E-11 U: 465.0000 S	3.02E-11 U: 465.0000 S
F14	3.02E-11 U: 1365.0000 N	3.02E-11 U: 465.0000 S	3.02E-11 U: 465.0000 S	3.02E-11 U: 1365.0000 N	3.02E-11 U: 1365.0000 N	3.02E-11 U: 1365.0000 N	3.02E-11 U: 465.0000 S	3.02E-11 U: 1365.0000 N	3.02E-11 U: 1365.0000 N	3.02E-11 U: 465.0000 S	3.02E-11 U: 465.0000 S
F15	3.02E-11 U: 465.0000 S	3.02E-11 U: 465.0000 S	3.02E-11 U: 465.0000 S	3.02E-11 U: 1365.0000 N	3.02E-11 U: 1365.0000 N	3.02E-11 U: 1365.0000 N	3.02E-11 U: 465.0000 S	2.92E-11 U: 1365.0000 N	3.02E-11 U: 1365.0000 N	3.02E-11 U: 465.0000 S	3.02E-11 U: 465.0000 S
F16	0.78446 U: 896.0000 E	0.000284 U: 669.0000 S	3.02E-11 U: 465.0000 S	0.888303 U: 925.0000 E	0.002499 U: 710.0000 S	0.016285 U: 1078.0000 N	3.02E-11 U: 465.0000 S	3.02E-11 U: 465.0000 S	0.118817 U: 809.0000 E	3.02E-11 U: 465.0000 S	3.02E-11 U: 465.0000 S
F17	0.019883 U: 757.0000 N	6.07E-11 U: 472.0000 S	3.02E-11 U: 465.0000 S	0.025101 U: 1067.0000 S	3.02E-11 U: 1365.0000 N	3.82E-10 U: 1339.0000 N	3.02E-11 U: 465.0000 S	5.57E-10 U: 495.0000 S	3.02E-11 U: 1365.0000 N	3.02E-11 U: 465.0000 S	3.02E-11 U: 465.0000 S
F18	6.64E-11 U: 483.0000 S	0.004764 U: 744.0000 S	0.682368 U: 936.5000 E	1.58E-11 U: 469.0000 S	6.03E-09 U: 534.0000 S	7.35E-11 U: 484.0000 S	1.34E-10 U: 490.0000 S	0.37355 U: 865.0000 E	4E-11 U: 478.0000 S	1.95E-11 U: 471.0000 S	2.2E-10 U: 495.0000 N
F19	1.21E-12 U: 465.0000 S	1.21E-12 U: 915.0000 E	1.21E-12 U: 915.0000 E	1.21E-12 U: 465.0000 S	4.79E-08 U: 600.0000 S	1.21E-12 U: 465.0000 S	1.21E-12 U: 465.0000 S	1.21E-12 U: 915.0000 E	1.21E-12 U: 465.0000 S	1.21E-12 U: 465.0000 S	1.21E-12 U: 465.0000 S
F20	1.21E-12 U: 915.0000 E	1.21E-12 U: 915.0000 E	2.21E-06 U: 915.0000 E	1.21E-12 U: 915.0000 E	1.21E-12 U: 915.0000 E	1.21E-12 U: 915.0000 E	1.21E-12 U: 915.0000 E	2.21E-06 U: 915.0000 E	1.21E-12 U: 915.0000 E	1.21E-12 U: 465.0000 S	1.21E-12 U: 465.0000 S
F21	1.21E-12 U: 465.0000 S	1.21E-12 U: 915.0000 E	1.66E-11 U: 915.0000 E	1.21E-12 U: 465.0000 S	1.66E-11 U: 495.0000 S	1.21E-12 U: 465.0000 S	1.21E-12 U: 465.0000 S	2.21E-06 U: 660.0000 S	1.21E-12 U: 465.0000 S	1.21E-12 U: 465.0000 S	1.21E-12 U: 465.0000 S
F22	1.21E-12 U: 1365.0000 N	9.76E-10 U: 501.0000 S	3.34E-11 U: 466.0000 S	2.68E-06 U: 597.0000 S	1.21E-12 U: 1365.0000 N	8.17E-11 U: 1349.0000 N	0.695215 U: 888.0000 E	1.21E-12 U: 1365.0000 N	1.21E-12 U: 1365.0000 N	3.02E-11 U: 465.0000 S	3.02E-11 U: 465.0000 S
F23	7.39E-11 U: 1356.0000 N	0.297272 U: 986.0000 E	7.38E-10 U: 1332.0000 N	0.695215 U: 942.0000 E	6.53E-08 U: 1281.0000 N	0.000377 U: 1156.0000 N	3.02E-11 U: 465.0000 S	0.153667 U: 1012.0000 E	1.16E-07 U: 1274.0000 N	3.02E-11 U: 465.0000 S	7.77E-09 U: 1306.0000 N
F24	1.21E-12 U: 465.0000 S	1.21E-12 U: 915.0000 E	1.21E-12 U: 915.0000 E	2.21E-06 U: 465.0000 S	1.21E-12 U: 600.0000 S	1.21E-12 U: 465.0000 S	1.21E-12 U: 465.0000 S	1.21E-12 U: 915.0000 E	2.21E-06 U: 465.0000 S	1.21E-12 U: 465.0000 S	1.21E-12 U: 465.0000 S
F25	1.46E-10 U: 481.0000 S	0.72646 U: 939.0000 E	2.88E-09 U: 513.0000 S	3.47E-10 U: 490.0000 S	5.61E-05 U: 642.0000 S	7.38E-10 U: 498.0000 S	3.02E-11 U: 465.0000 S	1.29E-09 U: 504.0000 S	1.25E-07 U: 557.0000 S	3.02E-11 U: 465.0000 S	1.46E-10 U: 481.0000 S

Table A13. Wilcoxon sum rank test results over 50 benchmarks (F26–F50), run = 30, FES = 1000, agents No. = 30.

Function	WOA	PSO	MFO	SHIO	ZOA	GWO	SCA	DOA	SCSO	GA	SA
F26	3.08E-08 U: 540.0000 S	0.761828 U: 894.0000 E	0.706171 U: 941.0000 E	0.673495 U: 886.0000 E	0.761828 U: 936.0000 E	0.77312 U: 895.0000 E	3.02E-11 U: 465.0000 S	1.53E-05 U: 622.0000 S	2E-05 U: 626.0000 S	3.02E-11 U: 465.0000 S	0.055546 U: 785.0000 E
F27	1.21E-12 U: 915.0000 E	1.21E-12 U: 915.0000 E	1.21E-12 U: 915.0000 E	1.21E-12 U: 915.0000 E	1.21E-12 U: 915.0000 E	1.21E-12 U: 915.0000 E	1.21E-12 U: 915.0000 E	1.21E-12 U: 915.0000 E	1.21E-12 U: 915.0000 E	1.21E-12 U: 465.0000 S	1.21E-12 U: 465.0000 S
F28	2.36E-12 U: 465.0000 S	0.654333 U: 900.0000 E	0.160742 U: 945.0000 E	2.36E-12 U: 465.0000 S	4.95E-09 U: 555.0000 S	2.36E-12 U: 465.0000 S	2.36E-12 U: 465.0000 S	3.81E-05 U: 690.0000 N	2.36E-12 U: 465.0000 S	2.36E-12 U: 465.0000 S	2.36E-12 U: 465.0000 S
F29	0.333711 U: 900.0000 E	1.21E-12 U: 915.0000 E	1.21E-12 U: 915.0000 E	1.21E-12 U: 915.0000 E	1.21E-12 U: 915.0000 E	1.21E-12 U: 915.0000 E	1.21E-12 U: 915.0000 E	1.21E-12 U: 915.0000 E	1.21E-12 U: 915.0000 E	1.21E-12 U: 465.0000 S	1.21E-12 U: 465.0000 S
F30	4.45E-12 U: 480.0000 S	1.21E-12 U: 915.0000 E	1.21E-12 U: 915.0000 E	1.21E-12 U: 915.0000 E	1.21E-12 U: 915.0000 E	1.21E-12 U: 915.0000 E	1.21E-12 U: 915.0000 E	1.21E-12 U: 915.0000 E	1.21E-12 U: 915.0000 E	1.21E-12 U: 465.0000 S	1.21E-12 U: 465.0000 S
F31	0.001767 U: 703.0000 N	5.11E-10 U: 1331.0000 N	3.27E-10 U: 1337.0000 N	1.03E-06 U: 584.0000 S	0.005801 U: 1102.0000 N	5.53E-08 U: 547.0000 S	3.02E-11 U: 465.0000 S	6.19E-10 U: 1329.0000 N	0.000318 U: 671.0000 S	3.02E-11 U: 465.0000 S	9.76E-10 U: 501.0000 S
F32	2.08E-11 U: 465.0000 S	0.667292 U: 888.0000 E	0.231069 U: 839.5000 E	2.08E-11 U: 465.0000 S	2.03E-08 U: 540.5000 S	2.08E-11 U: 465.0000 S	2.08E-11 U: 465.0000 S	2.12E-06 U: 601.0000 S	2.08E-11 U: 465.0000 S	2.08E-11 U: 465.0000 S	2.08E-11 U: 465.0000 S
F33	7.66E-05 U: 647.0000 S	7.02E-07 U: 579.0000 S	9.17E-06 U: 614.5000 S	1.75E-05 U: 624.0000 S	0.000399 U: 675.0000 N	3.16E-05 U: 633.0000 S	1.56E-08 U: 532.0000 S	0.830227 U: 930.0000 E	0.000149 U: 658.0000 N	1.78E-10 U: 483.0000 S	4.44E-07 U: 573.0000 S
F34	3.02E-11 U: 465.0000 S	0.661701 U: 945.0000 E	0.183929 U: 825.0000 E	3.02E-11 U: 465.0000 S	3.02E-11 U: 465.0000 S	3.02E-11 U: 465.0000 S	3.02E-11 U: 465.0000 S	0.026028 U: 1065.0000 S	3.02E-11 U: 465.0000 S	3.02E-11 U: 465.0000 S	3.02E-11 U: 465.0000 S
F35	3.02E-11 U: 465.0000 S	0.007258 U: 1095.0000 S	0.001816 U: 1125.0000 S	3.02E-11 U: 465.0000 S	3.02E-11 U: 465.0000 S	3.02E-11 U: 465.0000 S	3.02E-11 U: 465.0000 S	0.001689 U: 1125.0000 S	3.02E-11 U: 465.0000 S	3.02E-11 U: 465.0000 S	3.02E-11 U: 465.0000 S
F36	3.02E-11 U: 465.0000 S	6.77E-08 U: 1275.0000 S	0.075258 U: 1035.0000 E	3.02E-11 U: 465.0000 S	3.02E-11 U: 465.0000 S	3.02E-11 U: 465.0000 S	3.02E-11 U: 465.0000 S	0.075997 U: 1035.0000 E	3.02E-11 U: 465.0000 S	3.02E-11 U: 465.0000 S	3.02E-11 U: 465.0000 S
F37	9.92E-11 U: 477.0000 S	0.004427 U: 1108.0000 N	0.706171 U: 941.0000 E	2.88E-06 U: 598.0000 S	0.00238 U: 709.0000 S	9.53E-07 U: 583.0000 S	1.86E-09 U: 508.0000 S	0.559231 U: 955.0000 E	4.12E-06 U: 603.0000 S	3.02E-11 U: 465.0000 S	4.74E-06 U: 605.0000 S
F38	4.08E-11 U: 468.0000 S	2.13E-05 U: 1203.0000 N	0.17145 U: 1008.0000 E	0.311188 U: 984.0000 E	0.004427 U: 1108.0000 N	0.099258 U: 803.0000 E	3.34E-11 U: 466.0000 S	0.000903 U: 1140.0000 S	0.176128 U: 823.0000 E	3.02E-11 U: 465.0000 S	8.84E-07 U: 582.0000 S
F39	1.01E-11 U: 465.0000 S	0.008547 U: 1030.5000 S	0.001305 U: 1050.0000 N	1.01E-11 U: 465.0000 S	1.01E-11 U: 465.0000 S	1.01E-11 U: 465.0000 S	1.01E-11 U: 465.0000 S	0.342316 U: 861.0000 E	1.01E-11 U: 465.0000 S	1.01E-11 U: 465.0000 S	1.01E-11 U: 465.0000 S
F40	0.911709 U: 907.0000 E	0.156048 U: 1011.0000 E	4.79E-06 U: 1217.0000 N	0.077272 U: 1035.0000 E	1.47E-07 U: 1271.0000 N	0.946956 U: 910.0000 E	3.82E-10 U: 491.0000 S	6.66E-06 U: 1219.0000 N	0.853382 U: 902.0000 E	3.02E-11 U: 465.0000 S	1.11E-06 U: 1245.0000 N
F41	1.21E-12 U: 1365.0000 N	0.009468 U: 739.0000 S	3.02E-11 U: 465.0000 S	0.006056 U: 1101.0000 N	1.21E-12 U: 1365.0000 N	2.98E-11 U: 1339.0000 N	8.15E-11 U: 475.0000 S	1.21E-12 U: 1365.0000 N	1.21E-12 U: 1365.0000 N	3.02E-11 U: 465.0000 S	3.02E-11 U: 465.0000 S
F42	1.87E-11 U: 1365.0000 N	3.02E-11 U: 465.0000 S	3.02E-11 U: 465.0000 S	3.02E-11 U: 1365.0000 N	1.21E-12 U: 1365.0000 N	2.28E-11 U: 1365.0000 N	3.02E-11 U: 465.0000 S	4.08E-12 U: 1365.0000 N	1.21E-12 U: 1365.0000 N	3.02E-11 U: 465.0000 S	3.02E-11 U: 465.0000 S
F43	3.02E-11 U: 1365.0000 N	3.02E-11 U: 1365.0000 N	3.02E-11 U: 465.0000 S	0.045146 U: 779.0000 S	0.78446 U: 896.0000 E	5.49E-11 U: 1359.0000 N	3.02E-11 U: 465.0000 S	1.01E-08 U: 527.0000 S	6.74E-06 U: 1220.0000 N	3.02E-11 U: 465.0000 S	3.02E-11 U: 465.0000 S
F44	3.02E-11 U: 1365.0000 N	3.02E-11 U: 1365.0000 N	4.69E-08 U: 545.0000 S	0.051877 U: 783.0000 E	2.61E-10 U: 487.0000 S	8.99E-11 U: 1354.0000 N	3.02E-11 U: 465.0000 S	3.69E-11 U: 467.0000 S	1.33E-10 U: 480.0000 S	3.02E-11 U: 465.0000 S	3.02E-11 U: 465.0000 S
F45	1.21E-12 U: 465.0000 S	0.160742 U: 885.0000 E	1.21E-12 U: 915.0000 E	1.21E-12 U: 465.0000 S	1.93E-10 U: 525.0000 S	1.21E-12 U: 465.0000 S	1.21E-12 U: 465.0000 S	7.28E-07 U: 645.0000 S	1.21E-12 U: 465.0000 S	1.21E-12 U: 465.0000 S	1.21E-12 U: 465.0000 S
F46	1.17E-09 U: 503.0000 S	0.500506 U: 869.0000 E	0.034716 U: 772.0000 S	0.3871 U: 974.0000 E	0.002157 U: 707.0000 S	0.005322 U: 726.0000 S	3.02E-11 U: 465.0000 S	2.03E-07 U: 563.0000 S	0.000158 U: 659.0000 S	3.02E-11 U: 465.0000 S	5.49E-11 U: 471.0000 S
F47	7.12E-09 U: 523.0000 S	0.070111 U: 792.0000 E	0.007956 U: 735.0000 S	0.78446 U: 896.0000 E	0.001301 U: 697.0000 S	0.037782 U: 774.0000 S	3.02E-11 U: 465.0000 S	3.5E-09 U: 515.0000 S	0.000189 U: 662.0000 S	3.02E-11 U: 465.0000 S	1.03E-06 U: 584.0000 S
F48	1.27E-11 U: 465.0000 S	0.000662 U: 1065.0000 N	0.000662 U: 1065.0000 N	1.27E-11 U: 465.0000 S	8.71E-09 U: 535.0000 S	1.27E-11 U: 465.0000 S	1.27E-11 U: 465.0000 S	0.12526 U: 817.5000 E	1.27E-11 U: 465.0000 S	1.27E-11 U: 465.0000 S	1.27E-11 U: 465.0000 S
F49	0.000104 U: 652.0000 S	5.6E-05 U: 642.0000 S	0.549316 U: 874.0000 E	1.17E-05 U: 618.0000 S	9.79E-05 U: 651.0000 S	2.77E-05 U: 631.0000 S	1.1E-08 U: 528.0000 S	0.020679 U: 758.0000 S	0.000377 U: 674.0000 S	6.07E-11 U: 472.0000 S	0.001236 U: 696.0000 S
F50	3.82E-10 U: 491.0000	8.08E-10 U: 499.0000	7.6E-07 U: 580.0000	6.72E-10 U: 497.0000	8.15E-11 U: 475.0000	3.26E-07 U: 569.0000	3.02E-11 U: 465.0000	3.96E-08 U: 543.0000	7.12E-09 U: 523.0000	3.02E-11 U: 465.0000	3.69E-11 U: 467.0000
Total	S:28, N:14, E:8	S:21, N:8, E:21	S:24, N:6, E:20	S:26, N:10, E:14	S:25, N:17, E:8	S:24, N:16, E:10	S:43, N:0, E:7	S:20, N:14, E:16	S:25, N:15, E:10	S:50, N:0, E:0	S:45, N:3, E:2

Appendix F

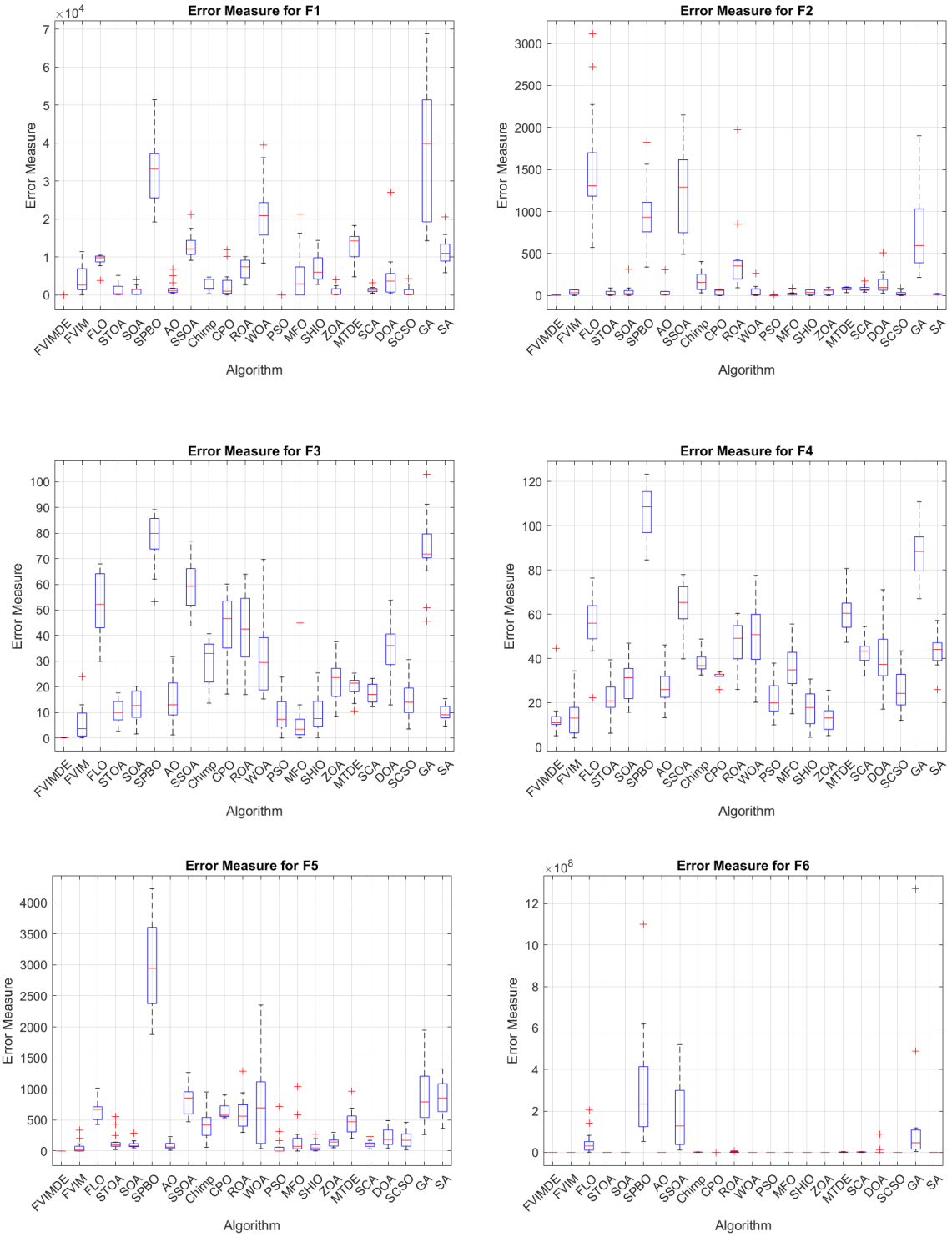

Figure A1. Error measure box plot analysis over CEC2022 benchmark functions (F1–F6).

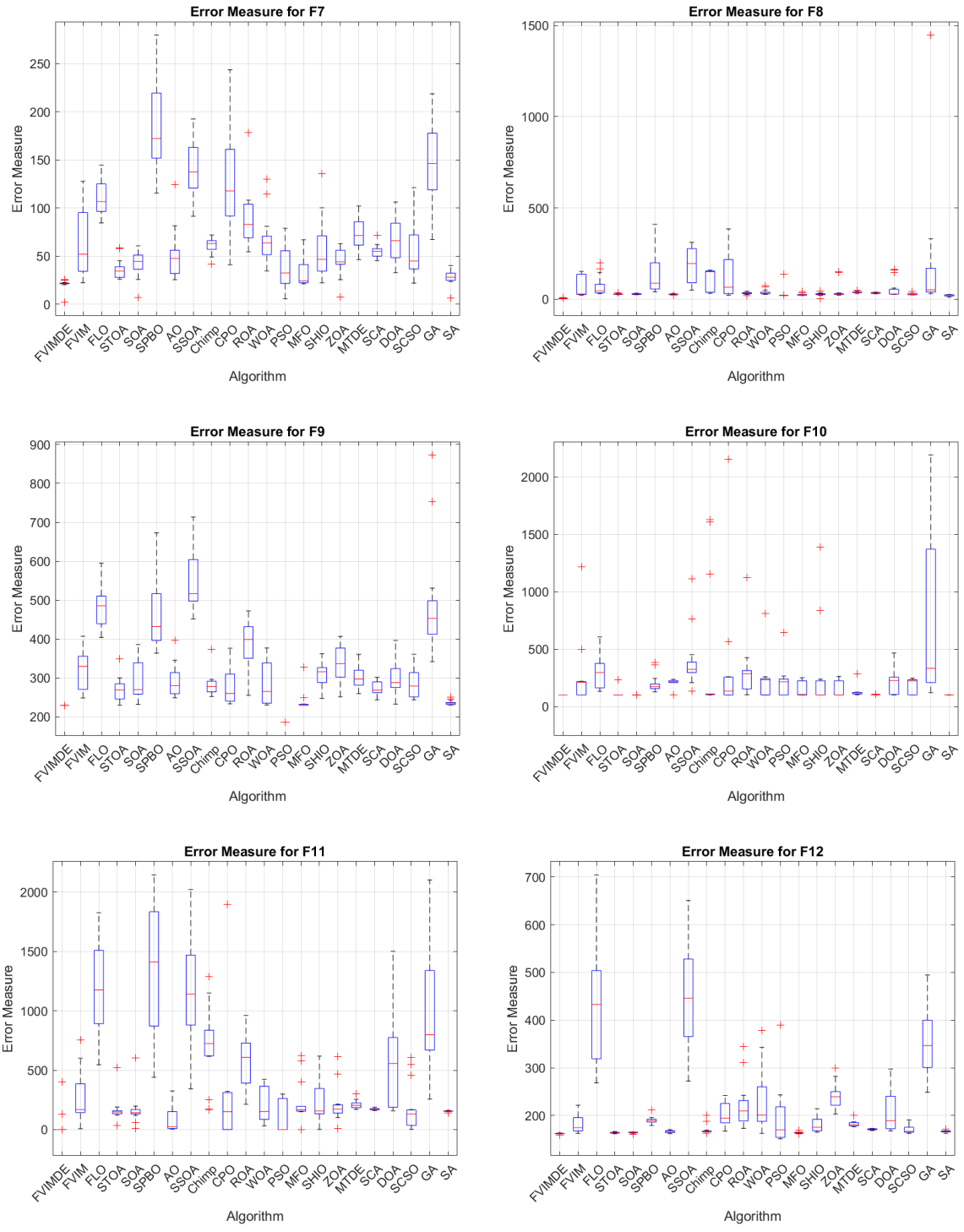

Figure A2. Error measure box plot analysis over CEC2022 benchmark functions (F7–F12).

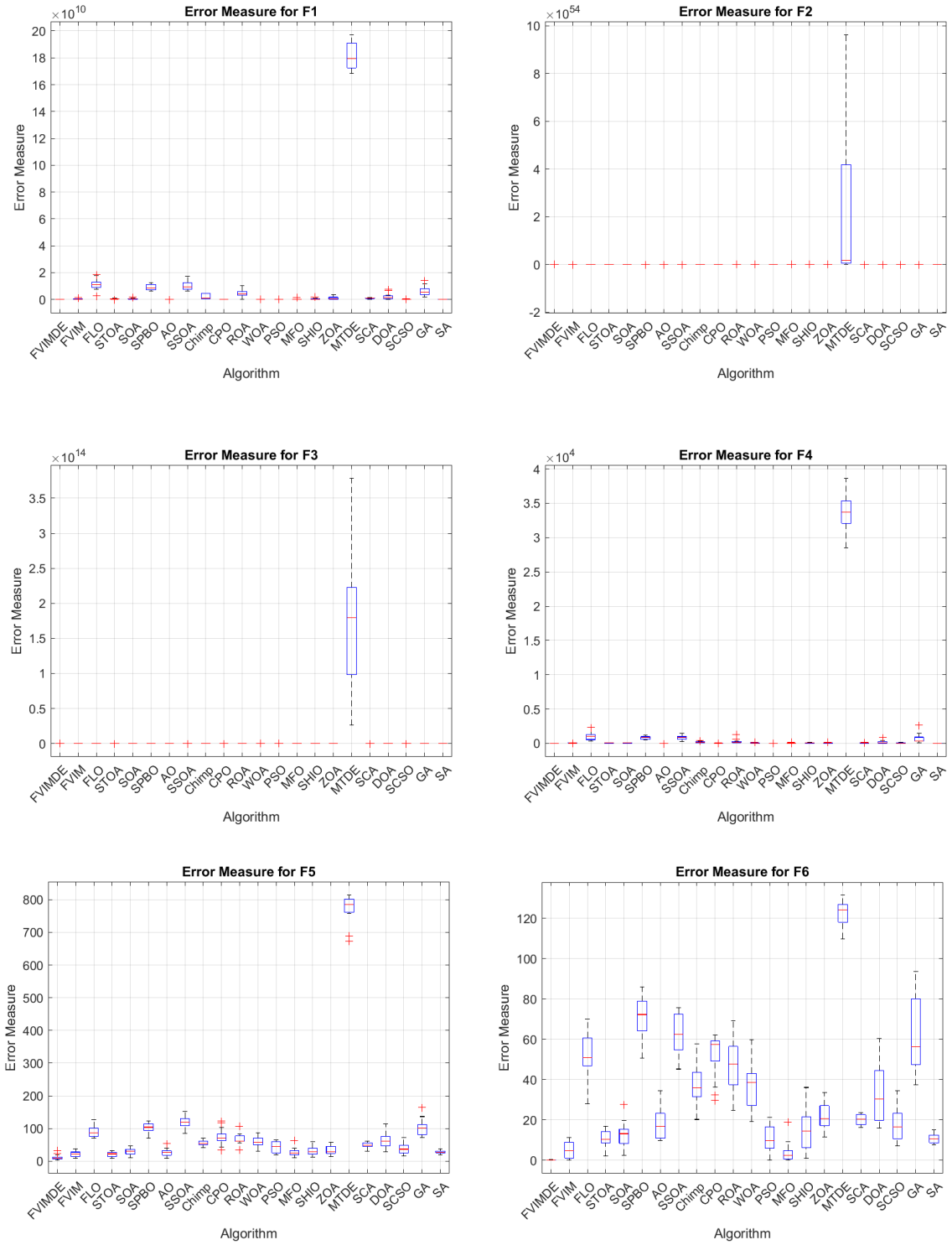

Figure A3. Error measure box plot analysis over CEC2017 benchmark functions (F1–F6).

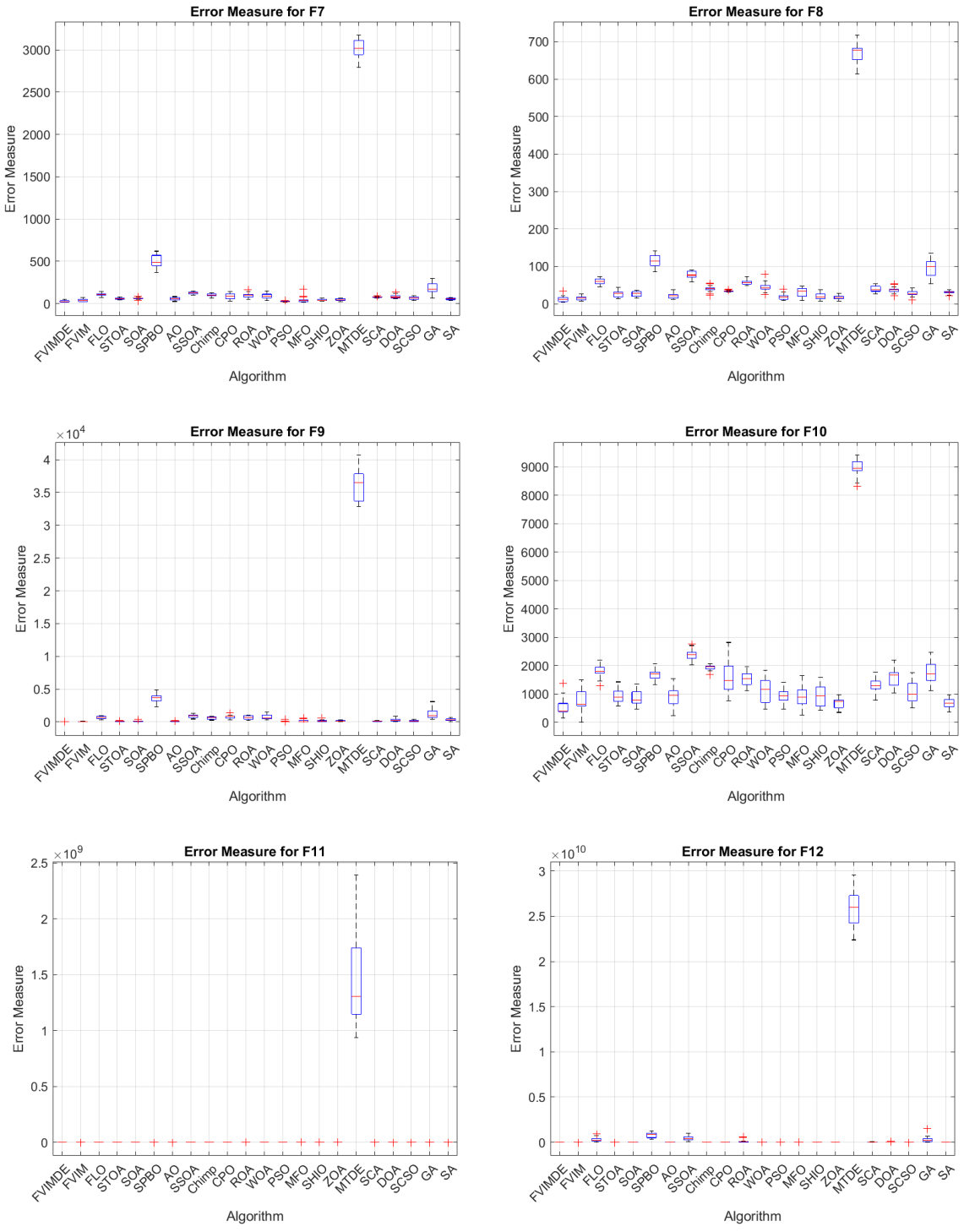

Figure A4. Error measure box plot analysis over CEC2017 benchmark functions (F7–F12).

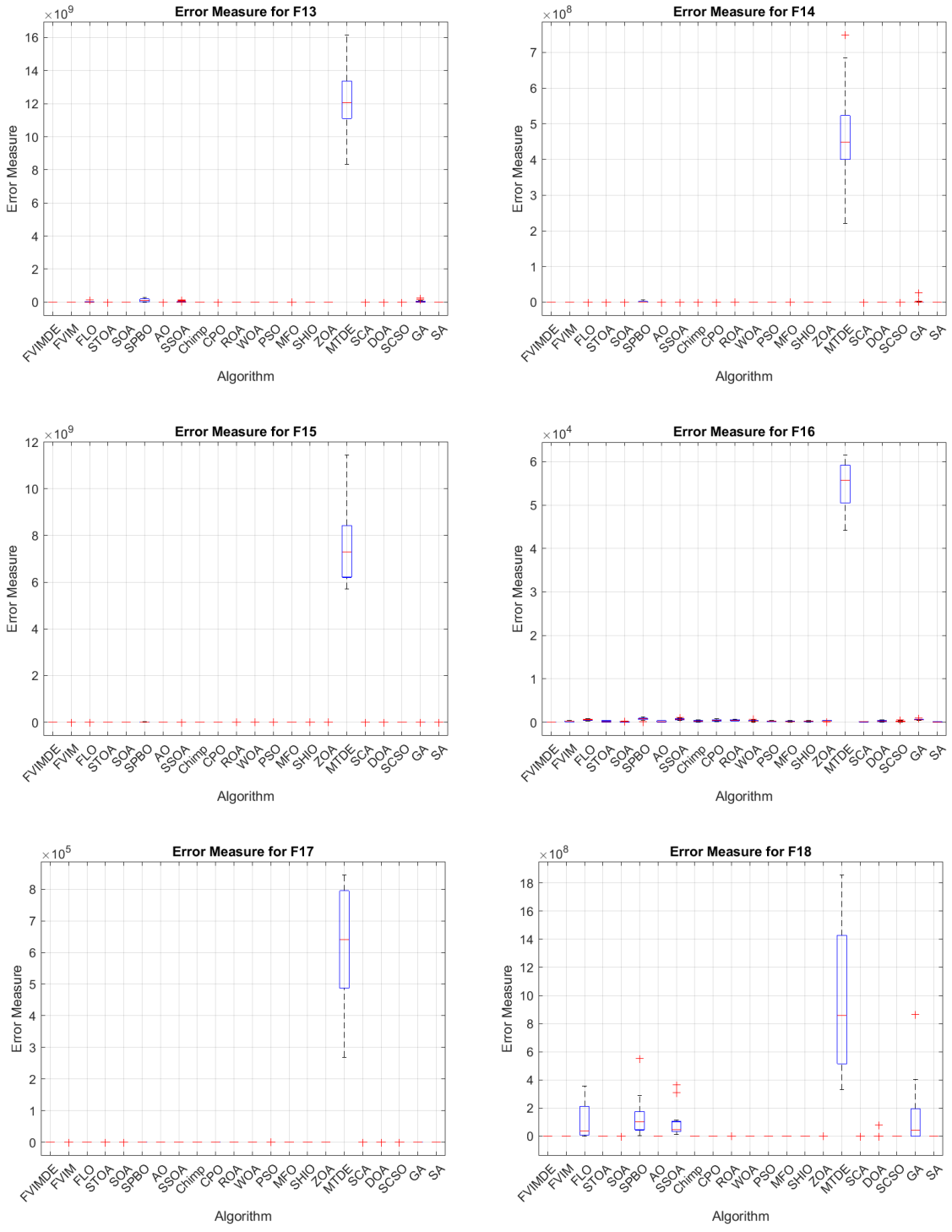

Figure A5. Error measure box plot analysis over CEC2017 benchmark functions (F13–F18).

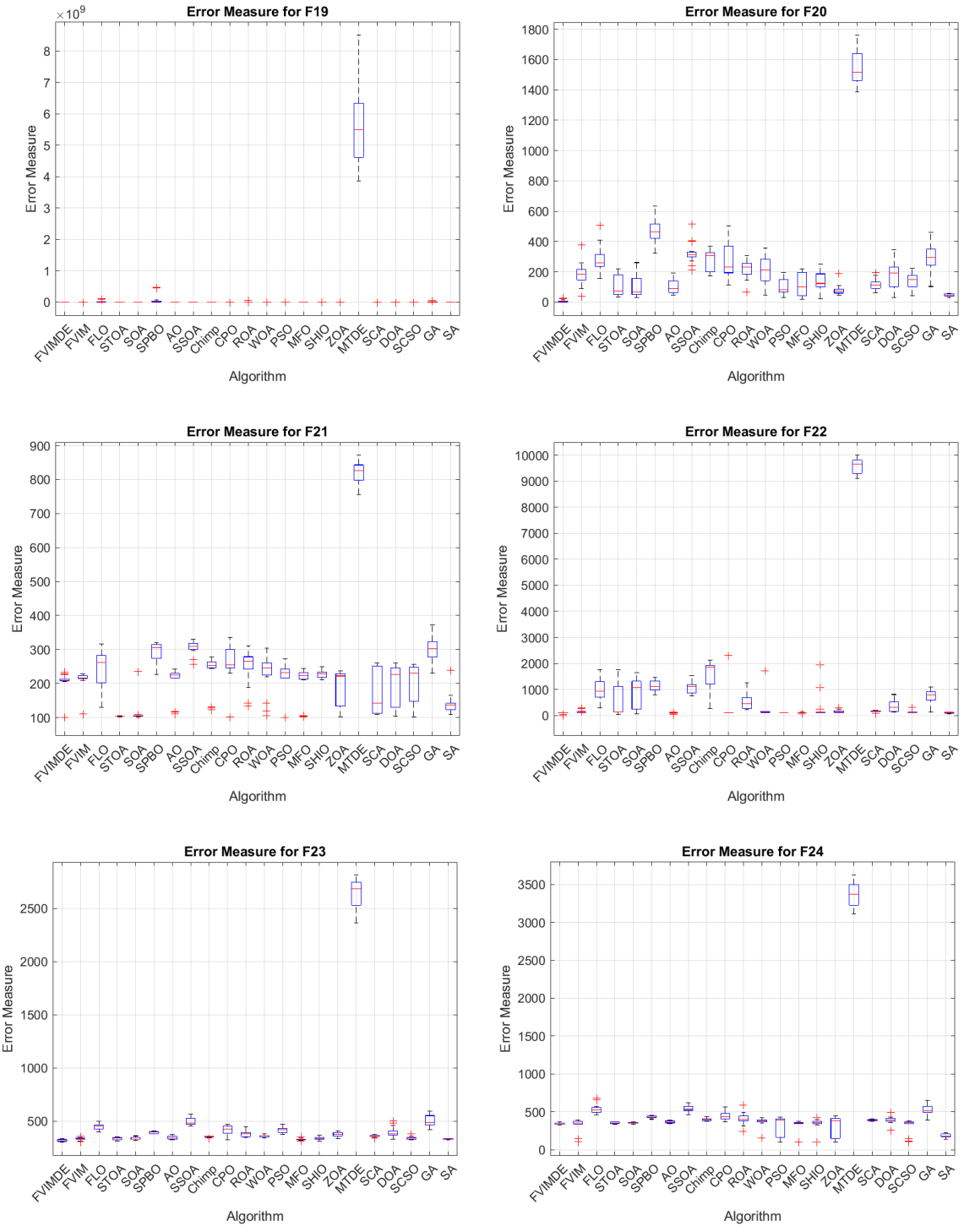

Figure A6. Error measure box plot analysis over CEC2017 benchmark functions (F19–F24).

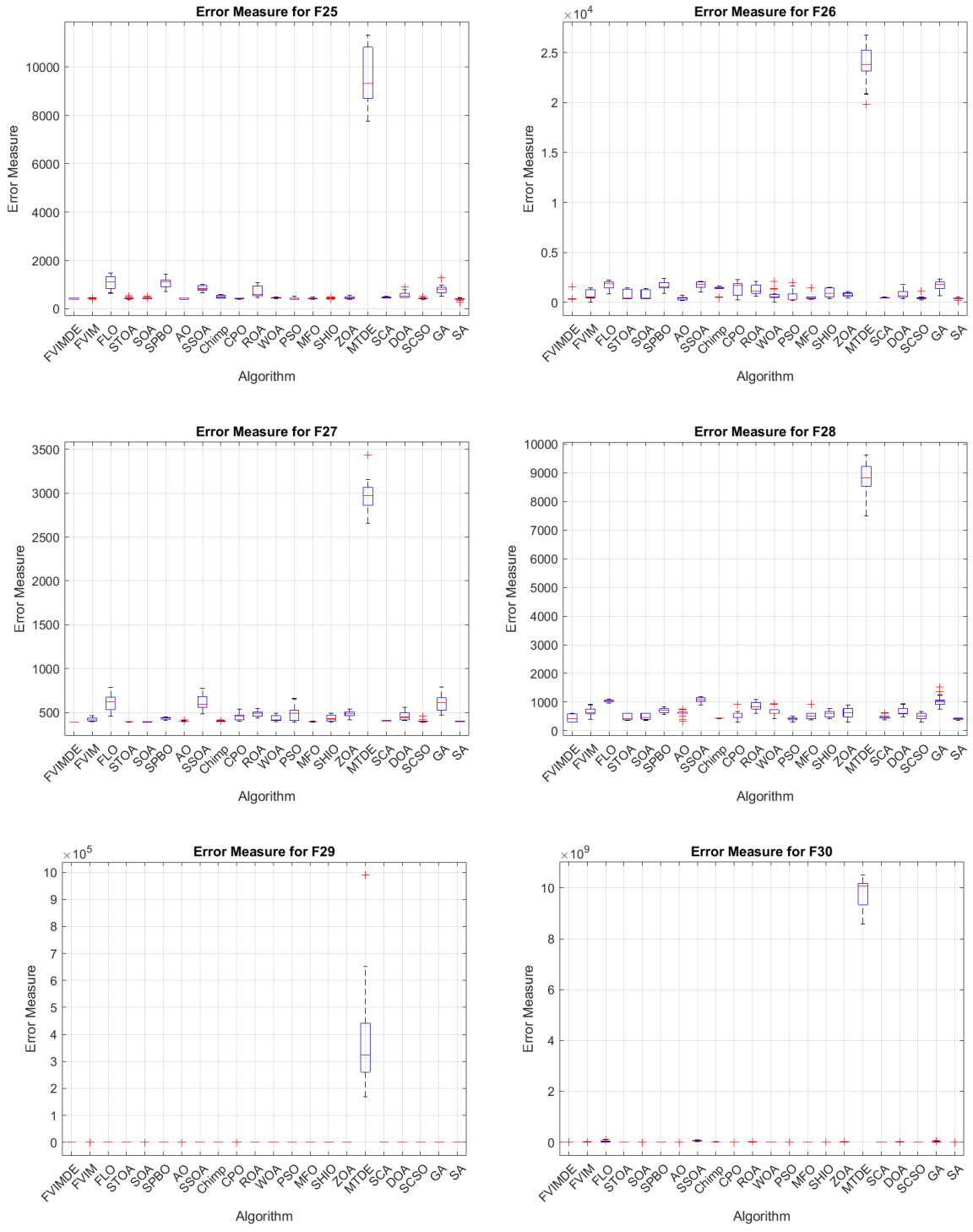

Figure A7. Error measure box plot analysis over CEC2017 benchmark functions (F25–F30).

References

1. Abualigah, L.; Elaziz, M.A.; Khasawneh, A.M.; Alshinwan, M.; Ibrahim, R.A.; Al-Qaness, M.A.; Mirjalili, S.; Sumari, P.; Gandomi, A.H. Metaheuristic optimization algorithms for solving real-world mechanical engineering design problems: A comprehensive survey, applications, comparative analysis, and results. *Neural Comput. Appl.* **2022**, *34*, 4081–4110. [CrossRef]
2. Sharma, M.; Kaur, P. A comprehensive analysis of nature-inspired meta-heuristic techniques for feature selection problem. *Arch. Comput. Methods Eng.* **2021**, *28*, 1103–1127. [CrossRef]
3. Eshelman, L.J. Genetic algorithms. In *Evolutionary Computation 1*; CRC Press: Boca Raton, FL, USA, 2018; pp. 102–118.
4. Kirkpatrick, S.; Gelatt, C.D., Jr.; Vecchi, M.P. Optimization by simulated annealing. *Science* **1983**, *220*, 671–680. [CrossRef] [PubMed]

5. Fakhouri, H.N.; Alawadi, S.; Awaysheh, F.M.; Hamad, F. Novel hybrid success history intelligent optimizer with gaussian transformation: Application in CNN hyperparameter tuning. *Clust. Comput.* **2024**, *27*, 3717–3739. [CrossRef]
6. Karimi-Mamaghan, M.; Mohammadi, M.; Meyer, P.; Karimi-Mamaghan, A.M.; Talbi, E.-G. Machine learning at the service of meta-heuristics for solving combinatorial optimization problems: A state-of-the-art. *Eur. J. Oper. Res.* **2022**, *296*, 393–422. [CrossRef]
7. Wang, Z.; Schafer, B.C. Machine learming to set meta-heuristic specific parameters for high-level synthesis design space exploration. In Proceedings of the 2020 57th ACM/IEEE Design Automation Conference (DAC), San Francisco, CA, USA, 20–24 July 2020; IEEE: Piscataway, NJ, USA, 2020; pp. 1–6.
8. Vikhar, P.A. Evolutionary algorithms: A critical review and its future prospects. In Proceedings of the 2016 International Conference on Global Trends in Signal Processing, Information Computing and Communication (ICGTSPICC), Jalgaon, India, 22–24 December 2016; IEEE: Piscataway, NJ, USA, 2016; pp. 261–265.
9. Beni, G. Swarm intelligence. In *Complex Social and Behavioral Systems: Game Theory and Agent-Based Models*; Springer: New York, NY, USA, 2020; pp. 791–818.
10. Kennedy, J.; Eberhart, R. Particle swarm optimization. In Proceedings of the ICNN'95-International Conference on Neural Networks, Perth, WA, Australia, 27 November–1 December 1995; IEEE: Piscataway, NJ, USA, 1995; Volume 4, pp. 1942–1948.
11. Dorigo, M.; Stützle, T. *Ant Colony Optimization: Overview and Recent Advances*; Springer: Cham, Switzerland, 2019.
12. Rashedi, E.; Rashedi, E.; Nezamabadi-Pour, H. A comprehensive survey on gravitational search algorithm. *Swarm Evol. Comput.* **2018**, *41*, 141–158. [CrossRef]
13. Fakhouri, H.N.; Hudaib, A.; Sleit, A. Hybrid particle swarm optimization with sine cosine algorithm and nelder–mead simplex for solving engineering design problems. *Arab. J. Sci. Eng.* **2020**, *45*, 3091–3109. [CrossRef]
14. Soler-Dominguez, A.; Juan, A.A.; Kizys, R. A survey on financial applications of metaheuristics. *ACM Comput. Surv. (CSUR)* **2017**, *50*, 15. [CrossRef]
15. Kumar, A.; Pant, S.; Ram, M.; Yadav, O. *Meta-Heuristic Optimization Techniques: Applications in Engineering*; Walter de Gruyter GmbH & Co KG: Berlin, Germany, 2022; Volume 10.
16. Fakhouri, H.N.; Ishtaiwi, A.; Makhadmeh, S.N.; Al-Betar, M.A.; Alkhalaileh, M. Novel hybrid crayfish optimization algorithm and self-adaptive differential evolution for solving complex optimization problems. *Symmetry* **2024**, *16*, 927. [CrossRef]
17. Chopard, B.; Tomassini, M.; Chopard, B.; Tomassini, M. Performance and limitations of metaheuristics. In *An Introduction to Metaheuristics for Optimization*; Springer: Berlin/Heidelberg, Germany, 2018; pp. 191–203.
18. Adam, S.P.; Alexandropoulos, S.-A.N.; Pardalos, P.M.; Vrahatis, M.N. No free lunch theorem: A review. In *Approximation and Optimization: Algorithms, Complexity and Applications*; Springer: Cham, Switzerland, 2019; pp. 57–82.
19. Huang, J.; Hu, H. Hybrid beluga whale optimization algorithm with multi-strategy for functions and engineering optimization problems. *J. Big Data* **2024**, *11*, 3. [CrossRef]
20. Tang, W.; Cao, L.; Chen, Y.; Chen, B.; Yue, Y. Solving Engineering Optimization Problems Based on Multi-Strategy Particle Swarm Optimization Hybrid Dandelion Optimization Algorithm. *Biomimetics* **2024**, *9*, 298. [CrossRef] [PubMed]
21. Liu, H.; Duan, S.; Luo, H. A hybrid engineering algorithm of the seeker algorithm and particle swarm optimization. *Mater. Test.* **2022**, *64*, 1051–1089. [CrossRef]
22. Cheng, J.; Lu, W.; Liu, Z.; Wu, D.; Gao, W.; Tan, J. Robust optimization of engineering structures involving hybrid probabilistic and interval uncertainties. *Struct. Multidiscip. Optim.* **2021**, *63*, 1327–1349. [CrossRef]
23. Dhiman, G. SSC: A hybrid nature-inspired meta-heuristic optimization algorithm for engineering applications. *Knowl.-Based Syst.* **2021**, *222*, 106926. [CrossRef]
24. Qin, C.; Han, B. A novel hybrid quantum particle swarm optimization with marine predators for engineering design problems. *IEEE Access* **2022**, *10*, 129322–129343. [CrossRef]
25. Chu, S.-C.; Guo, B.; Sun, B.; Pan, J.-S. A hybrid parallel willow catkin optimization algorithm applied for engineering optimization problems. *IEEE Access* **2024**, *12*, 102396–102415. [CrossRef]
26. Cuevas, E.; Diaz, P.; Camarena, O. Experimental analysis between exploration and exploitation. In *Metaheuristic Computation: A Performance Perspective*; Springer: Berlin/Heidelberg, Germany, 2021; pp. 249–269.
27. Dokeroglu, T.; Sevinc, E.; Kucukyilmaz, T.; Cosar, A. A survey on new generation metaheuristic algorithms. *Comput. Ind. Eng.* **2019**, *137*, 106040. [CrossRef]
28. Fakhouri, H.N.; Awaysheh, F.M.; Alawadi, S.; Alkhalaileh, M.; Hamad, F. Four vector intelligent metaheuristic for data optimization. *Computing* **2024**, *106*, 2321–2359. [CrossRef]
29. Storn, R.; Price, K. Differential evolution—A simple and efficient heuristic for global optimization over continuous spaces. *J. Glob. Optim.* **1997**, *11*, 341–359. [CrossRef]
30. Pant, M.; Zaheer, H.; Garcia-Hernandez, L.; Abraham, A. Differential evolution: A review of more than two decades of research. *Eng. Appl. Artif. Intell.* **2020**, *90*, 103479.
31. Luo, W.; Lin, X.; Li, C.; Yang, S.; Shi, Y. Benchmark functions for CEC 2022 competition on seeking multiple optima in dynamic environments. *arXiv* **2022**, arXiv:2201.00523.

32. Wu, G.; Mallipeddi, R.; Suganthan, P.N. Problem Definitions and Evaluation Criteria for the CEC 2017 Competition on Constrained Real-Parameter Optimization. Available online: https://www.researchgate.net/profile/Guohua-Wu-5/publication/317228117_Problem_Definitions_and_Evaluation_Criteria_for_the_CEC_2017_Competition_and_Special_Session_on_Constrained_Single_Objective_Real-Parameter_Optimization/links/5982cdbaa6fdcc8b56f59104/Problem-Definitions-and-Evaluation-Criteria-for-the-CEC-2017-Competition-and-Special-Session-on-Constrained-Single-Objective-Real-Parameter-Optimization.pdf (accessed on 17 July 2024).
33. Salgotra, R.; Singh, U.; Saha, S. Improved cuckoo search with better search capabilities for solving CEC2017 benchmark problems. In Proceedings of the 2018 IEEE Congress on Evolutionary Computation (CEC), Rio de Janeiro, Brazil, 8–13 July 2018; IEEE: Piscataway, NJ, USA, 2018; pp. 1–7.
34. Stanovov, V.; Akhmedova, S.; Semenkin, E. LSHADE algorithm with rank-based selective pressure strategy for solving CEC 2017 benchmark problems. In Proceedings of the 2018 IEEE Congress on Evolutionary Computation (CEC), Rio de Janeiro, Brazil, 8–13 July 2018; IEEE: Piscataway, NJ, USA, 2018; pp. 1–8.
35. Zhao, W.; Wang, L.; Mirjalili, S. Artificial hummingbird algorithm: A new bio-inspired optimizer with its engineering applications. *Comput. Methods Appl. Mech. Eng.* **2022**, *388*, 114194. [CrossRef]
36. Jamil, M.; Yang, X.-S. A literature survey of benchmark functions for global optimisation problems. *Int. J. Math. Model. Numer. Optim.* **2013**, *4*, 150–194. [CrossRef]
37. Alzoubi, S.; Abualigah, L.; Sharaf, M.; Daoud, M.S.; Khodadadi, N.; Jia, H. *Synergistic Swarm Optimization Algorithm*; Tech Science Press: Henderson, NV, USA , 2024.
38. Falahah, I.A.; Al-Baik, O.; Alomari, S.; Bektemyssova, G.; Gochhait, S.; Leonova, I.; Malik, O.P.; Werner, F.; Dehghani, M. Frilled lizard optimization: A novel nature-inspired metaheuristic algorithm for solving optimization problems. *Preprints* **2024**, 2024030898. [CrossRef]
39. Zhang, F.; Wu, S.; Cen, P. The past, present and future of the pangolin in mainland China. *Glob. Ecol. Conserv.* **2022**, 33, e01995. [CrossRef]
40. Jahn, J. *Vector Optimization*; Springer: Berlin/Heidelberg, Germany, 2009.
41. Fakhouri, H.N.; Hamad, F.; Alawamrah, A. Success history intelligent optimizer. *J. Supercomput.* **2022**, 78, 6461–6502. [CrossRef]
42. Mohapatra, S.; Mohapatra, P. American zebra optimization algorithm for global optimization problems. *Sci. Rep.* **2023**, 13, 5211. [CrossRef] [PubMed]
43. Bairwa, A.K.; Joshi, S.; Singh, D. Dingo optimizer: A nature-inspired metaheuristic approach for engineering problems. *Math. Probl. Eng.* **2021**, 2021, 2571863. [CrossRef]
44. Jia, H.; Peng, X.; Lang, C. Remora optimization algorithm. *Expert Syst. Appl.* **2021**, 185, 115665. [CrossRef]
45. Abualigah, L.; Yousri, D.; Abd Elaziz, M.; Ewees, A.A.; Al-Qaness, M.A.A.; Gandomi, A.H. Aquila optimizer: A novel meta-heuristic optimization algorithm. *Comput. Ind. Eng.* **2021**, 157, 107250. [CrossRef]
46. Khishe, M.; Mosavi, M.R. Chimp optimization algorithm. *Expert Syst. Appl.* **2020**, 149, 113338. [CrossRef]
47. Singh, A.; Sharma, A.; Rajput, S.; Mondal, A.K.; Bose, A.; Ram, M. Parameter extraction of solar module using the sooty tern optimization algorithm. *Electronics* **2022**, 11, 564. [CrossRef]
48. Dhiman, G.; Kumar, V. Seagull optimization algorithm: Theory and its applications for large-scale industrial engineering problems. *Knowl.-Based Syst.* **2019**, 165, 169–196. [CrossRef]
49. Wu, D.; Rao, H.; Wen, C.; Jia, H.; Liu, Q.; Abualigah, L. Modified sand cat swarm optimization algorithm for solving constrained engineering optimization problems. *Mathematics* **2022**, 10, 4350. [CrossRef]
50. Mirjalili, S.; Mirjalili, S.M.; Hatamlou, A. Multi-verse optimizer: A nature-inspired algorithm for global optimization. *Neural Comput. Appl.* **2016**, 27, 495–513. [CrossRef]
51. Mirjalili, S.; Lewis, A. The whale optimization algorithm . *Adv. Eng. Softw.* **2016**, *95*, 51–67. [CrossRef]
52. Mirjalili, S. SCA: A sine cosine algorithm for solving optimization problems. *Knowl.-Based Syst.* **2016**, 96, 120–133. [CrossRef]
53. Mirjalili, S. Moth-flame optimization algorithm: A novel nature-inspired heuristic paradigm. *Knowl.-Based Syst.* **2015**, *89*, 228–249. [CrossRef]
54. Mirjalili, S.; Mirjalili, S.M.; Lewis, A. Grey wolf optimizer. *Adv. Eng. Softw.* **2014**, 69, 46–61. [CrossRef]
55. Wang, D.; Tan, D.; Liu, L. Particle swarm optimization algorithm: An overview. *Soft Comput.* **2018**, 22, 387–408. [CrossRef]
56. Nikolaev, A.G.; Jacobson, S.H. Simulated annealing. In *Handbook of Metaheuristics*; Springer: Berlin/Heidelberg, Germany, 2010; pp. 1–39.
57. Mathew, T.V. Genetic Algorithm. Available online: https://datajobs.com/data-science-repo/Genetic-Algorithm-Guide-[Tom-Mathew].pdf (accessed on 17 July 2024).
58. Deb, K. An efficient constraint handling method for genetic algorithms. *Comput. Methods Appl. Mech. Eng.* **2000**, *186*, 311–338. [CrossRef]
59. Faramarzi, A.; Heidarinejad, M.; Stephens, B.; Mirjalili, S. Equilibrium optimizer: A novel optimization algorithm. *Knowl.-Based Syst.* **2020**, *191*, 105190. [CrossRef]
60. Hashim, F.A.; Houssein, E.H.; Mabrouk, M.S.; Al-Atabany, W.; Mirjalili, S. Henry gas solubility optimization: A novel physics-based algorithm. *Future Gener. Comput. Syst.* **2019**, *101*, 646–667. [CrossRef]

61. Zhao, S.; Zhang, T.; Ma, S.; Wang, M. Sea-horse optimizer: A novel nature-inspired meta-heuristic for global optimization problems. *Appl. Intell.* **2023**, *53*, 11833–11860. [CrossRef]
62. Abualigah, L.; Elaziz, M.A.; Sumari, P.; Geem, Z.W.; Gandomi, A.H. Reptile search algorithm (rsa): A nature-inspired meta-heuristic optimizer. *Expert Syst. Appl.* **2022**, *191*, 116158. [CrossRef]
63. Mirjalili, S. Dragonfly algorithm: A new meta-heuristic optimization technique for solving single-objective, discrete, and multi-objective problems. *Neural Comput. Appl.* **2016**, *27*, 1053–1073. [CrossRef]
64. Tzanetos, A.; Blondin, M. A qualitative systematic review of metaheuristics applied to tension/compression spring design problem: Current situation, recommendations, and research direction. *Eng. Appl. Artif. Intell.* **2023**, *118*, 105521. [CrossRef]
65. Kamil, A.T.; Saleh, H.M.; Abd-Alla, I.H. A multi-swarm structure for particle swarm optimization: Solving the welded beam design problem. *J. Phys. Conf. Ser.* **2021**, 1804, 012012. [CrossRef]
66. Yildirim, A.E.; Karci, A. Application of three bar truss problem among engineering design optimization problems using artificial atom algorithm. In Proceedings of the 2018 International Conference on Artificial Intelligence and Data Processing (IDAP), Malatya, Turkey, 28–30 September 2018; IEEE: Piscataway, NJ, USA, 2018; pp. 1–5.
67. Fenves, S.J. Tabular decision logic for structural design. *J. Struct. Div.* **1966**, *92*, 473–490. [CrossRef]